Supporting information for "Controllable Thermal Conductivity in Twisted Homogeneous Interfaces of Graphene and Hexagonal Boron Nitride"

Wengen Ouyang,[1] Huasong Qin,[2] Michael Urbakh,[1] and Oded Hod[1]*

[1]Department of Physical Chemistry, School of Chemistry, The Raymond and Beverly Sackler Faculty of Exact Sciences and The Sackler Center for Computational Molecular and Materials Science, Tel Aviv University, Tel Aviv 6997801, Israel.

[2]State Key Laboratory for Strength and Vibration of Mechanical Structures, School of Aerospace, Xi'an Jiaotong University, Xi'an 710049, China

The Supporting information includes following sections:

1. Methodology
2. Convergence Tests
3. Comparision of the phonon spectrum and density of states calculated using the ILP and the Lennard-Jones potential
4. Thermal conductivity of twisted bilayer graphene
5. Brillouin zone integration procedure
6. Temperature dependence of cross-plane thermal conductivity
7. Derivation of Fermi's golden rule

1 Methodology

1.1 Model system

The initial intralayer carbon-carbon covalent bond length was taken as 1.420 Å (the equilibrium value obtained using the REBO intralayer potential for single layer graphene) and the initial intralayer boron-nitrogen covalent bond length was taken as 1.442 Å (the equilibrium value obtained using the Tersoff intralayer potential for single layer *h*-BN). The initial interlayer distance across the layered stack was set equal to 3.4 Å and 3.3 Å for graphite and bulk *h*-BN, respectively. Periodic boundary conditions were applied in all directions. It should be noted that the lattice structure is rigorously periodic only at some specific twist angles, the values of which are listed in **Table S1** in section 3 below. While the cross-sectional area for each misfit angle, θ, is different, all systems considered have a contact area exceeding 12 nm^2, which was shown to provide converged results with respect to unit-cell dimensions (see Section 2.4).[1] The intralayer interactions within each graphene and *h*-BN layer were modeled via the second generation REBO potential[2] and Tersoff potential,[3] respectively. The interlayer interactions between the layers of graphite and bulk *h*-BN were described via our dedicated interlayer potential (ILP),[4] which is implemented in the LAMMPS[5] suite of codes.[6]

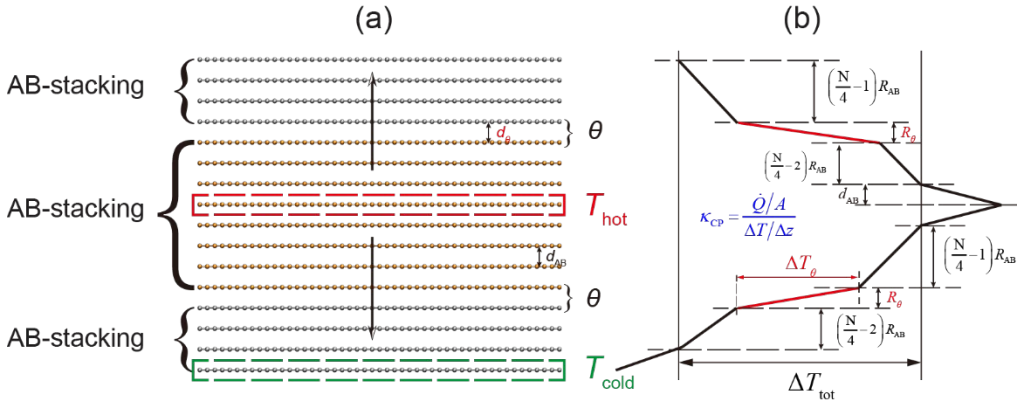

Figure S1. Schematic representation of the simulation setup (a) and steady-state temperature profile (b), respectively. In panel (a), two identical AB-stacked graphite slabs (gray and orange, respectively) are twisted with respect to each other to create a stacking fault of misfit angle θ. A thermal bias is induced by applying Langevin thermostats to the two layers marked by dashed red (T_{hot}) and green (T_{cold}) rectangles. The arrows indicate the direction of the vertical heat flux. Since periodic boundary conditions are applied also in the vertical direction, two twisted interfaces are, shown across which heat flows in opposite directions. The steady-state temperature profiles are illustrated in panel (b), where N is the total number of layers in the model system and R_{AB}, d_{AB} and R_θ, and d_θ mark the interfacial Kapitza resistance[7, 8] and interlayer distance for contacting graphene layers with AB-stacking and misfit angle θ, respectively. The red lines in panel (b) mark the temperature variation across the twisted interface, where the vertical axis corresponds to the position of the various layers along the stack and the horizontal axis marks the temperature of the various layers.

1.2 Simulation Protocol

All MD simulations were performed with the LAMMPS simulation package.[5] The velocity-Verlet algorithm with a time-step of 0.5 fs was used to propagate the equations of motion. A Nosé-Hoover thermostat with a time constant of 0.25 ps was used for constant temperature simulations. To maintain a specified hydrostatic pressure, the three translational vectors of the simulation cell were adjusted independently by a Nosé-Hoover barostat with a time constant of 1.0 ps.[9] To relax the box, we first equilibrated the systems in the NPT ensemble at a temperature of T = 300 K and zero pressure for 250 ps (see **Figure S2**). After equilibration, Langevin thermostats with damping coefficients 1.0 ps^{-1} were applied to the bottom and middle layer of the graphene stack (see **Figure S1**) with target temperatures T_{hot} = 375 K (hot reservoir) and T_{cold} = 225 K (cold reservoir), respectively. Then the system was allowed to reach steady-state over a subsequent simulation period of 750 ps (see **Figure S2**), during which the dynamics of all non-thermostated layers followed the NVE ensemble. For the larger model systems, the length of the NPT and Langevin stages was doubled (for the 32 and 48 layers systems) or tripled (for the 104 layers graphitic system) to ensure convergence of the obtained steady-state. Once steady-state was obtained, the last 500 ps were used to calculate the thermal conductivity of the twisted graphite and bulk *h*-BN. The statistical errors were estimated using ten different data sets, each calculated over a time interval of 50 ps.

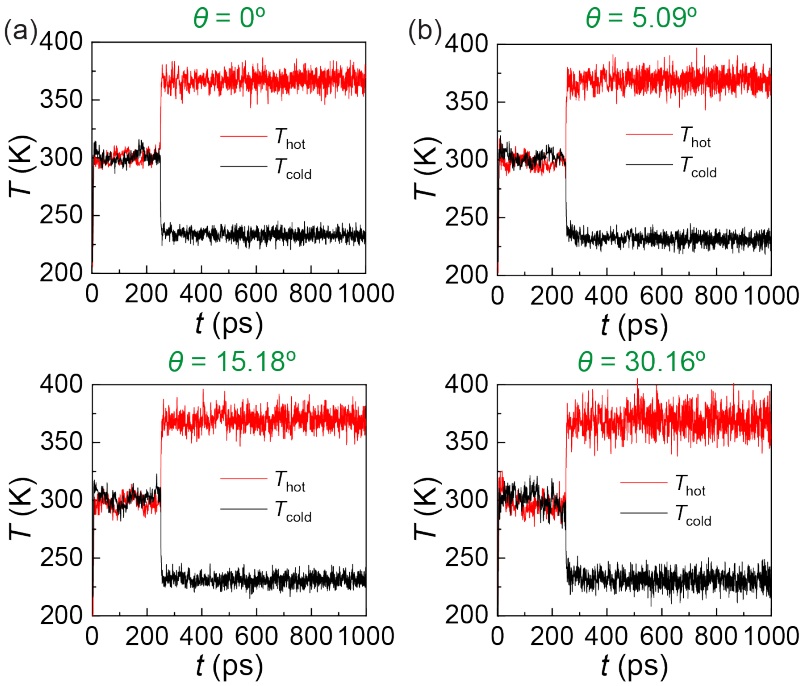

Figure S2. Time evolution of the temperature of the thermostated layers for 16 layers twisted graphite with misfit angle (a) θ = 0°, (b) θ = 5.09°, (c) θ = 15.18°, and (d) θ = 30.16°. Note that the thermal fluctuations increase with increasing the misfit angle due to the growing interfacial thermal resistance that enhances phonon back scattering at the twisted junction.

1.3 Calculation of the interfacial thermal resistance

According to Fourier's law, the cross-plane thermal conductivity (κ_{CP}) of a twisted graphitic interface of misfit angle θ can be calculated as:

$$\kappa_{\mathrm{CP}} = \frac{\dot{Q}/A}{\Delta T/\Delta z}, \tag{S1.1}$$

where $\dot{Q}$ is the heat flux, A is the cross-section area and $\Delta T/\Delta z$ is the temperature gradient along the direction of heat flux (perpendicular to the basal plane in our case). **Figure S1**(b) shows a schematic temperature profile along the z-direction, where the vertical axis corresponds to the position of the various layers along the stack and the horizontal axis marks the temperature of the various layers. The actual temperature profiles extracted from the NEMD simulations for twisted graphite with different number of layers can be found in **Figure S3** . For Bernal-stacked graphite (i.e., $\theta = 0°$, red circles in **Figure S3**), only the linear region of the temperature profile was used to calculate κ_{CP} and the points corresponding to the layers where the thermostats were applied were omitted (marked with green triangle in **Figure S3**). The κ_{CP} of the system was calculated using Eq. (S1.1) by averaging over the two linear regions of the temperature profiles. For the twisted case ($\theta \neq 0°$), we found a sudden temperature decrease ΔT_θ at the position of the twisted interface (see black squares in **Figure S3**). κ_{CP}, in this case, was calculated using the temperature gradient calculated for the same layer range as that for $\theta = 0°$. To characterize the thermal properties of the twisted interface, the concept of interfacial thermal resistance (ITR), i.e., Kapitza resistance,[7, 8] was introduced. Using the definition of the Kapitza resistance,[7] $R = A\Delta T/\dot{Q}$, and noticing that $\Delta T_{\mathrm{tot}} = (N/2-3)\Delta T_{\mathrm{AB}} + \Delta T_\theta$ and $\Delta z = (N/2-3)d_{\mathrm{AB}} + d_\theta$, where N is the number of layers and d_{AB}, ΔT_{AB} and d_θ, ΔT_θ are the interlayer distance and temperature difference for adjacent AB-stacked and twisted graphene layers, respectively, Eq. (S1.1) can be rewritten as follows [see **Figure S1**(b)]:

$$\left(\frac{N}{2}-3\right)R_{\mathrm{AB}} + R_\theta = \left[\left(\frac{N}{2}-3\right)d_{\mathrm{AB}} + d_\theta\right]/\kappa_{\mathrm{CP}}, \tag{S1.2}$$

where R_{AB} and R_θ are the ITRs of adjacent AB-stacked and twisted graphene layers, respectively. The first term on the left-hand side is just the sum of resistances of the various interfaces within the two optimally stacked slabs. The number of layers is divided by two to account only for one part of the system that is located between the two thermostats (see **Figure S1**) and we remove the three interfaces corresponding to the thermostats and the twisted interface. The second term on the left-hand side is the resistance of the twisted interface itself. On the right-hand side we have the overall

resistance (not to be confused with the resistivity) expressed as the inverse of the overall junction conductivity multiplied by the thickness. For the aligned contact $(\theta = 0°, R_\theta = R_{AB})$, the ITR can be simply calculated as $R_{\mathrm{AB}} = d_{\mathrm{AB}}/\kappa_{\mathrm{AB}}$. Once $R_{\mathrm{AB}}(N)$ is known, $R_\theta(N)$ can be calculated from Eq. (S1.2) using the value of $\kappa_{\mathrm{CP}}(N)$. We note that the sharp temperature drop at the twisted interface indicates that R_θ should be much larger than R_{AB}.

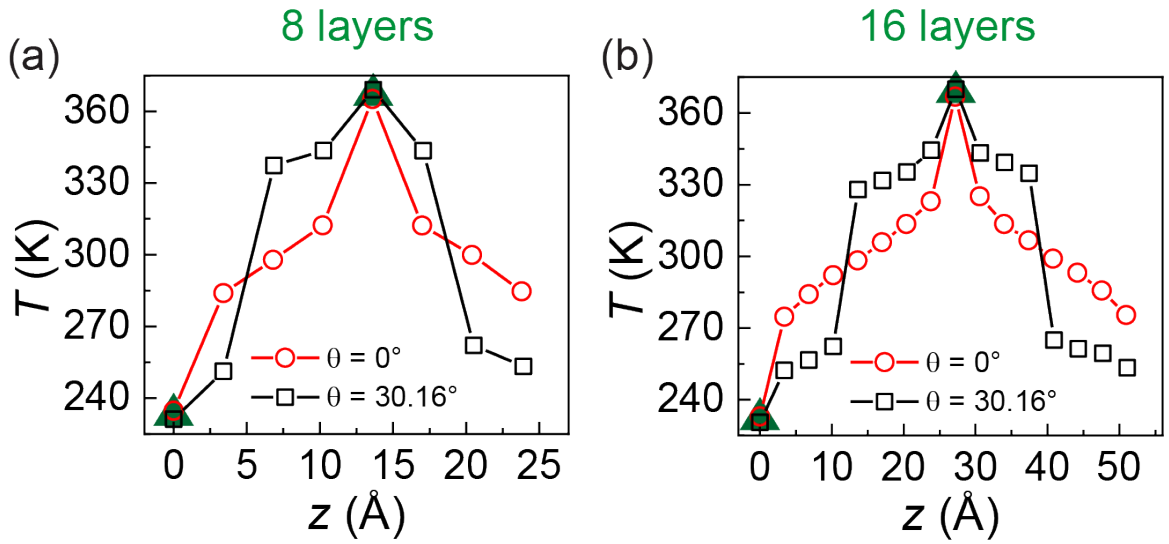

Figure S3. Temperature profiles for graphitic stacks consisting of (a) 8 and (b) 16 layers. The red circles and black squares represent the temperature profiles for the aligned $(\theta = 0°)$ and twisted $(\theta = 30.16°)$ junctions, respectively. Green triangles represent data points that were omitted in the κ_{CP} calculation.

2 Convergence Tests

2.1 Effect of NPT simulation time on the calculated thermal conductivity

According to our simulation protocol, the simulation box of the systems were relaxed using the NPT esemble for at least 250 ps (see Section 1.2) prior to the non-equilibrium simulation stage. To check the effect of the NPT equilibration time on the evaluated thermal conductivity, we performed additional convergence tests for the 8-layer graphite stack with θ = 0° by increasing the NPT simulation time to 1 ns. The results are summarized in **Figure S4**a,d. We find that the box size is already fully relaxed at 250 ps. More specifically, the averaged lattice constants for NPT simulation times of 250 ps and 1 ns were 2.4604 ± 0.0004 Å and 2.4605 ± 0.0003 Å, respectively. The relative difference between them is smaller than 0.01%. The corresponding calculated thermal conductivities were 0.196 ± 0.024 $Wm^{-1}K^{-1}$ and 0.184 ± 0.023 $Wm^{-1}K^{-1}$, respectively (see **Figure S5**a). Furthermore, the residual in-plane stresses obtained at a simulation time of 250 ps in both *x* (-0.025 ± 0.138 GPa) and *y* (-0.012 ± 0.128 GPa) directions also indicate that the system is satisfactorily relaxed. Similar behavior was found for θ = 30.16° (see **Figure S5**b). Therefore, we conclude that the NPT simulation time used in our protocol (250 ps) is sufficiently long to obtain converged results.

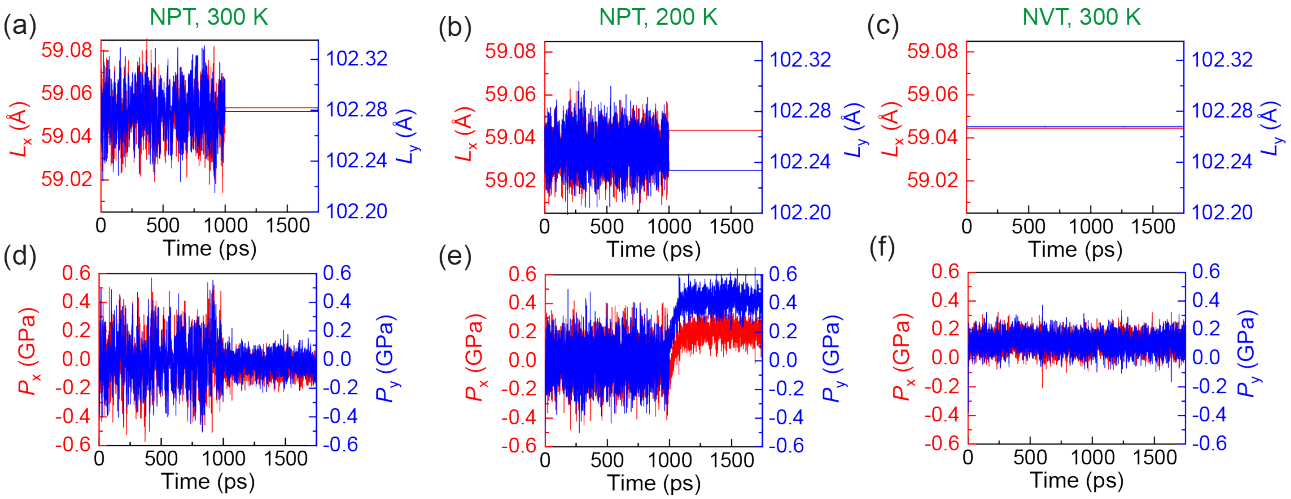

Figure S4. The size of the simulation box (a)-(c) and in-plane stress (d)-(f) as a function of simulation time calculated for the aligned (θ = 0°) 8-layer graphite stack using the NPT protocols at 300K (a, d) or at 200 K (b, e) and the NVT protocol at 300 K (c, f). After 1 ns, the equilibration protocol is terminated and Langevin thermostats are applied as explained in the main text. The left and right vertical axes represent the values obtained along the *x* (red lines) and *y* (blue lines) directions (see **Figure S10**a), respectively.

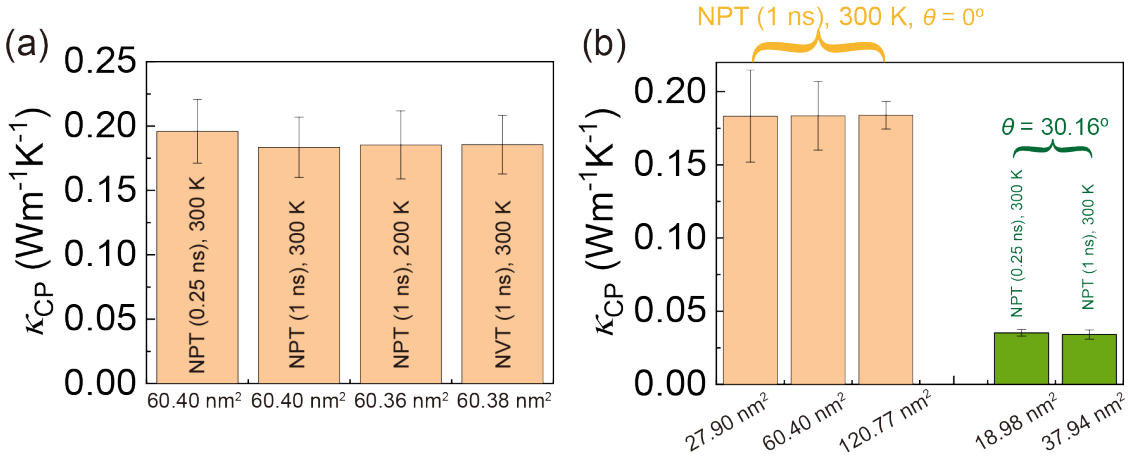

Figure S5. Convergence tests of the thermal conductivity for 8-layers graphite. (a) Evaluation of the effect of the equilibration time and protocol for $\theta = 0°$; (b) Evaluation of the effect of the size of the simulation box and equilibration time for $\theta = 0°$ (orange) and $\theta = 30.16°$ (green), respectively. In panel (a), the small difference between the cross-section area comes from the different simulation protocols. In panel (b), all the systems for $\theta = 0°$ are equilibrated under NPT conditions for 1 ns at 300 K and zero pressure. For $\theta = 30.16°$, the systems with smaller and larger cross-section areas are equilibrated under NPT conditions at 300 K and zero pressure for 0.25 ns and 1 ns, respectively. The method for estimating the error bars can be found in Section 1.2.

2.2 Effect of residual in-plane stress on the calculated thermal conductivity

Our original simulation protocol starts from an initial configuration, where all graphene layeres have the equilibrium carbon-carbon covalent bond-length obtained from the REBO intralayer potential (1.420 Å) and an interlayer distance of 3.4 Å. First, the system is equilibrated using an NPT ensemble simulation at 300 K and zero pressure with the REBO potential augmented by the ILP. This is followed by non-equilibrium NVE simulations with Langevin thermostats coupling the system to implicit heat baths, during which the simulation box dimensions are kept fixed and the thermal conductivity is evaluated. Since a previous study argued that the cross-plane thermal conductivity of graphite may be sensitive to in-plane stress,[10] we validated that any residual stress due to the difference in equilibration and non-equillibrium simulation protocols has minor effect on the calculated thermal conductivity. To this end, we performed additional simulations for the 8-layer graphitic stacks with $\theta = 0°$, replacing the NPT ensemble equilibration step by an NVT equilibration step (see **Figure S4**c,f). Consequently, the unit-cell was not relaxed during the equilibration step and the residual in-plane stress was ~0.11 ± 0.06 GPa in both the *x* and *y* directions. The average lattice parameter obtained using the NPT and NVT equilibration protocols were 2.4605 ± 0.0003 Å, and 2.4602 Å, respectively, with a relative difference of ~0.01%. The corresponding calculated thermal

conductivities were 0.184 ± 0.023 $Wm^{-1}K^{-1}$ and 0.186 ± 0.023 $Wm^{-1}K^{-1}$, respectively (see **Figure S5**a). The small variations (within the error bar) in lattice parameters and calculated thermal conductivity values indicates that the residual stress due to the different protocols used during the equillibration and non-equillibrium dynamics simulation stages has minor effect on our predictions.

2.3 Effect of NPT equillibration temperature

Our original simulation protocol starts from an initial configuration, where all graphene layeres have the equilibrium carbon-carbon covalent bond-length obtained from the REBO intralayer potential (1.420 Å) and an interlayer distance of 3.4 Å. First, the system is equilibrated using an NPT ensemble simulation at 300 K and zero pressure with the REBO potential augmented by the ILP. This is followed by non-equilibrium NVE simulations with Langevin thermostats coupling the system to implicit heat baths, during which the thermal conductivity is evaluated. To evaluate the effect of the equilibration step temperature, we repeated the calculations while setting the equilibration step temperature to 200 K and keeping the average temperature during the non-equilibrium calculation at 300 K. The results are presented in **Figure S4**b,e. We found that the time-averaged lattice parameter at steady-state during the thermal conductivity simulation stage was 2.4601 Å and the residual in-plane stress was 0.21 ± 0.06 GPa (0.43 ± 0.06 GPa) along x (y) direction. The small differences in lattice parameters between the original (2.4605 ± 0.0003 Å) and control simulations (~0.016%) have a minor effect on the calculated thermal conductivity (see **Figure S5**a).

2.4 Effect of supercell cross-section area on the calculated thermal conductivity

To evaluate the convergence of our results with respect to the simulated supercell dimensions, we performed additional calculations for the 8-layer graphite stacks with θ = 0° and θ = 30.16° by increasing the supercell sizes (see **Figure S5**b). Supercells of cross-section areas of 26.83 nm^2, 60.40 nm^2, and 120.77 nm^2 were used for the aligned (θ = 0°) interface and 18.98 nm^2 and 37.94 nm^2 sized models were used for the twisted interface (θ = 30.16°). For the θ = 0° interface, following a 1 ns equilibration step under NPT conditions at 300 K and zero pressure, the corresponding calculated thermal conductivities were 0.183 ± 0.032 $Wm^{-1}K^{-1}$, 0.184 ± 0.023 $Wm^{-1}K^{-1}$, and 0.184 ± 0.010 $Wm^{-1}K^{-1}$, respectively. Similarly, for the θ = 30.16° twisted interface, we equilibrated the smaller and larger systems under NPT conditions at 300 K and zero pressure for 0.25 ns and 1 ns, respectively. The corresponding thermal conductivities were 0.035 ± 0.002 $Wm^{-1}K^{-1}$ and 0.034 ± 0.003 $Wm^{-1}K^{-1}$, respectively. These results clearly indicate that our calculated thermal conductivities are well converged with respect to the model interface cross-section area.

3 Comparision of the phonon spectrum and density of states calculated using the ILP and the Lennard-Jones potential

A proper description of the phonon dispersion is very important for studying the thermal transport properties. We already showed in the main text that the ILP gives more accurate values of the cross-plane thermal conductivity for graphite than those predicted by the Lennard-Jones (LJ) potential. To further understand this finding, we repeated the phonon spectrum calculations for AB-stacked graphite obtained using the REBO interlayer potential and the ILP,[4] now using the AIREBO potential (with LJ parameters, $\varepsilon = 2.84$ meV and $\sigma = 3.4$ Å). The results are illustrated in **Figure S6**a. To identify the effect of interlayer potential on the phonon dispersions, we also calculated the phonon spectrum of monolayer graphene with the second generation REBO and AIREBO potential, respectively (see **Figure S6**b). Comparing **Figure S6**a and **Figure S6**b, we find that the interlayer potential mainly influences the phonon properties at the low energy regime. Therefore, the differences between the phonon dispersion curves calculated using the two potentials at the high energy regime mainly results from the intralayer potential terms. The comparison with the experimental phonon spectrum of graphite[11] shows that the phonon spectrum calculated by REBO+ILP agrees better with the experimental data in the low phonon energy regime, which is relevant for the cross-plane thermal conductivity calculation, than the spectrum obtained using AIREBO (see **Figure S6**c). The corresponding phonon density of states (DOS), as plotted in **Figure S6**d, also demonstrates the difference between the two force fields. This supports the reliability of the ILP for performing cross-plane thermal conductivity calculations.

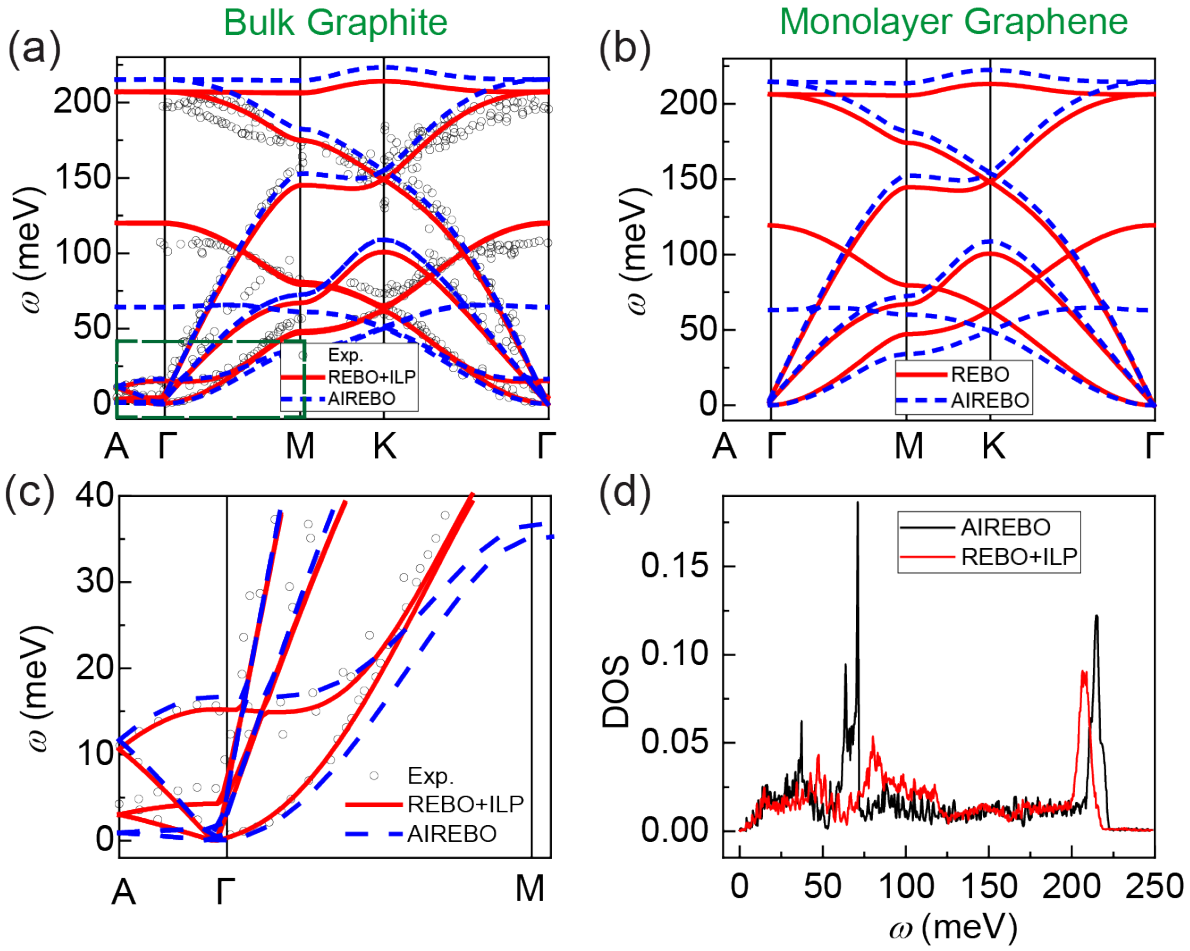

Figure S6. Phonon spectrum of (a) bulk graphite and (b) monolayer graphene. Red solid lines and blue dashed lines are dispersion curves calculated using the REBO+ILP (when applicable) and AIREBO force fields, respectively. Experimental results of bulk graphite[11] are presented by the open black circles. Panel (c) shows a zoom-in on the low energy phonon modes around the Γ-point (green rectangles in panels (a)) for graphite. Panel (d) shows the phonon density of states for graphite calculated using the REBO+ILP and the AIREBO potential, respectively.

4 Thermal conductivity of twisted bilayer graphene

4.1 Transient MD protocol

For comparison purposes we also calculated the interfacial thermal conductivity (ITC) and resistance (ITR) of twisted bilayer graphene (tBLG) with the transient MD simulation approach[12-14] since the NEMD simulation protocol used in the main text becomes invalid in this case. In this protocol, the system was first equilibrated within the NPT ensemble at T = 200 K and zero pressure for 100 ps, which was followed by a 100 ps NVT ensemble equilibration stage and a 100 ps of NVE ensemble equilibration stage. After the system reached equilibrium, an ultrafast heat impulse was imposed on the top layer of the t-BLG for 50 fs to increase the temperature of the top layer from 200 K to 400 K, while that of bottom layer of tBLG remained unchanged. After the external heat source was removed, thermal energy flowed from the top layer to the bottom layer due to the temperature difference and the temperature of both layers approached 300 K when quasi-steady-state was reached. During the thermal relaxation time interval (500 ps), the temperature and energy of the system sections were recorded. The ITR could then be extracted using the following equation:[12-14]

$$\frac{\partial E_{\mathrm{t}}}{\partial t} = \frac{A}{R}\left[T_{\mathrm{bot}}(t) - T_{\mathrm{top}}(t)\right], \tag{S4.1}$$

where E_{t} is the total energy of the top graphene layer, R is the ITR of the tBLG, A is the interfacial cross-section area, and T_{bot} and T_{top} are the instantaneous temperatures measured for the bottom and top layers of the tBLG, respectively. Note that in Eq. (S4.1) we assume a linear dependence of the heat flux on the temperature difference between the layers. The ITC of the tBLG is simply defined as $\mathrm{ITC} \equiv d/\mathrm{ITR}$, where d is the average interlayer distance. Note that, for tBLG, the ITC is equivalent to the κ_{CP} in the main text since there exists only one interface.

The ITC and ITR of tBLG as functions of misfit angle calculated with the transient MD simulation protocol are illustrated in **Figure S7**, demonstrating similar misfit-angle dependence as that for the NEMD protocol with Langevin thermostats exercised to obtain the results presented in the main text. This further validates the reliability of the simulation protocol adopted in the main text, which is more suitable to treat thick slabs and allows to obtain a true steady-state.

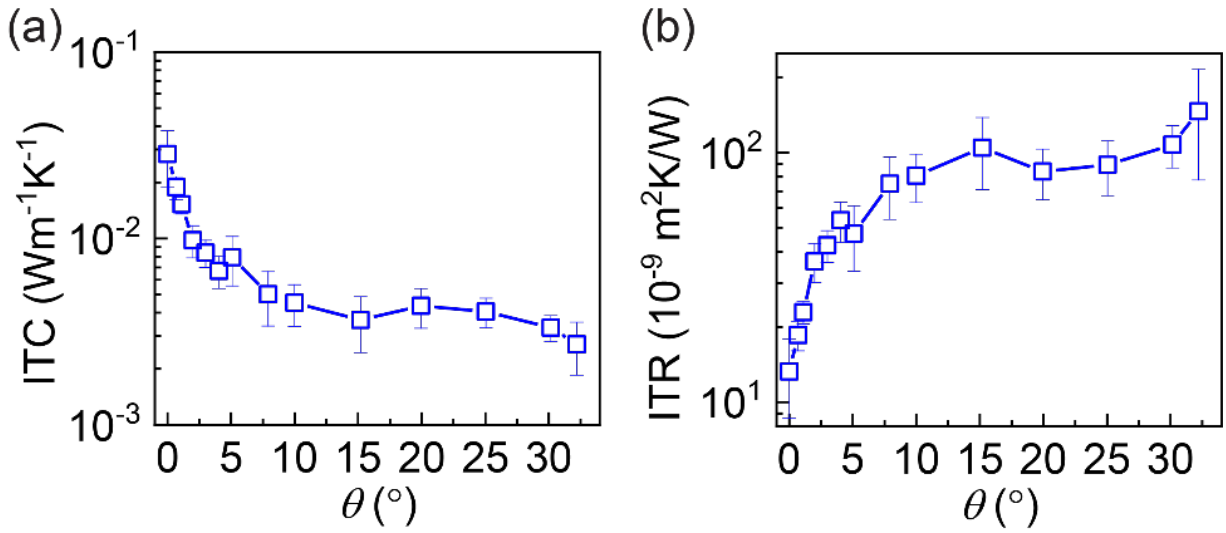

Figure S7. Misfit-angle dependence of (a) ITC and (b) ITR for a twisted bilayer graphene obtained using the transient MD simulation approach.

4.2 Comparison between the transient MD and Langevin thermostat protocols

Comparing κ_{CP} calculated for the multi-layered graphitic systems using the Langevin thermostat protocol (Figure 2a of the main text) and the ITC (=κ_{CP} in the bilayer case) calculated for bilayer graphene using the transient MD approach (**Figure S7**), a ~10 fold difference in magnitude is observed. We identify two main reasons for this discrepancy: (i) The dependence of κ_{CP} on the number of layers (see Figure 2a in the main text); and (ii) the different simulation protocols implemented for the two systems due to their different thickness. Regarding the latter issue we would like to stress that in the bilayer system we cannot use the Langevin thermostat approach as coupling the interface layer directly to the implicit heat bath without any buffer layers may result in an unphysical behavior. To estimate the relative importance of the two contributions we extrapolated the κ_{CP} data obtained using the Langevin thermostat approach (see Figure 4a in the main text) to the bilayer limit using a power-law fitting function. The extrapolated κ_{CP} values obtained were 0.076 $\mathrm{Wm^{-1}K^{-1}}$ and 0.0061 $\mathrm{Wm^{-1}K^{-1}}$ for the 0° and 30.16° rotated interfaces, respectively (see **Figure S8**). Comparing to the values obtained for the bilayer system using the transient MD approach (0.028 $\mathrm{Wm^{-1}K^{-1}}$ and 0.0033 $\mathrm{Wm^{-1}K^{-1}}$, respectively), we find a difference of a factor of 2.7 and 1.8 for the 0° and 30.16° rotated interfaces, respectively. The remaining difference can be therefore attributed to the difference between the two simulation approaches.

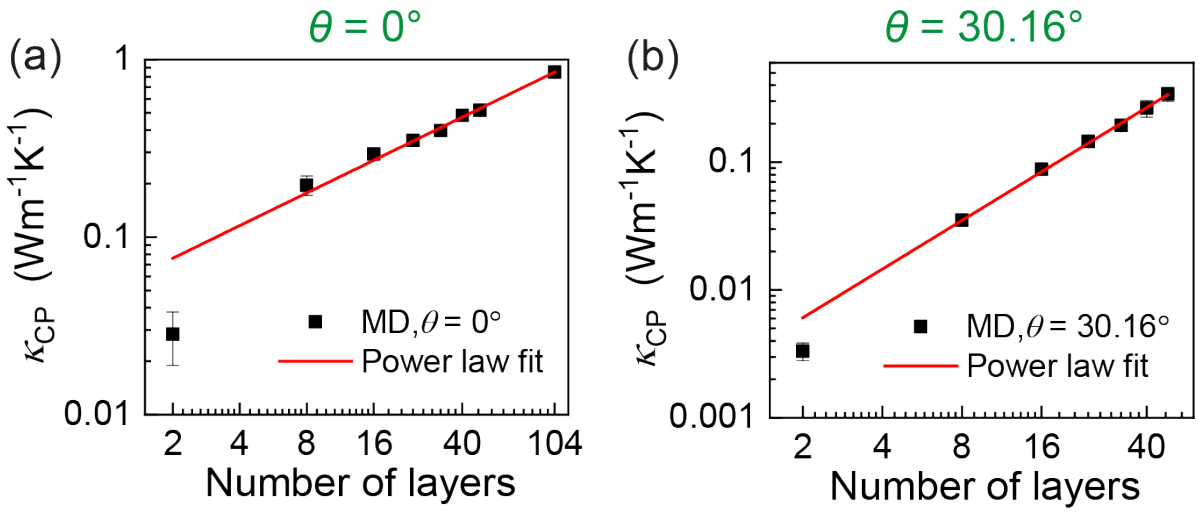

Figure S8. Interpolation of the cross-plane thermal conductivity (κ_{CP}) with the number of layers (N) for (a) 0° and (b) 30.16° rotated graphitic interfaces. Black squares and red lines represent the MD simulations and power-law fit, respectively. The power-law fit reads as $\kappa_{CP} = \alpha N^{\beta}$, where α and β are fitting parameters. In panels (a) and (b), the optimal fitting parameters are $\alpha = 0.04973$, $\beta = 0.61111$ and $\alpha = 0.00253$, $\beta = 1.26412$, respectively. The MD results for $N > 2$ and $N = 2$ were obtained with the Langevin thermostat approach and transient MD approach, respectively.

To explain the stronger thickness dependence of κ_{CP} observed for twisted interfaces, we note that there are two main factors (see Eq. (S1.2)) influencing the dependence of the cross-plane thermal conductivity on the thickness: (i) The ITR, R_θ, which measures the resistance of the twisted interface alone; and (ii) the resistance, R_{AB}, of the interface between each two optimally stacked layers within the slabs residing above and below the twisted interface. Thus, the equation for the thermal conductivity as a function of the number of layers, N, may be written as follows (see Eq. (S1.2) for a full explanation):

$$\kappa_{\mathrm{CP}}(N) = \frac{(N/2-3)d_{\mathrm{AB}}+d_\theta}{(N/2-3)R_{\mathrm{AB}}+R_\theta}. \qquad \text{(S4.2)}$$

To investigate the origin of the higher slope of $\kappa_{\mathrm{CP}}(N)$ for the twisted interface, we varied the value of R_θ artificially. In **Figure S9** below we compare the $\kappa_{\mathrm{CP}}(N)$ curves extracted from the simulations of the aligned and 30.16° twisted interfaces (open red circles and black squares, respectively) with the curve of the twisted interface, where we artificially reduce the value of R_θ by half (open blue triangles). Clearly, reducing R_θ results in a reduction of the slope of the curve and a weaker thickness dependence of κ_{CP}. Thus, we can conclude that the stronger thickness dependence of the twisted system stems from the larger interfacial thermal resistance at the twisted interface.

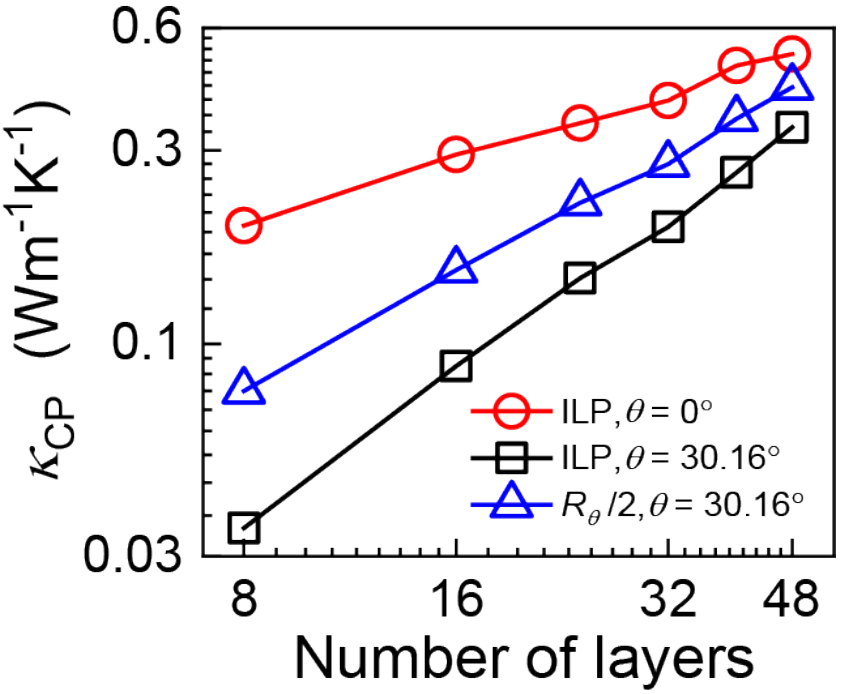

Figure S9. Thickness dependence of the thermal conductivity, κ_{CP}, of the aligned (open red circles) and 30.16° twisted (open black squares) graphite junctions. Blue triangles represented the κ_{CP} of graphite stacks with θ = 30.16°, where the ITR is artificially reduced by a factor of 2. Eq. (S4.2) is used to perform this calculation.

5 Brillouin zone integration procedure

5.1 Brillouin zone of supercell in tBLG

For tBLG, the lattice structure is rigorously periodic only at some specific misfit angles, θ, where the lattice vector $\boldsymbol{L}_1 = n_1\boldsymbol{a}_1 + n_2\boldsymbol{a}_2$ in the bottom layer equals the vector $\boldsymbol{L}_2 = m_1\boldsymbol{a}_1 + m_2\boldsymbol{a}_2$ in the top layer with certain integers m_1, m_2 and n_1, n_2. Here, $\boldsymbol{a}_1 = a(1,0)$ and $\boldsymbol{a}_2 = a\left(1/2, \sqrt{3}/2\right)$ are the primitive lattice vectors of the bottom layer and a is the lattice constant of monolayer graphene. Thus, the exact superlattice period is then given by:[15]

$$L = |n_1\boldsymbol{a}_1 + n_2\boldsymbol{a}_2| = a\sqrt{n_1^2 + n_2^2 + n_1 n_2} = \frac{|n_1 - n_2|a}{2\sin(\theta/2)}, \tag{S5.1}$$

where θ is the angle between two lattice vectors $\boldsymbol{L}_1$ and $\boldsymbol{L}_2$. In the simulations below, we always rotated the supercell such that its lattice vector is $\boldsymbol{L}_1 = L(1,0)$ and $\boldsymbol{L}_2 = L\left(1/2, \sqrt{3}/2\right)$.

Table S1. The parameters used to construct periodic supercells of various misfit angles.

$\boldsymbol{\theta}$ (°)	$\boldsymbol{A}$ ($\mathbf{nm^2}$)	$\boldsymbol{n_1}$	$\boldsymbol{n_2}$	$\boldsymbol{m_1}$	$\boldsymbol{m_2}$
0	60.383688	24	0	24	0
0.696407	709.613169	48	47	47	48
1.121311	273.718420	30	29	29	30
2.000628	85.648391	17	16	16	17
3.006558	152.322047	23	21	21	23
4.048894	189.013524	26	23	23	26
5.085849	53.255058	14	12	12	14
7.926470	49.376245	14	11	11	14
9.998709	86.277388	19	14	14	19
15.178179	31.554670	15	4	4	15
19.932013	42.876612	15	8	8	15
25.039660	13.942761	9	4	4	9
30.158276	18.974735	11	4	4	11
32.204228	21.805221	12	4	4	12

In this case, the corresponding reciprocal lattice vector of the moiré superlattice satisfies the relation $\boldsymbol{G}_i \cdot \boldsymbol{L}_j = 2\pi\delta_{ij}$, such that:

$$\boldsymbol{G}_1 = \frac{4\pi}{\sqrt{3}L}\left(\frac{\sqrt{3}}{2}, -\frac{1}{2}\right), \ \boldsymbol{G}_2 = \frac{4\pi}{\sqrt{3}L}(0,1). \tag{S5.2}$$

Both the lattice vectors and the corresponding reciprocal lattice vectors of the superlattice of the tBLG are presented in **Figure S10**. **Table S1** reports the parameters used to construct rhombus periodic supercells of different misfit angles that can be duplicated to construct a rectangular periodic supercell.

5.2 Special points for Brillouin zone integration

The calculation of the sum over wave vector $\boldsymbol{q}$ in eq 4 in the main text can be transformed to an integral using the relation $\sum_{\boldsymbol{q}}(\cdots) = \frac{1}{V_b}\int_{\mathrm{BZ}}(\cdots)\,\mathrm{d}\boldsymbol{q}$, where $V_b = (2\pi)^3/V$ is the volume of the Brillouin zone (BZ) and V is volume of the real-space unit-cell. The calculation of integral is usually inefficient since it requires calculating the value of the function over a large set of k points in the first BZ. To calculate such integrations more efficiently, simple k-point meshes can be replaced by a carefully selected set of special points in the BZ, $\boldsymbol{q}_i$,[16-19] over which the function is evaluated. The integral can then be estimated via:

$$I = \frac{1}{V_b}\int_{\mathrm{BZ}} f(\boldsymbol{q})\,\mathrm{d}\boldsymbol{q} \approx \frac{1}{N}\sum_i w_i f(\boldsymbol{q}_i), \tag{S5.3}$$

where w_i is the weight of the i^{th} data point, and $N = \sum_i w_i$ normalizes the weighting factors to unity. The set of selected $\{\boldsymbol{q}_i\}$ forms a grid in the irreducible Brillouin zone (IBZ), as is illustrated by the red points in **Figure S10**b. The coordinates of these points for a hexagonal lattice are presented in Eq. (S5.4).

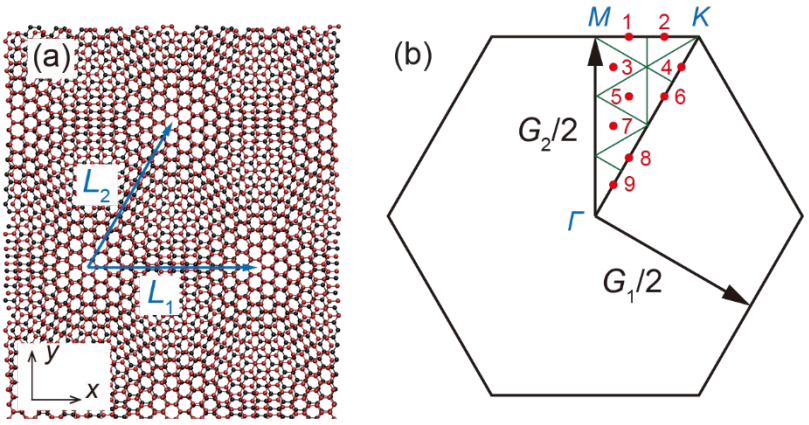

Figure S10. (a) Twisted bilayer graphene of misfit angle θ = 5.09°. $\boldsymbol{L}_1$ and $\boldsymbol{L}_2$ are the superlattice vectors. (b) The corresponding first Brillouin zone of (a). $\boldsymbol{G}_1$ and $\boldsymbol{G}_2$ are the reciprocal lattice vectors of the superlattice. The triangle $\Delta\Gamma MK$ represents the irreducible Brillouin zone. Red circles mark the position of the special points used to evaluate the integral over the first Brillouin zone.

$$\begin{cases} \boldsymbol{q}_1 = \left(\frac{1}{9}, \frac{t}{3}\right), \boldsymbol{q}_2 = \left(\frac{2}{9}, \frac{t}{3}\right), \boldsymbol{q}_3 = \left(\frac{1}{18}, \frac{5t}{18}\right) \\ \boldsymbol{q}_4 = \left(\frac{5}{18}, \frac{5t}{18}\right), \boldsymbol{q}_5 = \left(\frac{1}{9}, \frac{2t}{9}\right), \boldsymbol{q}_6 = \left(\frac{2}{9}, \frac{2t}{9}\right). \\ \boldsymbol{q}_7 = \left(\frac{1}{18}, \frac{3t}{18}\right), \boldsymbol{q}_8 = \left(\frac{1}{9}, \frac{t}{9}\right), \boldsymbol{q}_9 = \left(\frac{1}{18}, \frac{t}{18}\right) \end{cases} \quad \text{(S5.4)}$$

Here, $t = \sqrt{3}$ and the units of the coordinates are $2\pi/L$. The weighting factors $\{w_i\}$ are [16]:

$$w_{1,2,4,6,8,9} = \frac{1}{12}, w_{3,5,7} = \frac{1}{6}, \quad \text{(S5.5)}$$

Using Eqs. (S5.3)-(S5.5), eq 4 in the main text can be evaluated as follows:

$$\Gamma_{\text{tot}} = \frac{\pi\hbar^3}{2} \sum_{k=1}^{9} w_k \sum_{\lambda} \frac{e^{-\beta E_{\boldsymbol{q_k}\lambda}}}{Z} \frac{\rho\left(E_{\boldsymbol{q_k}\lambda}\right) \left| V_{\lambda,\lambda+\frac{3r}{2}}(\boldsymbol{q_k}) \right|^2}{E^2_{\boldsymbol{q_k}\lambda}}. \quad \text{(S5.6)}$$

This equation was used to calculate the transition rate presented in Figure 3 of the main text.

6 Temperature dependence of interfacial thermal conductivity

In the main text, the target temperatures of the Langevin thermostats for the bottom and middle layers of graphene and *h*-BN were set to 225 K and 375 K, respectively. After reaching the steady-state, the average temperature of the system was found to be ~300 K. To check the effect of average temperature on our results, we calculated the cross-plane thermal conductivity (κ_{CP}) and the corresponding interfacial thermal resistance (ITR) at a different temperature gradient (325 K – 475 K), resulting the average steady-state temperature of ~400 K. The protocol described in Section 1 above was used to perform these calculations, as well. Both ILP and Lennard-Jones (LJ) potential were tested for graphite whereas for the bulk *h*-BN simulations only the ILP was used. The results for graphite and bulk *h*-BN are illustrated in **Figure S11** and **Figure S12**, respectively. For the ILP we find that the overall values of κ_{CP} (ITR) decrease (increase) slightly with increasing average temperature. The LJ potential calculations, as well, exhibit very week dependence on average temperature within the range studied. Altogether, the thickness dependences of both quantities remain mostly insensitive to the average temperature.

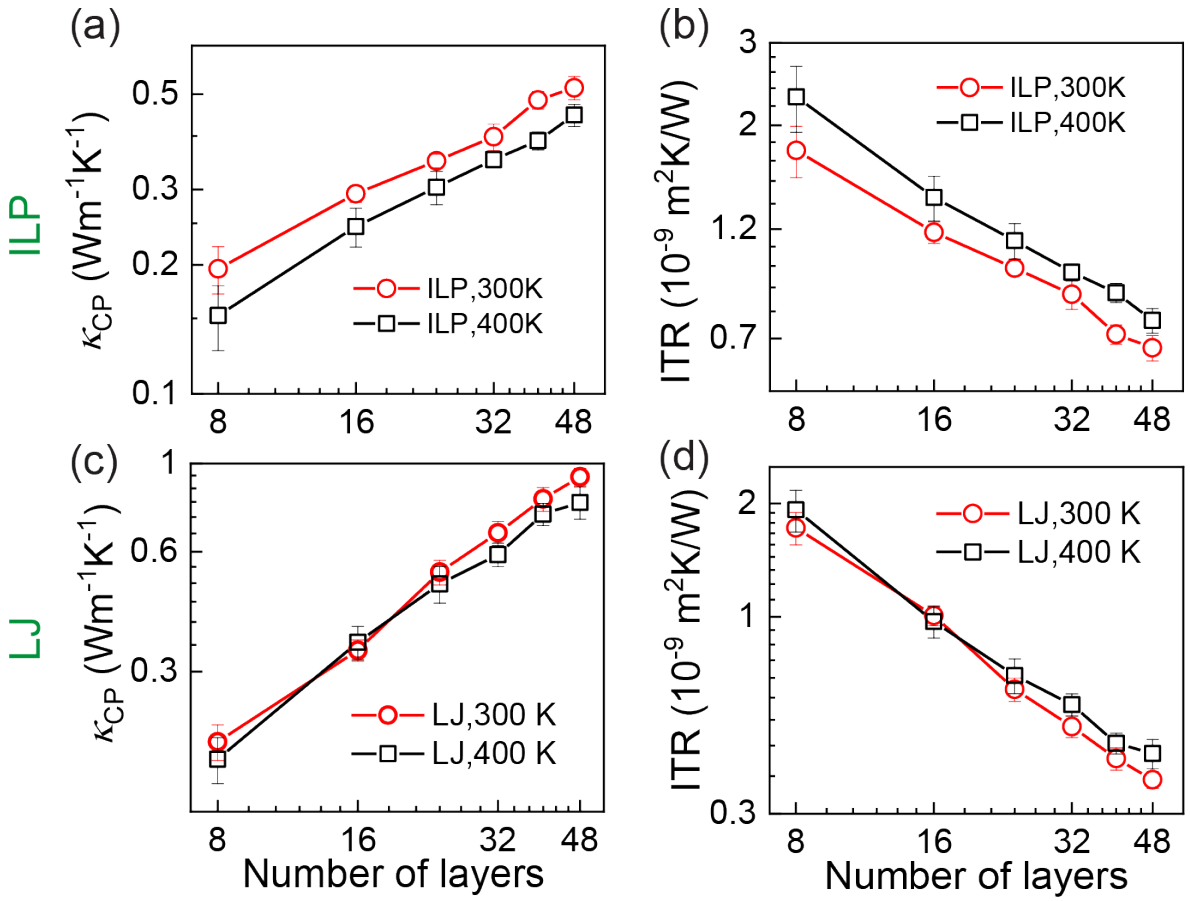

Figure S11. Thickness dependence of κ_{CP} (a, c) and ITR (b, d) for Bernal-stacked graphite at average steady-state temperatures of 300 K (red circles) and 400 K (black squares). The left and right columns correspond to the κ_{CP} and ITR calculated with ILP (top panels) and LJ potential (bottom panels), respectively.

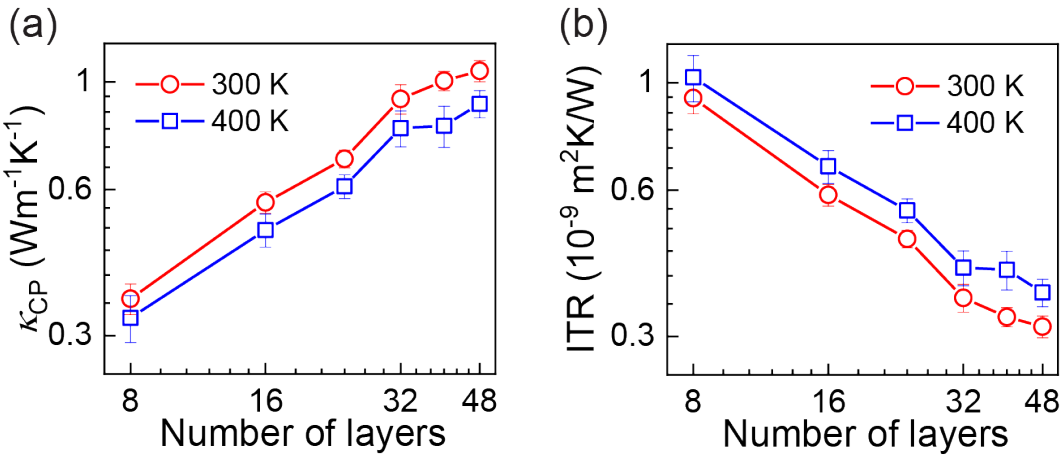

Figure S12. Thickness dependence of κ_{CP} (a) and ITR (b) for AA'-stacked *h*-BN at average temperatures of 300 K (red circles) and 400 K (blue squares).

7 Derivation of Fermi's golden rule

7.1 Basic theory for phonons

7.1.1 Basic notations

Let us consider a 3D crystal with a total of $N = N_1N_2N_3$ unit cells and periodic boundary conditions. To be specific, let $\boldsymbol{a}_i, i = 1,2,3$ be the lattice vectors that define the unit cell. We index unit cells with $\boldsymbol{n}$ = (n_1,n_2,n_3) where each n_i = 1,2, ···, N_i, and their locations are $\boldsymbol{R}_n = \sum_{i=1}^{3} n_i\boldsymbol{a}_i$. Assume that there are r atoms in each unit cell, which are indexed with $s = 1, \cdots, r$. The mass and the equilibrium distance of the s^{th} atom are notated as M_s and $\boldsymbol{R}_s^0$, respectively. Then the location of the s^{th} atom in the $\boldsymbol{n}^{\text{th}}$ unit cell at time t can be expressed as:

$$\boldsymbol{r}_{ns}(t) = \boldsymbol{R}_n + \boldsymbol{R}_s^0 + \boldsymbol{u}_{ns}(t), \tag{S7.1}$$

where $\boldsymbol{u}_{ns}(t)$ is its displacement from its equilibrium position.

The Lagrangian for this classical problem can be written as

$$\mathcal{L} = \sum_{n=1}^{N}\sum_{s=1}^{r}\frac{M_s|\dot{\boldsymbol{r}}_{ns}|^2(t)}{2} - V, \tag{S7.2}$$

where the second term is the sum of interactions between all pairs of atoms.

Under the harmonic approximation, i.e., expanding the total potential energy V around the equilibrium positions, The Lagrangian can be simplified as

$$\mathcal{L} = \sum_{n=1}^{N}\sum_{s=1}^{r}\frac{M_s|\dot{\boldsymbol{u}}_{ns}|^2(t)}{2} - \frac{1}{2}\sum_{n,n'}\sum_{s,s'}\sum_{\alpha\alpha'}\phi_{\alpha\alpha'}\begin{pmatrix}n,n'\\s,s'\end{pmatrix}u_{ns\alpha}u_{n's'\alpha'}, \tag{S7.3}$$

where $u_{ns\alpha}, \alpha = 1,2,3$ are the Cartesian coordinates of the displacement $\boldsymbol{u}_{ns}(t)$ and

$$\phi_{\alpha\alpha'}\begin{pmatrix}n,n'\\s,s'\end{pmatrix} = \frac{\partial^2 V}{\partial r_{ns\alpha}r_{n's'\alpha'}}\bigg|_{\text{eq}} = \phi_{\alpha'\alpha}\begin{pmatrix}n',n\\s',s\end{pmatrix} = \phi_{\alpha\alpha'}\begin{pmatrix}n-n'\\s,\ s'\end{pmatrix}. \tag{S7.4}$$

Note that the first order term vanishes because we are expanding around the equilibrium positions. $\phi_{\alpha\alpha'}\begin{pmatrix}n,n'\\s,s'\end{pmatrix}$ represents the component of the force acted on the s^{th} atom in the n^{th} unit cell along α direction when the atom s' in the unit cell n' moves a unit displacement along α' direction. The symmetries of $\phi_{\alpha\alpha'}\begin{pmatrix}n,n'\\s,s'\end{pmatrix}$ appearing in Eq. (S7.4) arise from the intechangability of the second derivative and the translational invariance of the interactions.

7.1.2 Dynamical matrix

The equation of motion of the s^{th} atom in the n^{th} unit cell can be derived using the Euler–Lagrange equation as follows:

$$M_s\ddot{u}_{ns\alpha} = -\sum_{n's'\alpha'}\phi_{\alpha\alpha'}\begin{pmatrix}n-n'\\s,\ s'\end{pmatrix}u_{n's'\alpha'}, \tag{S7.5}$$

If we displace all atoms equally, i.e. shifting $u_{n's'\alpha'}$ to $u_{n's'\alpha'} + \delta$, the total force on the s^{th} atom in

the n^{th} unit cell does not change. From the above equation we have

$$\sum_{n'\alpha'} \phi_{\alpha\alpha'} \binom{n-n'}{s,\ s'} = 0, \tag{S7.6}$$

We are looking for normal modes (because any general solution can be written as a linear combination of them); these are solutions where all atoms oscillate with the same frequency. Moreover, because of the lattice structure, we expect solutions to reflect this periodicity. So we guess solutions of the form

$$\tilde{u}_{ns\alpha}(t) = \frac{1}{\sqrt{M_s}} e_{s\alpha} e^{i(\boldsymbol{q}\cdot\boldsymbol{R}_n - \omega t)}, \tag{S7.7}$$

where $e_{s\alpha}$ are real-space solutions that will be determined later and $\boldsymbol{q}$ is the wave-vector in reciprocal space. Substituting Eq. (S7.7) into Eq. (S7.5), we can get

$$\omega^2 e_{s\alpha}(\boldsymbol{q}) = \sum_{s'\alpha'} D_{s\alpha}^{s'\alpha'}(\boldsymbol{q}) e_{s'\alpha'}(\boldsymbol{q}), \tag{S7.8}$$

where

$$D_{s\alpha}^{s'\alpha'}(\boldsymbol{q}) = \sum_{n'} \frac{1}{\sqrt{M_s M_{s'}}} \phi_{\alpha\alpha'} \binom{n-n'}{s,\ s'} e^{-i\boldsymbol{q}\cdot(\boldsymbol{R}_n - \boldsymbol{R}_{n'})} = \sum_{l} \frac{1}{\sqrt{M_s M_{s'}}} \phi_{\alpha\alpha'} \binom{l}{s,\ s'} e^{-i\boldsymbol{q}\cdot\boldsymbol{R}_l}, \tag{S7.9}$$

is called dynamical matrix (dimension $3r \times 3r$). Note that we have defined the relative cell distance vector $\boldsymbol{R}_l \equiv \boldsymbol{R}_n - \boldsymbol{R}_{n'}$ and number index, $l \equiv n - n'$, where the infinite sum over n' can be replaced by the sum over l for any value of the index n. Note that dynamical matrix is Hermitian symmetric (i.e., $\left[D_{s\alpha}^{s'\alpha'}(\boldsymbol{q})\right]^* = D_{s'\alpha'}^{s\alpha}(-\boldsymbol{q})$) because ϕ is symmetric, so all the eigenvalues of Eq. (S7.8) ($\omega_\lambda(\boldsymbol{q}), \lambda = 1,2\cdots,3r$) are real for each $\boldsymbol{q}$ in the Brillouin zone (BZ), which is determined by

$$\det\left|\omega_\lambda^2(\boldsymbol{q})\delta_{s\alpha}\delta_{s'\alpha'} - D_{s\alpha}^{s'\alpha'}(\boldsymbol{q})\right| = 0. \tag{S7.10}$$

Taking the conjugate of this equation, we have

$$0 = \det\left|\left[\omega_\lambda^2(\boldsymbol{q})\right]^*\delta_{s\alpha}\delta_{s'\alpha'} - \left[D_{s\alpha}^{s'\alpha'}(\boldsymbol{q})\right]^*\right| = \det\left|\omega_\lambda^2(\boldsymbol{q})\delta_{s\alpha}\delta_{s'\alpha'} - D_{s\alpha}^{s'\alpha'}(-\boldsymbol{q})\right|, \tag{S7.11}$$

while replacing $\boldsymbol{q}$ by $-\boldsymbol{q}$ in Eq. (S7.10), we have $\det\left|\omega_\lambda^2(-\boldsymbol{q})\delta_{s\alpha}\delta_{s'\alpha'} - D_{s\alpha}^{s'\alpha'}(-\boldsymbol{q})\right| = 0$.

It's clear that $\omega_\lambda^2(\boldsymbol{q})$ and $\omega_\lambda^2(-\boldsymbol{q})$ obey the same equation, thus we have:

$$\omega_\lambda(-\boldsymbol{q}) = \omega_\lambda(\boldsymbol{q}). \tag{S7.12}$$

The corresponding eigenvectors are orthonormal:

$$\sum_{s\alpha}\left(e_{s\alpha}^\lambda\right)^* e_{s\alpha}^{\lambda'} = \delta_{\lambda\lambda'}. \tag{S7.13}$$

The complex conjugate of Eq. (S7.8) gives

$$\omega^2 e_{s\alpha}^*(\boldsymbol{q}) = \sum_{s'\alpha'}\left[D_{s\alpha}^{s'\alpha'}(\boldsymbol{q})\right]^* e_{s'\alpha'}^*(\boldsymbol{q}) = \sum_{s'\alpha'} D_{s'\alpha'}^{s\alpha}(-\boldsymbol{q}) e_{s'\alpha'}^*(\boldsymbol{q}), \tag{S7.14}$$

While replacing $\boldsymbol{q}$ by $-\boldsymbol{q}$ in Eq. (S7.8) we get the following equation:

$$\omega^2 e_{s\alpha}(-\boldsymbol{q}) = \sum_{s'\alpha'} D_{s\alpha}^{s'\alpha'}(-\boldsymbol{q}) e_{s'\alpha'}(-\boldsymbol{q}), \tag{S7.15}$$

From Eq. (S7.14) and Eq. (S7.15), we see that eigenvectors $\left[e_{s\alpha}^\lambda(-\boldsymbol{q})\right]^*$ and $e_{s\alpha}^\lambda(\boldsymbol{q})$ obey the same

eigenvalue equation. Since the eigenvectors are normalized, we get the following property:

$$\left[e_{s\alpha}^{\lambda}(-\boldsymbol{q})\right]^{*} = e_{s\alpha}^{\lambda}(\boldsymbol{q}). \tag{S7.16}$$

7.2 Second quantization

The general solution is a linear combination of all these normal modes, thus we have

$$u_{ns\alpha}(t) = \sum_{\boldsymbol{q}\lambda} \frac{C_{\lambda}(\boldsymbol{q})}{\sqrt{NM_s}} \left[e_{s\alpha}^{\lambda}(\boldsymbol{q}) e^{-i\omega_{q\lambda}t}\right] e^{i\boldsymbol{q}\cdot\boldsymbol{R}_n} = \sum_{\boldsymbol{q}\lambda} \frac{Q_{\lambda}(\boldsymbol{q},t)}{\sqrt{NM_s}} e_{s\alpha}^{\lambda}(\boldsymbol{q}) e^{i\boldsymbol{q}\cdot\boldsymbol{R}_n}, \tag{S7.17}$$

where the we define the normal coordinates as $Q_{\lambda}(\boldsymbol{q},t) \equiv C_{\lambda}(\boldsymbol{q}) e^{-i\omega_{\lambda}(\boldsymbol{q})t}$ in the eigenvectors representation. To ensure that the displacements $u_{ns\alpha}(t)$ are real (namely, $u_{ns\alpha}^{*}(t) = u_{ns\alpha}(t)$), the following relation on $Q_{\lambda}(\boldsymbol{q},t)$ and $e_{s\alpha}^{\lambda}$ is enforced:

$$\left[Q_{\lambda}(\boldsymbol{q},t) e_{s\alpha}^{\lambda}(\boldsymbol{q})\right]^{*} = Q_{\lambda}(-\boldsymbol{q},t) e_{s\alpha}^{\lambda}(-\boldsymbol{q}), \tag{S7.18}$$

where we used the fact that the sum over $\boldsymbol{q}$ runs symmetrically over both negative and positive values. Using Eq. (S7.16), we have

$$[Q_{\lambda}(\boldsymbol{q},t)]^{*} = Q_{\lambda}(-\boldsymbol{q},t), \tag{S7.19}$$

7.2.1 Kinetic energy term

Using Eq. (S7.17), the kinetic energy of the system can be expressed as

$$T = \frac{1}{2}\sum_{ns\alpha} M_s \dot{u}_{ns\alpha}^{2}(t) = \frac{1}{2}\sum_{s\alpha} \frac{M_s}{NM_s} \sum_{\boldsymbol{q}\lambda}\sum_{\boldsymbol{q}'\lambda'} \left[\dot{Q}_{\lambda}(\boldsymbol{q},t)\dot{Q}_{\lambda'}(\boldsymbol{q}',t)\right]\left[e_{s\alpha}^{\lambda}(\boldsymbol{q}) e_{s\alpha}^{\lambda'}(\boldsymbol{q}')\right] \sum_n e^{i(\boldsymbol{q}+\boldsymbol{q}')\cdot\boldsymbol{R}_n} =$$

$$\frac{1}{2}\sum_{s\alpha}\sum_{\boldsymbol{q}\boldsymbol{q}'\lambda'} \left[\dot{Q}_{\lambda}(\boldsymbol{q},t)\dot{Q}_{\lambda'}(-\boldsymbol{q},t)\right]\left[e_{s\alpha}^{\lambda}(\boldsymbol{q}) e_{s\alpha}^{\lambda'}(-\boldsymbol{q})\right] =$$

$$\frac{1}{2}\sum_{\boldsymbol{q}\lambda\lambda'} \left[\dot{Q}_{\lambda}(\boldsymbol{q},t)\dot{Q}_{\lambda'}^{*}(\boldsymbol{q},t)\right] \sum_{s\alpha} \left\{e_{s\alpha}^{\lambda}(\boldsymbol{q})\left[e_{s\alpha}^{\lambda'}(\boldsymbol{q})\right]^{*}\right\} = \frac{1}{2}\sum_{\boldsymbol{q}\lambda} \left[\dot{Q}_{\lambda}(\boldsymbol{q},t)\dot{Q}_{\lambda}^{*}(\boldsymbol{q},t)\right] =$$

$$\frac{1}{2}\sum_{\boldsymbol{q}\lambda} \left[\dot{Q}_{\lambda}(\boldsymbol{q},t)\dot{Q}_{\lambda}(-\boldsymbol{q},t)\right],$$

i.e.,

$$T = \frac{1}{2}\sum_{\boldsymbol{q}\lambda} \left[\dot{Q}_{\lambda}(\boldsymbol{q},t)\dot{Q}_{\lambda}(-\boldsymbol{q},t)\right], \tag{S7.20}$$

To derive Eq. (S7.20), we used Eqs. (S7.13) and (S7.16), as well as the following equations:

$$\frac{1}{N}\sum_n e^{i(\boldsymbol{q}+\boldsymbol{q}')\cdot\boldsymbol{R}_n} = \delta_{\boldsymbol{q}+\boldsymbol{q}',\boldsymbol{0}}, \tag{S7.21}$$

7.2.2 Potential energy term

Similarity, the potential energy can be rewritten in terms of the normal coordinates as follows:

$$
\begin{aligned}
U &= \frac{1}{2}\sum_{n,n'}\sum_{s,s'}\sum_{\alpha\alpha'}\phi_{ns\alpha}^{n's'\alpha'}u_{ns\alpha}u_{n's'\alpha'} = \frac{1}{2}\sum_{s,s'}\sum_{\alpha\alpha'}\sum_{nn'}\phi_{\alpha\alpha'}\binom{n-n'}{s,s'}\frac{e^{i(\boldsymbol{q}\cdot\boldsymbol{R}_n+\boldsymbol{q}'\cdot\boldsymbol{R}_{n'})}}{N\sqrt{M_sM_s'}}\sum_{\boldsymbol{q}\lambda}\sum_{\boldsymbol{q}'\lambda'}[Q_\lambda(\boldsymbol{q},t)Q_{\lambda'}(\boldsymbol{q}',t)]\left[e_{s\alpha}^{\lambda}(\boldsymbol{q})e_{s'\alpha'}^{\lambda'}(\boldsymbol{q}')\right] \\
&= \frac{1}{2}\sum_{s,s'}\sum_{\alpha\alpha'}\sum_{nl}\phi_{\alpha\alpha'}\binom{l}{s,s'}\frac{e^{i(\boldsymbol{q}+\boldsymbol{q}')\cdot\boldsymbol{R}_n}e^{-i\boldsymbol{q}'\cdot\boldsymbol{R}_l}}{N\sqrt{M_sM_s'}}\sum_{\boldsymbol{q}\lambda}\sum_{\boldsymbol{q}'\lambda'}[Q_\lambda(\boldsymbol{q},t)Q_{\lambda'}(\boldsymbol{q}',t)]\left[e_{s\alpha}^{\lambda}(\boldsymbol{q})e_{s'\alpha'}^{\lambda'}(\boldsymbol{q}')\right] \\
&= \frac{1}{2}\sum_{s,s'}\sum_{\alpha\alpha'}\sum_{l}\phi_{\alpha\alpha'}\binom{l}{s,s'}\frac{e^{-i\boldsymbol{q}'\cdot\boldsymbol{R}_l}}{\sqrt{M_sM_s'}}\sum_{\boldsymbol{q}\lambda}\sum_{\boldsymbol{q}'\lambda'}[Q_\lambda(\boldsymbol{q},t)Q_{\lambda'}(\boldsymbol{q}',t)]\left[e_{s\alpha}^{\lambda}(\boldsymbol{q})e_{s'\alpha'}^{\lambda'}(\boldsymbol{q}')\right]\underbrace{\sum_{n}\frac{1}{N}e^{i(\boldsymbol{q}+\boldsymbol{q}')\cdot\boldsymbol{R}_n}}_{=\delta_{q+q'=0}} \\
&= \frac{1}{2}\sum_{s,s'}\sum_{\alpha\alpha'}\sum_{l}\phi_{\alpha\alpha'}\binom{l}{s,s'}\frac{e^{i\boldsymbol{q}\boldsymbol{R}_l}}{\sqrt{M_sM_s'}}\sum_{\boldsymbol{q}\lambda\lambda'}[Q_\lambda(\boldsymbol{q},t)Q_{\lambda'}(-\boldsymbol{q},t)]\left[e_{s\alpha}^{\lambda}(\boldsymbol{q})e_{s'\alpha'}^{\lambda'}(-\boldsymbol{q})\right] \\
&= \frac{1}{2}\sum_{\boldsymbol{q}\lambda\lambda'}[Q_\lambda(\boldsymbol{q},t)Q_{\lambda'}(-\boldsymbol{q},t)]\sum_{s\alpha}e_{s\alpha}^{\lambda}(\boldsymbol{q})\sum_{s'\alpha'}\left[D_{s\alpha}^{s'\alpha'}(-\boldsymbol{q})e_{s'\alpha'}^{\lambda'}(-\boldsymbol{q})\right] \\
&= \frac{1}{2}\sum_{\boldsymbol{q}\lambda\lambda'}[Q_\lambda(\boldsymbol{q},t)Q_{\lambda'}(-\boldsymbol{q},t)]\sum_{s\alpha}e_{s\alpha}^{\lambda}(\boldsymbol{q})\,\omega_\lambda^2(-\boldsymbol{q})e_{s\alpha}^{\lambda'}(-\boldsymbol{q}) \\
&= \frac{1}{2}\sum_{\boldsymbol{q}\lambda\lambda'}[Q_\lambda(\boldsymbol{q},t)Q_{\lambda'}(-\boldsymbol{q},t)]\omega_\lambda^2(\boldsymbol{q})\delta_{\lambda\lambda'} = \frac{1}{2}\sum_{\boldsymbol{q}\lambda}\omega_\lambda^2(\boldsymbol{q})Q_\lambda(\boldsymbol{q},t)Q_\lambda(-\boldsymbol{q},t)
\end{aligned}
$$

i.e.,

$$U = \frac{1}{2}\sum_{\boldsymbol{q}\lambda}\omega_\lambda^2(\boldsymbol{q})Q_\lambda(\boldsymbol{q},t)Q_\lambda(-\boldsymbol{q},t), \tag{S7.22}$$

where in above deriviation, the orthogonality of its eigenvectores and the symmetry of its eigenvalues are used. Thus the Lagrangian reads as:

$$\mathcal{L} = T - V = \frac{1}{2}\sum_{\boldsymbol{q}\lambda}\left[\dot{Q}_\lambda(-\boldsymbol{q},t)\dot{Q}_\lambda(\boldsymbol{q},t) - \omega_\lambda^2(\boldsymbol{q})Q_\lambda(-\boldsymbol{q},t)Q_\lambda(\boldsymbol{q},t)\right], \tag{S7.23}$$

Using the relation $P_\lambda(\boldsymbol{q},t) = \partial\mathcal{L}/\,\partial\dot{Q}_\lambda(\boldsymbol{q},t)$, the Hamiltonian of the system then can be written as:

$$H = T + V = \frac{1}{2}\sum_{\boldsymbol{q}\lambda}[P_\lambda(-\boldsymbol{q},t)P_\lambda(\boldsymbol{q},t) + \omega_\lambda^2(\boldsymbol{q})Q_\lambda(-\boldsymbol{q},t)Q_\lambda(\boldsymbol{q},t)], \tag{S7.24}$$

Now, we quantize H by asking the momenta and coordinates to be operators:

$$\hat{H} = \frac{1}{2}\sum_{\boldsymbol{q}\lambda}\left[\hat{P}_{-\boldsymbol{q}\lambda}\hat{P}_{\boldsymbol{q}\lambda} + \omega_{\boldsymbol{q}\lambda}^2\hat{Q}_{-\boldsymbol{q}\lambda}\hat{Q}_{\boldsymbol{q}\lambda}\right], \tag{S7.25}$$

here $\hat{P}_{\boldsymbol{q}\lambda}$ and $\hat{Q}_{\boldsymbol{q}\lambda}$ obey the following commutation relations:

$$\begin{cases} \left[\hat{Q}_{\boldsymbol{q}\lambda},\hat{P}_{\boldsymbol{q}'\lambda'}\right] = i\hbar\delta_{\boldsymbol{q}\boldsymbol{q}'}\delta_{\lambda\lambda'} \\ \left[\hat{Q}_{\boldsymbol{q}\lambda},\hat{Q}_{\boldsymbol{q}'\lambda'}\right] = 0,\ \left[\hat{P}_{\boldsymbol{q}\lambda},\hat{P}_{\boldsymbol{q}'\lambda'}\right] = 0 \end{cases}. \tag{S7.26}$$

Similar to the case of ordinary quantum harmonic oscillators, it is convenient to define ladder operators for each mode as follows:

$$\hat{Q}_{\boldsymbol{q}\lambda} = \sqrt{\frac{\hbar}{2\omega_{\boldsymbol{q}\lambda}}}\left(\hat{b}_{\boldsymbol{q}\lambda} + \hat{b}_{-\boldsymbol{q}\lambda}^\dagger\right), \hat{P}_{\boldsymbol{q}\lambda} = i\sqrt{\frac{\hbar\omega_{\boldsymbol{q}\lambda}}{2}}\left(\hat{b}_{\boldsymbol{q}\lambda}^\dagger - \hat{b}_{-\boldsymbol{q}\lambda}\right), \tag{S7.27}$$

where $\hat{b}_{\boldsymbol{q}\lambda}^\dagger$ and $\hat{b}_{\boldsymbol{q}\lambda}$ are Bosonic creation and annihilation operators for phonons with momentum $\boldsymbol{q}$, branch index λ, and frequency $\omega_{\boldsymbol{q}\lambda}$, which obeys the Bosonic commutation relation:

$$\begin{cases} \left[\hat{b}_{\boldsymbol{q}\lambda}, \hat{b}^{\dagger}_{\boldsymbol{q}'\lambda'}\right] = \delta_{\boldsymbol{q}\boldsymbol{q}'}\delta_{\lambda\lambda'} \\ \left[\hat{b}_{\boldsymbol{q}\lambda}, \hat{b}_{\boldsymbol{q}'\lambda'}\right] = \hat{0},\ \left[\hat{b}^{\dagger}_{\boldsymbol{q}\lambda}, \hat{b}^{\dagger}_{\boldsymbol{q}'\lambda'}\right] = \hat{0} \end{cases}. \tag{S7.28}$$

Substituting Eqs. (S7.27) into (S7.25) and using the properties Eq. (S7.26) and (S7.28), we have

$$\begin{aligned} H &= \frac{1}{2}\sum_{\boldsymbol{q}\lambda}\left[\hat{P}_{-\boldsymbol{q}\lambda}\hat{P}_{\boldsymbol{q}\lambda} + \omega^2_{\boldsymbol{q}\lambda}\hat{Q}_{-\boldsymbol{q}\lambda}\hat{Q}_{\boldsymbol{q}\lambda}\right] \\ &= \frac{1}{2}\sum_{\boldsymbol{q}\lambda}\left[-\frac{\hbar\omega_{\boldsymbol{q}\lambda}}{2}\left(\hat{b}^{\dagger}_{-\boldsymbol{q}\lambda} - \hat{b}_{\boldsymbol{q}\lambda}\right)\left(\hat{b}^{\dagger}_{\boldsymbol{q}\lambda} - \hat{b}_{-\boldsymbol{q}\lambda}\right) + \omega^2_{\boldsymbol{q}\lambda}\frac{\hbar}{2\omega_{\boldsymbol{q}\lambda}}\left(\hat{b}_{-\boldsymbol{q}\lambda} + \hat{b}^{\dagger}_{\boldsymbol{q}\lambda}\right)\left(\hat{b}_{\boldsymbol{q}\lambda} + \hat{b}^{\dagger}_{-\boldsymbol{q}\lambda}\right)\right] \\ &= \frac{\hbar}{4}\sum_{\boldsymbol{q}\lambda}\omega_{\boldsymbol{q}\lambda}\left[-\left(\hat{b}^{\dagger}_{-\boldsymbol{q}\lambda}\hat{b}^{\dagger}_{\boldsymbol{q}\lambda} - \hat{b}^{\dagger}_{-\boldsymbol{q}\lambda}\hat{b}_{-\boldsymbol{q}\lambda} - \hat{b}_{\boldsymbol{q}\lambda}\hat{b}^{\dagger}_{\boldsymbol{q}\lambda} + \hat{b}_{\boldsymbol{q}\lambda}\hat{b}_{-\boldsymbol{q}\lambda}\right)\right. \\ &\left. + \left(\hat{b}_{-\boldsymbol{q}\lambda}\hat{b}_{\boldsymbol{q}\lambda} + \hat{b}_{-\boldsymbol{q}\lambda}\hat{b}^{\dagger}_{-\boldsymbol{q}\lambda} + \hat{b}^{\dagger}_{\boldsymbol{q}\lambda}\hat{b}_{\boldsymbol{q}\lambda} + \hat{b}^{\dagger}_{\boldsymbol{q}\lambda}\hat{b}^{\dagger}_{-\boldsymbol{q}\lambda}\right)\right] \\ &= \frac{\hbar}{4}\sum_{\boldsymbol{q}\lambda}\omega_{\boldsymbol{q}\lambda}\left[\left(\hat{b}^{\dagger}_{-\boldsymbol{q}\lambda}\hat{b}_{-\boldsymbol{q}\lambda} + \hat{b}_{-\boldsymbol{q}\lambda}\hat{b}^{\dagger}_{-\boldsymbol{q}\lambda}\right) + \left(\hat{b}_{\boldsymbol{q}\lambda}\hat{b}^{\dagger}_{\boldsymbol{q}\lambda} + \hat{b}^{\dagger}_{\boldsymbol{q}\lambda}\hat{b}_{\boldsymbol{q}\lambda}\right)\right] \\ &= \frac{\hbar}{4}\sum_{\boldsymbol{q}\lambda}\omega_{\boldsymbol{q}\lambda}\left[\left(2\hat{b}^{\dagger}_{-\boldsymbol{q}\lambda}\hat{b}_{-\boldsymbol{q}\lambda} + 1\right) + \left(2\hat{b}^{\dagger}_{\boldsymbol{q}\lambda}\hat{b}_{\boldsymbol{q}\lambda} + 1\right)\right] = \sum_{\boldsymbol{q}\lambda}\hbar\omega_{\boldsymbol{q}\lambda}\left(\hat{b}^{\dagger}_{\boldsymbol{q}\lambda}\hat{b}_{\boldsymbol{q}\lambda} + \frac{1}{2}\right) \end{aligned}$$

Therefore, we finally get the quantized representation of non-interacting phonons:

$$H = \sum_{\boldsymbol{q}\lambda}\hbar\omega_{\boldsymbol{q}\lambda}\left(\hat{b}^{\dagger}_{\boldsymbol{q}\lambda}\hat{b}_{\boldsymbol{q}\lambda} + \tfrac{1}{2}\right). \tag{S7.29}$$

The operator of atom displacements (Eq. 1.14) is expressed in terms of the phonon operators by:

$$\hat{u}_{ns\alpha} = \sum_{\boldsymbol{q}\lambda}\sqrt{\frac{\hbar}{2NM_s\omega_{\boldsymbol{q}\lambda}}}\,e^{\lambda}_{s\alpha}e^{i\boldsymbol{q}\cdot\boldsymbol{R}_n}\left(\hat{b}_{\boldsymbol{q}\lambda} + \hat{b}^{\dagger}_{-\boldsymbol{q}\lambda}\right). \tag{S7.30}$$

These equations will be used below.

7.3 Inter-phonon coupling within harmonic approximation

7.3.1 Hamiltonian with inter-phonon coupling

In this section, we consider systems that consist of two (or more) covalently bonded units that are weakly coupled between them. Unlike previous studies that considered phonon-phonon couplings resulting from anharmonicity effects,[20] here all phonon mode considered are Harmonic and the couplings arise from the division of the entire system into subunits. The Hamiltonian of the whole system can be written as:

$$H = H_1 + H_2 + H_{12}, \tag{S7.31}$$

To derive the expressions of H_1, H_2 and H_{12} in Eq. (S7.31), we consider the Hamiltonian of the whole system written as the function of the atomic displacements:

$$H = T + V = \sum_{ns\alpha}\frac{M_s\dot{u}^2_{ns\alpha}(t)}{2} + \frac{1}{2}\sum_{n,n'}\sum_{s,s'}\sum_{\alpha\alpha'}\phi_{\alpha\alpha'}\binom{n-n'}{s,\ s'}u_{ns\alpha}u_{n's'\alpha'}, \tag{S7.32}$$

Let's assume that subsystem I and II contain atoms with indeices ranging from $s = 1,2,\cdots,r/2$ and $s = \frac{r}{2}+1, \frac{r}{2}+2, \cdots, r$, respectively. Then the kinetic energy term in Eq. (S7.32) can be rewritten as:

$$T = \sum_{n\alpha}\left[\sum_{s=1}^{r/2}\frac{M_s\dot{u}_{nsa}^2(t)}{2} + \sum_{s=\frac{r}{2}+1}^{r}\frac{M_s\dot{u}_{nsa}^2(t)}{2}\right]. \tag{S7.33}$$

While the potential energy term is:

$$V = \frac{1}{2}\sum_{n,n'}\sum_{\alpha,\alpha'}\left\{\sum_{s,s'=1}^{r/2}\phi_{\alpha\alpha'}\binom{n-n'}{s,\ s'}u_{nsa}u_{n's'\alpha'} + \sum_{s,s'=r/2+1}^{r}\phi_{\alpha\alpha'}\binom{n-n'}{s,\ s'}u_{nsa}u_{n's'\alpha'} + \sum_{s=1}^{r/2}\sum_{s'=r/2+1}^{r}\phi_{\alpha\alpha'}\binom{n-n'}{s,\ s'}u_{nsa}u_{n's'\alpha'} + \sum_{s=r/2+1}^{r}\sum_{s'=1}^{r/2}\phi_{\alpha\alpha'}\binom{n-n'}{s,\ s'}u_{nsa}u_{n's'\alpha'}\right\} = V_{11}+V_{22}+V_{12}+V_{21}$$

Or equivalently,

$$\begin{cases} V_{11} = \frac{1}{2}\sum_{n,n'}\sum_{\alpha,\alpha'}\sum_{s,s'=1}^{\frac{r}{2}}\phi_{\alpha\alpha'}\binom{n-n'}{s,\ s'}u_{nsa}u_{n's'\alpha'} \\ V_{22} = \frac{1}{2}\sum_{n,n'}\sum_{\alpha,\alpha'}\sum_{s,s'=r/2+1}^{r}\phi_{\alpha\alpha'}\binom{n-n'}{s,\ s'}u_{nsa}u_{n's'\alpha'} \\ V_{12} = \frac{1}{2}\sum_{n,n'}\sum_{\alpha,\alpha'}\sum_{s=1}^{r/2}\sum_{s'=r/2+1}^{r}\phi_{\alpha\alpha'}\binom{n-n'}{s,\ s'}u_{nsa}u_{n's'\alpha'} \\ V_{21} = \frac{1}{2}\sum_{n,n'}\sum_{\alpha,\alpha'}\sum_{s=r/2+1}^{r}\sum_{s'=1}^{r/2}\phi_{\alpha\alpha'}\binom{n-n'}{s,\ s'}u_{nsa}u_{n's'\alpha'} \end{cases}, \tag{S7.34}$$

7.3.2 Second quantization

We may now quantize this Hamiltonian and write it in the basis of the eigenstates of the coupled subunits. In second quantization, the atomic displacement operators of the two subunits are given in the following form:

$$\hat{u}_{nsa} = \begin{cases} \sum_{\boldsymbol{q}\lambda}\sqrt{\frac{\hbar}{2NM_s\omega_{\boldsymbol{q}\lambda}}}e_{sa}^{\lambda}e^{i\boldsymbol{q}\cdot\boldsymbol{R}_n}\left(\hat{a}_{\boldsymbol{q}\lambda}+\hat{a}_{-\boldsymbol{q}\lambda}^{\dagger}\right), & s\in\left[1,\frac{r}{2}\right] \\ \sum_{\boldsymbol{q}'\lambda'}\sqrt{\frac{\hbar}{2NM_s\tilde{\omega}_{\boldsymbol{q}'\lambda'}}}\tilde{e}_{sa}^{\lambda'}e^{i\boldsymbol{q}'\cdot\boldsymbol{R}_n}\left(\hat{\tilde{a}}_{\ \boldsymbol{q}'\lambda'}+\hat{\tilde{a}}_{-\boldsymbol{q}'\lambda'}^{\dagger}\right), & s\in\left[\frac{r}{2}+1,r\right] \end{cases}. \tag{S7.35}$$

Here, we use different notations for the creation and annihilation operators ($\hat{a}_{\boldsymbol{q}\lambda}, \hat{a}_{-\boldsymbol{q}\lambda}^{\dagger}$ and $\hat{\tilde{a}}_{\boldsymbol{q}\lambda}, \tilde{\hat{a}}_{-\boldsymbol{q}\lambda}^{\dagger}$), eigenvalues ($\omega_{\boldsymbol{q}\lambda}, \tilde{\omega}_{\boldsymbol{q}\lambda}$) and eigenvectors ($e_{sa}^{\lambda}, \tilde{e}_{sa}^{\lambda}$) for the two subunits. Note that e_{sa}^{λ} and $\tilde{e}_{sa}^{\lambda}$ are of the dimensions of the whole system, however their non-zero elements appear only on the relevant subunits such that they obey the following relations: $\sum_{sa}\left(e_{sa}^{\lambda}\right)^{*}e_{sa}^{\lambda'} = \delta_{\lambda\lambda'}$; $\sum_{sa}\left(\tilde{e}_{sa}^{\lambda}\right)^{*}\tilde{e}_{sa}^{\lambda'} = \delta_{\lambda\lambda'}$; $\sum_{sa}\left(\tilde{e}_{sa}^{\lambda}\right)^{*}e_{sa}^{\lambda'} = \sum_{sa}\left(e_{sa}^{\lambda}\right)^{*}\tilde{e}_{sa}^{\lambda'} = 0$. Defining the normal coordinates of the two subunits as:

$$\hat{Q}_{\boldsymbol{q}\lambda} \equiv \sqrt{\frac{\hbar}{2\omega_{\boldsymbol{q}\lambda}}}\left(\hat{a}_{\boldsymbol{q}\lambda}+\hat{a}_{-\boldsymbol{q}\lambda}^{\dagger}\right) \ ; \ \hat{\tilde{Q}}_{\boldsymbol{q}\lambda} \equiv \sqrt{\frac{\hbar}{2\tilde{\omega}_{\boldsymbol{q}\lambda}}}\left(\hat{\tilde{a}}_{\boldsymbol{q}\lambda}+\hat{\tilde{a}}_{-\boldsymbol{q}\lambda}^{\dagger}\right), \tag{S7.36}$$

and the corresponding momenta operators as:

$$\hat{P}_{\boldsymbol{q}\lambda} = i\sqrt{\frac{\hbar\omega_{\boldsymbol{q}\lambda}}{2}}\left(\hat{a}_{\boldsymbol{q}\lambda}^{\dagger}-\hat{a}_{-\boldsymbol{q}\lambda}\right) \ ; \ \hat{\tilde{P}}_{\boldsymbol{q}\lambda} = i\sqrt{\frac{\hbar\tilde{\omega}_{\boldsymbol{q}\lambda}}{2}}\left(\hat{\tilde{a}}_{\boldsymbol{q}\lambda}^{\dagger}-\hat{\tilde{a}}_{-\boldsymbol{q}\lambda}\right), \tag{S7.37}$$

Eq. (S7.35) reads:

$$\hat{u}_{ns\alpha} = \begin{cases} \sum_{\boldsymbol{q}\lambda} \frac{e^{\lambda}_{s\alpha}(\boldsymbol{q})}{\sqrt{NM_s}} e^{i\boldsymbol{q}\cdot\boldsymbol{R}_n} \hat{Q}_{\boldsymbol{q}\lambda}\,, & s \in \left[1, \frac{r}{2}\right] \\ \sum_{\boldsymbol{q}\lambda} \frac{\tilde{e}^{\lambda}_{s\alpha}(\boldsymbol{q})}{\sqrt{NM_s}} e^{i\boldsymbol{q}\cdot\boldsymbol{R}_n} \hat{\tilde{Q}}_{\boldsymbol{q}\lambda}\,, & s \in \left[\frac{r}{2}+1, r\right] \end{cases}, \tag{S7.38}$$

The second quantized kinetic energy operator is then written as:

$$\hat{T} = \hat{T}_1 + \hat{T}_2 = \frac{1}{2}\sum_{\boldsymbol{q}\lambda} \hat{P}_{\boldsymbol{q}\lambda}\hat{P}_{-\boldsymbol{q}\lambda} + \frac{1}{2}\sum_{\boldsymbol{q}'\lambda'} \hat{\tilde{P}}_{\boldsymbol{q}'\lambda'}\hat{\tilde{P}}_{-\boldsymbol{q}'\lambda'}, \tag{S7.39}$$

Correspondingly, the various potential energy terms are obtained by substituting Eq. (S7.38) in Eq. (S7.34):

$$\begin{aligned}
\hat{V}_{11} &= \frac{1}{2}\sum_{\alpha,\alpha'}\sum_{s,s'=1}^{\frac{r}{2}}\sum_{n,n'} \phi_{\alpha\alpha'}\binom{n-n'}{s,\ s'} \sum_{\boldsymbol{q}\lambda,\boldsymbol{q}'\lambda'} \frac{e^{\lambda}_{s\alpha}(\boldsymbol{q}) e^{\lambda'}_{s'\alpha'}(\boldsymbol{q}')}{\sqrt{M_s M_{s'}}} \frac{1}{N} e^{i\boldsymbol{q}\cdot\boldsymbol{R}_n + i\boldsymbol{q}'\cdot\boldsymbol{R}_{n'}} \hat{Q}_{\boldsymbol{q}\lambda}\hat{Q}_{\boldsymbol{q}'\lambda'} \\
&= \frac{1}{2}\sum_{\alpha,\alpha'}\sum_{s,s'=1}^{\frac{r}{2}}\sum_{\boldsymbol{q}\boldsymbol{q}'\lambda,\lambda'} \hat{Q}_{\boldsymbol{q}\lambda}\hat{Q}_{\boldsymbol{q}'\lambda'}\, e^{\lambda}_{s\alpha}(\boldsymbol{q}) e^{\lambda'}_{s'\alpha'}(\boldsymbol{q}') \sum_{n'} \frac{1}{N} e^{i(\boldsymbol{q}+\boldsymbol{q}')\boldsymbol{R}_{n'}} \sum_{n} \phi_{\alpha\alpha'}\binom{n-n'}{s,\ s'} \frac{e^{i\boldsymbol{q}\cdot(\boldsymbol{R}_n - \boldsymbol{R}_{n'})}}{\sqrt{M_s M_{s'}}} \\
&= \frac{1}{2}\sum_{\alpha,\alpha'}\sum_{s,s'=1}^{\frac{r}{2}}\sum_{\boldsymbol{q}\boldsymbol{q}'\lambda,\lambda'} \hat{Q}_{\boldsymbol{q}\lambda}\hat{Q}_{\boldsymbol{q}'\lambda'}\, e^{\lambda}_{s\alpha}(\boldsymbol{q}) e^{\lambda'}_{s'\alpha'}(\boldsymbol{q}') \left[\sum_{l} \phi_{\alpha\alpha'}\binom{l}{s,\ s'} \frac{e^{i\boldsymbol{q}\cdot\boldsymbol{R}_l}}{\sqrt{M_s M_{s'}}}\right] \left[\sum_{n'} \frac{1}{N} e^{i(\boldsymbol{q}+\boldsymbol{q}')\cdot\boldsymbol{R}_{n'}}\right] \\
&= \frac{1}{2}\sum_{\alpha,\alpha'}\sum_{s,s'=1}^{\frac{r}{2}}\sum_{\boldsymbol{q}\lambda,\lambda'} \hat{Q}_{\boldsymbol{q}\lambda}\hat{Q}_{-\boldsymbol{q}\lambda'}\, e^{\lambda}_{s\alpha}(\boldsymbol{q}) e^{\lambda'}_{s'\alpha'}(-\boldsymbol{q}) \sum_{l} \phi_{\alpha\alpha'}\binom{l}{s,\ s'} \frac{e^{i\boldsymbol{q}\cdot\boldsymbol{R}_l}}{\sqrt{M_s M_{s'}}} \\
&= \frac{1}{2}\sum_{\alpha}\sum_{s=1}^{\frac{r}{2}}\sum_{\boldsymbol{q}\lambda,\lambda'} \hat{Q}_{\boldsymbol{q}\lambda}\hat{Q}_{-\boldsymbol{q}\lambda'}\, e^{\lambda}_{s\alpha}(\boldsymbol{q}) \sum_{s'=1}^{\frac{r}{2}}\sum_{\alpha'} D^{s'\alpha'}_{s\alpha}(-\boldsymbol{q}) e^{\lambda'}_{s'\alpha'}(-\boldsymbol{q}) \\
&= \frac{1}{2}\sum_{\boldsymbol{q}\lambda,\lambda'} \omega^2_{\boldsymbol{q}\lambda'} \hat{Q}_{\boldsymbol{q}\lambda}\hat{Q}_{-\boldsymbol{q}\lambda'} \sum_{\alpha}\sum_{s=1}^{\frac{r}{2}} e^{\lambda}_{s\alpha}(\boldsymbol{q}) \left[e^{\lambda'}_{s\alpha}(\boldsymbol{q})\right]^* = \frac{1}{2}\sum_{\boldsymbol{q}\lambda} \omega^2_{\boldsymbol{q}\lambda} \hat{Q}_{\boldsymbol{q}\lambda}\hat{Q}_{-\boldsymbol{q}\lambda'}
\end{aligned}$$

i.e.,

$$\hat{V}_{11} = \frac{1}{2}\sum_{\boldsymbol{q}\lambda} \omega^2_{\boldsymbol{q}\lambda} \hat{Q}_{\boldsymbol{q}\lambda}\hat{Q}_{-\boldsymbol{q}\lambda'}, \tag{S7.40}$$

Going from the second line to the third line we used the fact that the sum over n' runs between $\pm\infty$ and the summand depends only on the difference between n and n', hence the sum is independent of the value of the index n. Therefore, we can replace the sum over n' by a sum over $l \equiv n - n'$ amd define $\boldsymbol{R}_l \equiv \boldsymbol{R}_n - \boldsymbol{R}_{n'}$. Following the same procedure, we can get the corresponding expressions for the second diagonal term:

$$\hat{V}_{22} = \frac{1}{2}\sum_{\boldsymbol{q}\lambda} \tilde{\omega}^2_{\boldsymbol{q}\lambda} \hat{\tilde{Q}}_{\boldsymbol{q}\lambda}\hat{\tilde{Q}}_{-\boldsymbol{q}\lambda}, \tag{S7.41}$$

Similarly, for the off-diagonal terms we get:

$$\hat{V}_{12} = \frac{1}{2}\sum_{\alpha,\alpha'}\sum_{s=1}^{\frac{r}{2}}\sum_{s'=\frac{r}{2}+1}^{r}\sum_{n,n'}\phi_{\alpha\alpha'}\binom{n-n'}{s,\ s'}\sum_{\boldsymbol{q}\lambda,\boldsymbol{q}'\lambda'}\frac{e^{\lambda}_{s\alpha}(\boldsymbol{q})\tilde{e}^{\lambda'}_{s'\alpha'}(\boldsymbol{q}')}{\sqrt{M_s M_{s'}}}\frac{1}{N}e^{i\boldsymbol{q}\cdot\boldsymbol{R}_n+i\boldsymbol{q}'\cdot\boldsymbol{R}_{n'}}\hat{Q}_{\boldsymbol{q}\lambda}\hat{\tilde{Q}}_{\boldsymbol{q}'\lambda'}$$

$$= \frac{1}{2}\sum_{\alpha,\alpha'}\sum_{s=1}^{\frac{r}{2}}\sum_{s'=\frac{r}{2}+1}^{r}\sum_{\boldsymbol{q}\boldsymbol{q}'\lambda,\lambda'}\hat{Q}_{\boldsymbol{q}\lambda}\hat{\tilde{Q}}_{\boldsymbol{q}'\lambda'}\,e^{\lambda}_{s\alpha}(\boldsymbol{q})\tilde{e}^{\lambda'}_{s'\alpha'}(\boldsymbol{q}')\sum_{n'}\frac{1}{N}e^{i(\boldsymbol{q}+\boldsymbol{q}')\cdot\boldsymbol{R}_{n'}}\sum_{n}\phi_{\alpha\alpha'}\binom{n-n'}{s,\ s'}\frac{e^{i\boldsymbol{q}\cdot(\boldsymbol{R}_n-\boldsymbol{R}_{n'})}}{\sqrt{M_s M_{s'}}}$$

$$= \frac{1}{2}\sum_{\alpha,\alpha'}\sum_{s=1}^{\frac{r}{2}}\sum_{s'=\frac{r}{2}+1}^{r}\sum_{\boldsymbol{q}\boldsymbol{q}'\lambda,\lambda'}\hat{Q}_{\boldsymbol{q}\lambda}\hat{\tilde{Q}}_{\boldsymbol{q}'\lambda'}\,e^{\lambda}_{s\alpha}(\boldsymbol{q})\tilde{e}^{\lambda'}_{s'\alpha'}(\boldsymbol{q}')\left[\sum_{l}\phi_{\alpha\alpha'}\binom{l}{s,\ s'}\frac{e^{i\boldsymbol{q}\cdot\boldsymbol{R}_l}}{\sqrt{M_s M_{s'}}}\right]\left[\sum_{n'}\frac{1}{N}e^{i(\boldsymbol{q}+\boldsymbol{q}')\cdot\boldsymbol{R}_{n'}}\right]$$

$$= \frac{1}{2}\sum_{\alpha,\alpha'}\sum_{s=1}^{\frac{r}{2}}\sum_{s'=\frac{r}{2}+1}^{r}\sum_{\boldsymbol{q},\lambda,\lambda'}\hat{Q}_{\boldsymbol{q}\lambda}\hat{\tilde{Q}}_{-\boldsymbol{q}\lambda'}\,e^{\lambda}_{s\alpha}(\boldsymbol{q})\tilde{e}^{\lambda'}_{s'\alpha'}(-\boldsymbol{q})\sum_{l}\phi_{\alpha\alpha'}\binom{l}{s,\ s'}\frac{e^{i\boldsymbol{q}\cdot\boldsymbol{R}_l}}{\sqrt{M_s M_{s'}}}$$

$$= \frac{1}{2}\sum_{\boldsymbol{q}}\sum_{\lambda=1}^{3r/2}\sum_{\lambda'=\frac{3r}{2}+1}^{3r}\hat{Q}_{\boldsymbol{q}\lambda}\hat{\tilde{Q}}^{\dagger}_{\boldsymbol{q}\lambda'}\left[\sum_{\alpha\alpha'}\sum_{s=1}^{\frac{r}{2}}\sum_{s'=\frac{r}{2}+1}^{r}\left(\tilde{e}^{\lambda'}_{s'\alpha'}(\boldsymbol{q})\right)^{*}\sum_{l}\phi_{\alpha\alpha'}\binom{l}{s,\ s'}\frac{e^{i\boldsymbol{q}\cdot\boldsymbol{R}_l}}{\sqrt{M_s M_{s'}}}e^{\lambda}_{s\alpha}(\boldsymbol{q})\right]$$

$$= \frac{1}{2}\sum_{\boldsymbol{q}}\sum_{\lambda=1}^{3r/2}\sum_{\lambda'=\frac{3r}{2}+1}^{3r}V_{\lambda\lambda'}(\boldsymbol{q})\hat{Q}_{\boldsymbol{q}\lambda}\hat{\tilde{Q}}^{\dagger}_{\boldsymbol{q}\lambda'}$$

Where we have defined:

$$V_{\lambda\lambda'}(\boldsymbol{q}) \equiv \sum_{\alpha\alpha'}\sum_{s=1}^{\frac{r}{2}}\sum_{s'=\frac{r}{2}+1}^{r}\left(\tilde{e}^{\lambda'}_{s'\alpha'}(\boldsymbol{q})\right)^{*}V^{s'\alpha'}_{s\alpha}(\boldsymbol{q})e^{\lambda}_{s\alpha}(\boldsymbol{q}), \tag{S7.42}$$

where

$$V^{s'\alpha'}_{s\alpha}(\boldsymbol{q}) \equiv \sum_{l}\frac{e^{i\boldsymbol{q}\cdot\boldsymbol{R}_l}}{\sqrt{M_s M_{s'}}}\phi_{\alpha\alpha'}\binom{l}{s,\ s'}. \tag{S7.43}$$

It's easy to show that $V_{\lambda\lambda'}(\boldsymbol{q})$ has the following property:

$$V^{*}_{\lambda\lambda'}(\boldsymbol{q}) = V_{\lambda\lambda'}(-\boldsymbol{q}). \tag{S7.44}$$

Following the same procedure, we have:

$$\hat{V}_{21}=\frac{1}{2}\sum_{\alpha,\alpha'}\sum_{s'=1}^{\frac{r}{2}}\sum_{s=\frac{r}{2}+1}^{r}\sum_{n,n'}\phi_{\alpha\alpha'}\binom{n-n'}{s,\ s'}\sum_{\boldsymbol{q}\lambda,\boldsymbol{q}'\lambda'}\frac{\tilde{e}_{s\alpha}^{\lambda}(\boldsymbol{q})e_{s'\alpha'}^{\lambda'}(\boldsymbol{q}')}{\sqrt{M_sM_{s'}}}\frac{1}{N}e^{i\boldsymbol{q}\cdot\boldsymbol{R}_n+i\boldsymbol{q}'\cdot\boldsymbol{R}_{n'}}\hat{\tilde{Q}}_{\boldsymbol{q}\lambda}\hat{Q}_{\boldsymbol{q}'\lambda'}$$

$$=\frac{1}{2}\sum_{\alpha'\alpha}\sum_{s=1}^{\frac{r}{2}}\sum_{s'=\frac{r}{2}+1}^{r}\sum_{n',n}\phi_{\alpha'\alpha}\binom{n'-n}{s',s}\sum_{\boldsymbol{q}'\lambda',\boldsymbol{q}\lambda}\frac{\tilde{e}_{s'\alpha'}^{\lambda'}(\boldsymbol{q}')e_{s\alpha}^{\lambda}(\boldsymbol{q})}{\sqrt{M_{s'}M_s}}\frac{1}{N}e^{i\boldsymbol{q}'\cdot\boldsymbol{R}_{n'}+i\boldsymbol{q}\cdot\boldsymbol{R}_n}\hat{\tilde{Q}}_{\boldsymbol{q}'\lambda'}\hat{Q}_{\boldsymbol{q}\lambda}$$

$$=\frac{1}{2}\sum_{\alpha,\alpha'}\sum_{s=1}^{\frac{r}{2}}\sum_{s'=\frac{r}{2}+1}^{r}\sum_{\boldsymbol{q}\boldsymbol{q}'\lambda,\lambda'}\hat{\tilde{Q}}_{\boldsymbol{q}'\lambda'}\hat{Q}_{\boldsymbol{q}\lambda}\,\tilde{e}_{s'\alpha'}^{\lambda'}(\boldsymbol{q}')e_{s\alpha}^{\lambda}(\boldsymbol{q})\sum_{n'}\frac{1}{N}e^{i(\boldsymbol{q}+\boldsymbol{q}')\cdot\boldsymbol{R}_{n'}}\sum_{n}\phi_{\alpha\alpha'}\binom{n-n'}{s,s'}\frac{e^{i\boldsymbol{q}\cdot(\boldsymbol{R}_n-\boldsymbol{R}_{n'})}}{\sqrt{M_sM_{s'}}}$$

$$=\frac{1}{2}\sum_{\alpha,\alpha'}\sum_{s=1}^{\frac{r}{2}}\sum_{s'=\frac{r}{2}+1}^{r}\sum_{\boldsymbol{q}\boldsymbol{q}'\lambda,\lambda'}\hat{\tilde{Q}}_{\boldsymbol{q}'\lambda'}\hat{Q}_{\boldsymbol{q}\lambda}\,\tilde{e}_{s'\alpha'}^{\lambda'}(\boldsymbol{q}')e_{s\alpha}^{\lambda}(\boldsymbol{q})\left[\sum_{l}\phi_{\alpha\alpha'}\binom{l}{s,s'}\frac{e^{i\boldsymbol{q}\cdot\boldsymbol{R}_l}}{\sqrt{M_sM_{s'}}}\right]\left[\sum_{n'}\frac{1}{N}e^{i(\boldsymbol{q}+\boldsymbol{q}')\cdot\boldsymbol{R}_{n'}}\right]$$

$$=\frac{1}{2}\sum_{\alpha,\alpha'}\sum_{s=1}^{\frac{r}{2}}\sum_{s'=\frac{r}{2}+1}^{r}\sum_{\boldsymbol{q}'\lambda,\lambda'}\hat{\tilde{Q}}_{\boldsymbol{q}'\lambda'}\hat{Q}_{-\boldsymbol{q}'\lambda}\tilde{e}_{s'\alpha'}^{\lambda'}(\boldsymbol{q}')e_{s\alpha}^{\lambda}(-\boldsymbol{q}')\sum_{l}\phi_{\alpha\alpha'}\binom{l}{s,s'}\frac{e^{-i\boldsymbol{q}'\cdot\boldsymbol{R}_l}}{\sqrt{M_sM_{s'}}}$$

$$=\frac{1}{2}\sum_{\boldsymbol{q}'}\sum_{\lambda=1}^{3r/2}\sum_{\lambda'=\frac{3r}{2}+1}^{3r}\hat{\tilde{Q}}_{\boldsymbol{q}'\lambda'}\hat{Q}_{\boldsymbol{q}'\lambda}^{\dagger}\left[\sum_{\alpha\alpha'}\sum_{s=1}^{\frac{r}{2}}\sum_{s'=\frac{r}{2}+1}^{r}\left(e_{s\alpha}^{\lambda}(\boldsymbol{q}')\right)^{*}\sum_{l}\phi_{\alpha\alpha'}\binom{l}{s,s'}\frac{e^{-i\boldsymbol{q}'\cdot\boldsymbol{R}_l}}{\sqrt{M_sM_{s'}}}\tilde{e}_{s'\alpha'}^{\lambda'}(\boldsymbol{q}')\right]$$

$$=\frac{1}{2}\sum_{\boldsymbol{q}}\sum_{\lambda=1}^{3r/2}\sum_{\lambda'=\frac{3r}{2}+1}^{3r}\hat{\tilde{Q}}_{\boldsymbol{q}\lambda'}\hat{Q}_{\boldsymbol{q}\lambda}^{\dagger}\left[\sum_{\alpha\alpha'}\sum_{s=1}^{\frac{r}{2}}\sum_{s'=\frac{r}{2}+1}^{r}\left(e_{s\alpha}^{\lambda}(\boldsymbol{q})\right)^{*}\sum_{l}\phi_{\alpha\alpha'}\binom{l}{s,\ s'}\frac{e^{-i\boldsymbol{q}\cdot\boldsymbol{R}_l}}{\sqrt{M_sM_{s'}}}\tilde{e}_{s'\alpha'}^{\lambda'}(\boldsymbol{q})\right]$$

$$=\frac{1}{2}\sum_{\boldsymbol{q}}\sum_{\lambda=1}^{3r/2}\sum_{\lambda'=\frac{3r}{2}+1}^{3r}\left(\hat{Q}_{\boldsymbol{q}\lambda}\hat{\tilde{Q}}_{\boldsymbol{q}\lambda'}^{\dagger}\right)^{\dagger}\left[\sum_{\alpha\alpha'}\sum_{s=1}^{\frac{r}{2}}\sum_{s'=\frac{r}{2}+1}^{r}\left(\tilde{e}_{s'\alpha'}^{\lambda'}(\boldsymbol{q})\right)^{*}\sum_{l}\phi_{\alpha\alpha'}\binom{l}{s,\ s'}\frac{e^{i\boldsymbol{q}\cdot\boldsymbol{R}_l}}{\sqrt{M_sM_{s'}}}e_{s\alpha}^{\lambda}(\boldsymbol{q})\right]^{*}$$

$$=\left\{\frac{1}{2}\sum_{\boldsymbol{q}}\sum_{\lambda=1}^{\frac{3r}{2}}\sum_{\lambda'=\frac{3r}{2}+1}^{3r}V_{\lambda\lambda'}(\boldsymbol{q})\hat{Q}_{\boldsymbol{q}\lambda}\hat{\tilde{Q}}_{\boldsymbol{q}\lambda'}^{\dagger}\right\}^{\dagger}=V_{12}^{\dagger}$$

Define:

$$\begin{cases}\hat{H}_1=\hat{T}_{11}+\hat{V}_{11}\\ \hat{H}_2=\hat{T}_{22}+\hat{V}_{22}\\ \hat{H}_{12}=\hat{V}_{12}+\hat{V}_{21}\end{cases},\tag{S7.45}$$

we finally get the expressions of $\hat{H}_1$, $\hat{H}_2$ and $\hat{H}_{12}$ in Eq. (S7.31) as follows:

$$\begin{cases}\hat{H}_1=\sum_{\boldsymbol{q}}\sum_{\lambda=1}^{3r/2}\hbar\omega_{\boldsymbol{q}\lambda}\left(\hat{a}_{\boldsymbol{q}\lambda}^{\dagger}\hat{a}_{\boldsymbol{q}\lambda}+\frac{1}{2}\right)\\ \hat{H}_2=\sum_{\boldsymbol{q}}\sum_{\lambda'=1+\frac{3r}{2}}^{3r}\hbar\tilde{\omega}_{\boldsymbol{q}\lambda'}\left(\hat{\tilde{a}}_{\boldsymbol{q}\lambda'}^{\dagger}\hat{\tilde{a}}_{\boldsymbol{q}\lambda'}+\frac{1}{2}\right)\\ \hat{H}_{12}=\frac{1}{2}\sum_{\boldsymbol{q}}\left\{\sum_{\lambda=1}^{3r/2}\sum_{\lambda'=\frac{3r}{2}+1}^{3r}V_{\lambda\lambda'}(\boldsymbol{q})\hat{Q}_{\boldsymbol{q}\lambda}\hat{\tilde{Q}}_{\boldsymbol{q}\lambda'}^{\dagger}+\text{h. c.}\right\}\end{cases}.\tag{S7.46}$$

Here h.c. means the Hermitian conjugate. Since the indices of $\hat{a}_{\boldsymbol{q}\lambda}$, $\hat{\tilde{a}}_{\boldsymbol{q}\lambda'}$ and $\hat{Q}_{\boldsymbol{q}\lambda}$, $\hat{\tilde{Q}}_{\boldsymbol{q}\lambda'}$ belong to the two system sections, we can define an abbreviated notation $\hat{a}_{\boldsymbol{q}\lambda}$ and $\hat{Q}_{\boldsymbol{q}\lambda}$ using the index λ to identify which subsystem they belong to. In this case, the Hamiltonian of the coupled system can be

simplified as follows:

$$\widehat{H} = \widehat{H}_0 + \widehat{H}_C, \tag{S7.47}$$

where

$$\begin{cases} \widehat{H}_0 = \sum_{\boldsymbol{q}} \sum_{\lambda=1}^{3r} \hbar\omega_{\boldsymbol{q}\lambda} \left(\hat{a}_{\boldsymbol{q}\lambda}^{\dagger}\hat{a}_{\boldsymbol{q}\lambda} + \frac{1}{2}\right) \\ \widehat{H}_C = \frac{1}{2}\sum_{\boldsymbol{q}} \left\{ \sum_{\lambda=1}^{3r/2} \sum_{\lambda'=\frac{3r}{2}+1}^{3r} V_{\lambda\lambda'}(\boldsymbol{q}) \hat{Q}_{\boldsymbol{q}\lambda} \hat{Q}_{\boldsymbol{q}\lambda'}^{\dagger} + h.c. \right\} \end{cases}. \tag{S7.48}$$

7.4 Basic theory of many-body physics

7.4.1 Dynamics of the ladder operators

In order to describe the dynamics of the ladder operators appearing in the Hamiltonian of Eq. (S7.47) we express them in the Heisenberg picture as follows:

$$\hat{a}_p(\tau) = e^{\frac{i}{\hbar}\widehat{H}t} \hat{a}_p e^{-\frac{i}{\hbar}\widehat{H}t} = e^{\frac{\widehat{H}\tau}{\hbar}} \hat{a}_p e^{-\frac{\widehat{H}\tau}{\hbar}}, \tag{S7.49}$$

where we define the imaginary time $\tau \equiv it$ and introduce the notation $\boldsymbol{p} \equiv (\boldsymbol{q}, \lambda)$ and $\overline{\boldsymbol{p}} \equiv (-\boldsymbol{q}, \lambda)$. The corresponding equation of motion for the ladder operators is given by:

$$\hbar \frac{\partial \hat{a}_{\boldsymbol{p}}(\tau)}{\partial \tau} = \left[\widehat{H}, \hat{a}_{\boldsymbol{p}}(\tau)\right]. \tag{S7.50}$$

For the uncoupled system ($\widehat{H}_C = \hat{0}$) this gives:

$$\hbar \frac{\partial \hat{a}_{\boldsymbol{p}}(\tau)}{\partial \tau} = \left[\widehat{H}_0, \hat{a}_{\boldsymbol{p}}(\tau)\right] = \left[\widehat{H}_0, e^{\frac{\widehat{H}_0\tau}{\hbar}} \hat{a}_{\boldsymbol{p}} e^{-\frac{\widehat{H}_0\tau}{\hbar}}\right] = \widehat{H}_0 e^{\frac{\widehat{H}_0\tau}{\hbar}} \hat{a}_{\boldsymbol{p}} e^{-\frac{\widehat{H}_0\tau}{\hbar}} - e^{\frac{\widehat{H}_0\tau}{\hbar}} \hat{a}_{\boldsymbol{p}} e^{-\frac{\widehat{H}_0\tau}{\hbar}} \widehat{H}_0$$

$$= e^{\frac{\widehat{H}_0\tau}{\hbar}} \left(\widehat{H}_0 \hat{a}_{\boldsymbol{p}} - \hat{a}_{\boldsymbol{p}} \widehat{H}_0\right) e^{-\frac{\widehat{H}_0\tau}{\hbar}} = e^{\frac{\widehat{H}_0\tau}{\hbar}} \left[\widehat{H}_0, \hat{a}_{\boldsymbol{p}}\right] e^{-\frac{\widehat{H}_0\tau}{\hbar}}$$

i.e.,

$$\hbar \frac{\partial \hat{a}_{\boldsymbol{p}}(\tau)}{\partial \tau} = e^{\frac{\widehat{H}_0\tau}{\hbar}} \left[\widehat{H}_0, \hat{a}_{\boldsymbol{p}}\right] e^{-\frac{\widehat{H}_0\tau}{\hbar}}. \tag{S7.51}$$

The commutator on the right-hand-side of Eq. (S7.51) can be evaluated as follows:

$$\left[\widehat{H}_0, \hat{a}_{\boldsymbol{p}'}\right] = \left[\sum_{\boldsymbol{p}} \hbar\omega_{\boldsymbol{p}} \left(\hat{a}_{\boldsymbol{p}}^{\dagger}\hat{a}_{\boldsymbol{p}} + \frac{1}{2}\right), \hat{a}_{\boldsymbol{p}'}\right] = \sum_{\boldsymbol{p}} \hbar\omega_{\boldsymbol{p}} \left[\hat{a}_{\boldsymbol{p}}^{\dagger}\hat{a}_{\boldsymbol{p}}, \hat{a}_{\boldsymbol{p}'}\right] = \sum_{\boldsymbol{p}} \hbar\omega_{\boldsymbol{p}} \left(\hat{a}_{\boldsymbol{p}}^{\dagger}\hat{a}_{\boldsymbol{p}}\hat{a}_{\boldsymbol{p}'} - \hat{a}_{\boldsymbol{p}'}\hat{a}_{\boldsymbol{p}}^{\dagger}\hat{a}_{\boldsymbol{p}}\right) =$$

$$\sum_{\boldsymbol{p}} \hbar\omega_{\boldsymbol{p}} \left[\hat{a}_{\boldsymbol{p}}^{\dagger}\hat{a}_{\boldsymbol{p}}\hat{a}_{\boldsymbol{p}'} - \left(\delta_{\boldsymbol{p}'\boldsymbol{p}} + \hat{a}_{\boldsymbol{p}}^{\dagger}\hat{a}_{\boldsymbol{p}'}\right)\hat{a}_{\boldsymbol{p}}\right] = -\hbar\omega_{\boldsymbol{p}'}\hat{a}_{\boldsymbol{p}'} + \sum_{\boldsymbol{p}} \hbar\omega_{\boldsymbol{p}} \left[\hat{a}_{\boldsymbol{p}}^{\dagger}\hat{a}_{\boldsymbol{p}}\hat{a}_{\boldsymbol{p}'} - \hat{a}_{\boldsymbol{p}}^{\dagger}\hat{a}_{\boldsymbol{p}}\hat{a}_{\boldsymbol{p}'}\right] = -\hbar\omega_{\boldsymbol{p}'}\hat{a}_{\boldsymbol{p}'}.$$

i.e.,

$$\left[\widehat{H}_0, \hat{a}_{\boldsymbol{p}'}\right] = -\hbar\omega_{\boldsymbol{p}'}\hat{a}_{\boldsymbol{p}'}. \tag{S7.52}$$

Therefore, we have:

$$\hbar \frac{\partial \hat{a}_{\boldsymbol{p}}(\tau)}{\partial \tau} = e^{\frac{\widehat{H}_0\tau}{\hbar}} \left[\widehat{H}_0, \hat{a}_{\boldsymbol{p}}\right] e^{-\frac{\widehat{H}_0\tau}{\hbar}} = -\hbar\omega_{\boldsymbol{p}} e^{\frac{\widehat{H}_0\tau}{\hbar}} \hat{a}_{\boldsymbol{p}} e^{-\frac{\widehat{H}_0\tau}{\hbar}} = -\hbar\omega_{\boldsymbol{p}} \hat{a}_{\boldsymbol{p}}(\tau). \tag{S7.53}$$

The solution of Eq. (S7.53) is $\hat{a}_{\boldsymbol{p}}(\tau) = \hat{a}_{\boldsymbol{p}}(0) e^{-\omega_{\boldsymbol{p}}\tau} = \hat{a}_{\boldsymbol{p}} e^{-\omega_{\boldsymbol{p}}\tau}$. For $\hat{a}_{\boldsymbol{p}}^{\dagger}(\tau)$ we have

$$\left[\hat{H}_0, \hat{a}_{\boldsymbol{p}'}^{\dagger}(0)\right] = \left[\hat{H}_0, \hat{a}_{\boldsymbol{p}'}^{\dagger}\right] = \left[\sum_{\boldsymbol{p}} \hbar\omega_{\boldsymbol{p}} \left(\hat{a}_{\boldsymbol{p}}^{\dagger}\hat{a}_{\boldsymbol{p}} + \frac{1}{2}\right), \hat{a}_{\boldsymbol{p}'}^{\dagger}\right] = \sum_{\boldsymbol{p}} \hbar\omega_{\boldsymbol{p}}\left[\hat{a}_{\boldsymbol{p}}^{\dagger}\hat{a}_{\boldsymbol{p}}, \hat{a}_{\boldsymbol{p}'}^{\dagger}\right]$$

$$= \sum_{\boldsymbol{p}} \hbar\omega_{\boldsymbol{p}} \left(\hat{a}_{\boldsymbol{p}}^{\dagger}\hat{a}_{\boldsymbol{p}}\hat{a}_{\boldsymbol{p}'}^{\dagger} - \hat{a}_{\boldsymbol{p}'}^{\dagger}\hat{a}_{\boldsymbol{p}}^{\dagger}\hat{a}_{\boldsymbol{p}}\right) = \sum_{\boldsymbol{p}} \hbar\omega_{\boldsymbol{p}} \left[\hat{a}_{\boldsymbol{p}}^{\dagger}\left(\delta_{\boldsymbol{p}\boldsymbol{p}'} + \hat{a}_{\boldsymbol{p}'}^{\dagger}\hat{a}_{\boldsymbol{p}}\right) - \hat{a}_{\boldsymbol{p}'}^{\dagger}\hat{a}_{\boldsymbol{p}}^{\dagger}\hat{a}_{\boldsymbol{p}}\right]$$

$$= \hbar\omega_{\boldsymbol{p}'}\hat{a}_{\boldsymbol{p}'}^{\dagger} + \sum_{\boldsymbol{p}} \hbar\omega_{\boldsymbol{p}} \left[\hat{a}_{\boldsymbol{p}}^{\dagger}\hat{a}_{\boldsymbol{p}'}^{\dagger}\hat{a}_{\boldsymbol{p}} - \hat{a}_{\boldsymbol{p}'}^{\dagger}\hat{a}_{\boldsymbol{p}}^{\dagger}\hat{a}_{\boldsymbol{p}}\right] = \hbar\omega_{\boldsymbol{p}'}\hat{a}_{\boldsymbol{p}'}^{\dagger}$$

In summary, we have

$$\begin{cases} \hat{a}_{\boldsymbol{p}}(\tau) = \hat{a}_{\boldsymbol{p}}(0)e^{-\omega_{\boldsymbol{p}}\tau} = \hat{a}_{\boldsymbol{p}}e^{-\omega_{\boldsymbol{p}}\tau} \\ \hat{a}_{\boldsymbol{p}}^{\dagger}(\tau) = \hat{a}_{\boldsymbol{p}}^{\dagger}(0)e^{\omega_{\boldsymbol{p}}\tau} = \hat{a}_{\boldsymbol{p}}^{\dagger}e^{\omega_{\boldsymbol{p}}\tau} \end{cases}. \tag{S7.54}$$

7.4.2 Green's function

To describe thermal transport properties between different system sections, we use the formalism of thermal (or imaginary time) phonon Green's function.[21] To this end, we define the thermal Green's function for phonons as:

$$\hat{G}_{\boldsymbol{p}\boldsymbol{p}'}(\tau, \tau') = -\langle \hat{T}_{\tau}\hat{a}_{\boldsymbol{p}}(\tau)\hat{a}_{\boldsymbol{p}'}^{\dagger}(\tau')\rangle = -\mathrm{Tr}\left\{\hat{\rho}_H \hat{T}_{\tau}\left[\hat{a}_{\boldsymbol{p}}(\tau)\hat{a}_{\boldsymbol{p}'}^{\dagger}(\tau')\right]\right\}, \tag{S7.55}$$

where $\hat{T}_{\tau}$ is the time ordering operator and $\hat{\rho}_H$ is the statistical operator for the grand canonical ensemble (note that the chemical potential for phonons is zero):

$$\hat{\rho}_H = e^{-\beta\hat{H}}/Z_H. \tag{S7.56}$$

where the partition function is given by $Z_H \equiv \mathrm{Tr}\left(e^{-\beta\hat{H}}\right)$, and $\beta = 1/k_B T$, with k_B being Boltzmann's constant and T the temperature. For time independent Hamiltonians, $G_{\boldsymbol{p}\boldsymbol{p}'}(\tau, \tau')$ depends only on $\tau - \tau'$, i.e.,

$$G_{\boldsymbol{p}\boldsymbol{p}'}(\tau, \tau') = G_{\boldsymbol{p}\boldsymbol{p}'}(\tau - \tau', 0). \tag{S7.57}$$

To show this we shall first assume that $\tau > \tau'$ such that

$$G_{\boldsymbol{p}\boldsymbol{p}'}(\tau, \tau') = -\langle \hat{T}_{\tau}\hat{a}_{\boldsymbol{p}}(\tau)\hat{a}_{\boldsymbol{p}'}^{\dagger}(\tau')\rangle = -\mathrm{Tr}\left\{\hat{\rho}_H \hat{T}_{\tau}\left[\hat{a}_{\boldsymbol{p}}(\tau)\hat{a}_{\boldsymbol{p}'}^{\dagger}(\tau')\right]\right\} = -\mathrm{Tr}\left\{\hat{\rho}_H \hat{a}_{\boldsymbol{p}}(\tau)\hat{a}_{\boldsymbol{p}'}^{\dagger}(\tau')\right\}$$

$$= -\mathrm{Tr}\left\{\hat{\rho}_H e^{\frac{\hat{H}\tau}{\hbar}}\hat{a}_{\boldsymbol{p}}e^{-\frac{\hat{H}\tau}{\hbar}}e^{\frac{\hat{H}\tau'}{\hbar}}\hat{a}_{\boldsymbol{p}'}^{\dagger}e^{-\frac{\hat{H}\tau'}{\hbar}}\right\} = -\mathrm{Tr}\left\{\hat{\rho}_H e^{-\frac{\hat{H}\tau'}{\hbar}}e^{\frac{\hat{H}\tau}{\hbar}}\hat{a}_{\boldsymbol{p}}e^{-\frac{\hat{H}(\tau-\tau')}{\hbar}}\hat{a}_{\boldsymbol{p}'}^{\dagger}\right\}$$

$$= -\mathrm{Tr}\left\{\hat{\rho}_H e^{\frac{\hat{H}(\tau-\tau')}{\hbar}}\hat{a}_{\boldsymbol{p}}e^{-\frac{\hat{H}(\tau-\tau')}{\hbar}}\hat{a}_{\boldsymbol{p}'}^{\dagger}\right\} = -\mathrm{Tr}\left\{\hat{\rho}_H \hat{a}_{\boldsymbol{p}}(\tau-\tau')\hat{a}_{\boldsymbol{p}'}^{\dagger}(0)\right\}$$

$$= -\mathrm{Tr}\left\{\hat{\rho}_H \hat{T}_{\tau}\left[\hat{a}_{\boldsymbol{p}}(\tau-\tau')\hat{a}_{\boldsymbol{p}'}^{\dagger}(0)\right]\right\} = -\langle \hat{T}_{\tau}\hat{a}_{\boldsymbol{p}}(\tau-\tau')\hat{a}_{\boldsymbol{p}'}^{\dagger}(0)\rangle = G_{\boldsymbol{p}\boldsymbol{p}'}(\tau-\tau', 0)$$

Where we have used the commutativity of $\hat{\rho}_H$ and $e^{\pm\frac{\hat{H}\tau'}{\hbar}}$ and the invariance of the trace operation towards cyclic permutations. Similarly, for $\tau < \tau'$ we have:

$$
\begin{aligned}
G_{\boldsymbol{p}\boldsymbol{p}'}(\tau,\tau') &= -\langle \hat{T}_\tau \hat{a}_{\boldsymbol{p}}(\tau)\hat{a}^\dagger_{\boldsymbol{p}'}(\tau')\rangle = -\mathrm{Tr}\left\{\hat{\rho}_H \hat{T}_\tau\left[\hat{a}_{\boldsymbol{p}}(\tau)\hat{a}^\dagger_{\boldsymbol{p}'}(\tau')\right]\right\} = -\mathrm{Tr}\left\{\hat{\rho}_H \hat{a}^\dagger_{\boldsymbol{p}'}(\tau')\hat{a}_{\boldsymbol{p}}(\tau)\right\} \\
&= -\mathrm{Tr}\left\{\hat{\rho}_H e^{\frac{\hat{H}\tau'}{\hbar}}\hat{a}^\dagger_{\boldsymbol{p}'} e^{-\frac{\hat{H}\tau'}{\hbar}} e^{\frac{\hat{H}\tau}{\hbar}}\hat{a}_{\boldsymbol{p}} e^{-\frac{\hat{H}\tau}{\hbar}}\right\} = -\mathrm{Tr}\left\{\hat{\rho}_H \hat{a}^\dagger_{\boldsymbol{p}'} e^{\frac{\hat{H}(\tau-\tau')}{\hbar}}\hat{a}_{\boldsymbol{p}} e^{-\frac{\hat{H}\tau}{\hbar}} e^{\frac{\hat{H}\tau'}{\hbar}}\right\} \\
&= -\mathrm{Tr}\left\{\hat{\rho}_H \hat{a}^\dagger_{\boldsymbol{p}'} e^{\frac{\hat{H}(\tau-\tau')}{\hbar}}\hat{a}_{\boldsymbol{p}} e^{-\frac{\hat{H}(\tau-\tau')}{\hbar}}\right\} = -\mathrm{Tr}\left\{\hat{\rho}_H \hat{a}^\dagger_{\boldsymbol{p}'}(0)\hat{a}_{\boldsymbol{p}}(\tau-\tau')\right\} \\
&= -\mathrm{Tr}\left\{\hat{\rho}_H \hat{T}_\tau\left[\hat{a}^\dagger_{\boldsymbol{p}'}(0)\hat{a}_{\boldsymbol{p}}(\tau-\tau')\right]\right\} = -\mathrm{Tr}\left\{\hat{\rho}_H \hat{T}_\tau\left[\hat{a}_{\boldsymbol{p}}(\tau-\tau')\hat{a}^\dagger_{\boldsymbol{p}'}(0)\right]\right\} \\
&= -\langle \hat{T}_\tau \hat{a}_{\boldsymbol{p}}(\tau-\tau')\hat{a}^\dagger_{\boldsymbol{p}'}(0)\rangle = G_{\boldsymbol{p}\boldsymbol{p}'}(\tau-\tau',0)
\end{aligned}
$$

For simplicity, we will introduce the notation $G_{\boldsymbol{p}\boldsymbol{p}'}(\tau,0) \equiv G_{\boldsymbol{p}\boldsymbol{p}'}(\tau)$. We further note that when using imaginary time $G_{\boldsymbol{p}\boldsymbol{p}'}(\tau)$ is a periodic functions in the domain $[-\beta\hbar,\beta\hbar]$ with a period of $\beta\hbar$ (see Page 236 of Ref. [21]):

$$
\begin{cases} G_{\boldsymbol{p}\boldsymbol{p}'}(\tau+\beta\hbar,0) = G_{\boldsymbol{p}\boldsymbol{p}'}(\tau,0), \tau < 0 \\ G_{\boldsymbol{p}\boldsymbol{p}'}(\tau-\beta\hbar,0) = G_{\boldsymbol{p}\boldsymbol{p}'}(\tau,0), \tau > 0 \end{cases}. \tag{S7.58}
$$

To show this, we shall again assume first that $-\beta\hbar < \tau < 0$ to write, that is

$$
\begin{aligned}
G_{\boldsymbol{p}\boldsymbol{p}'}(\tau+\beta\hbar,0) &= -\langle \hat{T}_\tau \hat{a}_{\boldsymbol{p}}(\tau+\beta\hbar)\hat{a}^\dagger_{\boldsymbol{p}'}(0)\rangle = -\langle \hat{a}_{\boldsymbol{p}}(\tau+\beta\hbar)\hat{a}^\dagger_{\boldsymbol{p}'}(0)\rangle \\
&= -\mathrm{Tr}\left\{\hat{\rho}_H e^{\frac{\hat{H}(\tau+\beta\hbar)}{\hbar}}\hat{a}_{\boldsymbol{p}} e^{-\frac{\hat{H}(\tau+\beta\hbar)}{\hbar}}\hat{a}_{\boldsymbol{p}'}\right\} = -\mathrm{Tr}\left\{\hat{\rho}_H e^{\beta\hat{H}} e^{\frac{\hat{H}\tau}{\hbar}}\hat{a}_{\boldsymbol{p}} e^{-\frac{\hat{H}\tau}{\hbar}} e^{-\beta\hat{H}}\hat{a}_{\boldsymbol{p}'}\right\} \\
&= -\mathrm{Tr}\{\hat{\rho}_H e^{\beta\hat{H}}\hat{a}_{\boldsymbol{p}}(\tau)e^{-\beta\hat{H}}\hat{a}_{\boldsymbol{p}'}(0)\} = -\frac{1}{Z_H}\mathrm{Tr}\{e^{-\beta\hat{H}} e^{\beta\hat{H}}\hat{a}_{\boldsymbol{p}}(\tau)e^{-\beta\hat{H}}\hat{a}_{\boldsymbol{p}'}(0)\} \\
&= -\frac{1}{Z_H}\mathrm{Tr}\{\hat{a}_{\boldsymbol{p}}(\tau)e^{-\beta\hat{H}}\hat{a}_{\boldsymbol{p}'}(0)\} = -\frac{1}{Z_H}\mathrm{Tr}\{e^{-\beta\hat{H}}\hat{a}_{\boldsymbol{p}'}(0)\hat{a}_{\boldsymbol{p}}(\tau)\} \\
&= -\frac{1}{Z_H}\mathrm{Tr}\{e^{-\beta\hat{H}}\hat{T}_\tau[\hat{a}_{\boldsymbol{p}}(\tau)\hat{a}_{\boldsymbol{p}'}(0)]\} = -\mathrm{Tr}\{\hat{\rho}_H \hat{T}_\tau[\hat{a}_{\boldsymbol{p}}(\tau)\hat{a}_{\boldsymbol{p}'}]\} = G_{\boldsymbol{p}\boldsymbol{p}'}(\tau,0)
\end{aligned}
$$

Similarly, for $\beta\hbar > \tau > 0$ we have:

$$
\begin{aligned}
G_{\boldsymbol{p}\boldsymbol{p}'}(\tau-\beta\hbar,0) &= -\langle \hat{T}_\tau \hat{a}_{\boldsymbol{p}}(\tau-\beta\hbar)\hat{a}^\dagger_{\boldsymbol{p}'}(0)\rangle = -\langle \hat{a}^\dagger_{\boldsymbol{p}'}(0)\hat{a}_{\boldsymbol{p}}(\tau-\beta\hbar)\rangle \\
&= -\mathrm{Tr}\left\{\hat{\rho}_H \hat{a}_{\boldsymbol{p}'} e^{\frac{\hat{H}(\tau-\beta\hbar)}{\hbar}}\hat{a}_{\boldsymbol{p}} e^{-\frac{\hat{H}(\tau-\beta\hbar)}{\hbar}}\right\} = -\mathrm{Tr}\left\{\hat{\rho}_H \hat{a}_{\boldsymbol{p}'} e^{-\beta\hat{H}} e^{\frac{\hat{H}\tau}{\hbar}}\hat{a}_{\boldsymbol{p}} e^{-\frac{\hat{H}\tau}{\hbar}} e^{\beta\hat{H}}\right\} \\
&= -\mathrm{Tr}\{\hat{\rho}_H \hat{a}_{\boldsymbol{p}'}(0)e^{-\beta\hat{H}}\hat{a}_{\boldsymbol{p}}(\tau)e^{\beta\hat{H}}\} = -\frac{1}{Z_H}\mathrm{Tr}\{e^{-\beta\hat{H}}\hat{a}_{\boldsymbol{p}'}(0)e^{-\beta\hat{H}}\hat{a}_{\boldsymbol{p}}(\tau)e^{\beta\hat{H}}\} \\
&= -\frac{1}{Z_H}\mathrm{Tr}\{\hat{a}_{\boldsymbol{p}'}(0)e^{-\beta\hat{H}}\hat{a}_{\boldsymbol{p}}(\tau)\} = -\frac{1}{Z_H}\mathrm{Tr}\{e^{-\beta\hat{H}}\hat{a}_{\boldsymbol{p}}(\tau)\hat{a}_{\boldsymbol{p}'}(0)\} \\
&= -\frac{1}{Z_H}\mathrm{Tr}\{e^{-\beta\hat{H}}\hat{T}_\tau[\hat{a}_{\boldsymbol{p}}(\tau)\hat{a}_{\boldsymbol{p}'}(0)]\} = -\mathrm{Tr}\{\hat{\rho}_H \hat{T}_\tau[\hat{a}_{\boldsymbol{p}}(\tau)\hat{a}_{\boldsymbol{p}'}]\} = G_{\boldsymbol{p}\boldsymbol{p}'}(\tau,0)
\end{aligned}
$$

Therefore, $G_{\boldsymbol{p}\boldsymbol{p}'}(\tau)$ can be expanded as a Fourier series in the domain $[0,\beta\hbar]$ as follows:

$$G_{\boldsymbol{pp'}}(\tau) = \frac{1}{\beta\hbar}\sum_{-\infty}^{\infty} e^{-i\omega_n\tau} G_{\boldsymbol{pp'}}(i\omega_n). \tag{S7.59}$$

where $\omega_n = \frac{2\pi n}{\beta\hbar}$ and the associated Fourier coefficient is given by

$$G_{\boldsymbol{pp'}}(i\omega_n) = \int_0^{\beta\hbar} \mathrm{d}\tau e^{i\omega_n\tau} G_{\boldsymbol{pp'}}(\tau),\ \omega_n = \frac{2n\pi}{\beta\hbar}. \tag{S7.60}$$

Having proven the translational time invariance and the periodicity of the Green's functios we can now calculate it for the uncoupled system:

$$G^0_{\boldsymbol{pp'}}(\tau,\tau') = -\langle \hat{T}_\tau \hat{a}_{\boldsymbol{p}}(\tau)\hat{a}^\dagger_{\boldsymbol{p'}}(\tau')\rangle_0 = \begin{cases} -\langle \hat{a}_{\boldsymbol{p}}(0)e^{-\omega_p\tau}\hat{a}^\dagger_{\boldsymbol{p'}}(0)e^{\omega_{p'}\tau'}\rangle, & \tau-\tau'>0 \\ -\langle \hat{a}^\dagger_{\boldsymbol{p'}}(0)e^{\omega_{p'}\tau'}\hat{a}_{\boldsymbol{p}}(0)e^{-\omega_p\tau}\rangle, & \tau-\tau'<0 \end{cases}$$

$$= \begin{cases} -e^{-\omega_p\tau}e^{\omega_{p'}\tau'}\langle \hat{a}_{\boldsymbol{p}}(0)\hat{a}^\dagger_{\boldsymbol{p'}}(0)\rangle, & \tau-\tau'>0 \\ -e^{-\omega_p\tau}e^{\omega_{p'}\tau'}\langle \hat{a}^\dagger_{\boldsymbol{p'}}(0)\hat{a}_{\boldsymbol{p}}(0)\rangle, & \tau-\tau'<0 \end{cases}$$

$$= \begin{cases} -e^{-\omega_p\tau}e^{\omega_{p'}\tau'}\langle \hat{a}^\dagger_{\boldsymbol{p'}}(0)\hat{a}_{\boldsymbol{p}}(0) + \left[\hat{a}_{\boldsymbol{p}}(0),\hat{a}^\dagger_{\boldsymbol{p'}}(0)\right]\rangle, \tau-\tau'>0 \\ -e^{-\omega_p\tau}e^{\omega_{p'}\tau'}\langle \hat{a}^\dagger_{\boldsymbol{p'}}(0)\hat{a}_{\boldsymbol{p}}(0)\rangle, & \tau-\tau'<0 \end{cases}$$

$$= \begin{cases} -e^{-\omega_p\tau}e^{\omega_{p'}\tau'}\left[\langle \hat{a}^\dagger_{\boldsymbol{p'}}(0)\hat{a}_{\boldsymbol{p}}(0)\rangle + \delta_{\boldsymbol{pp'}}\right], \tau-\tau'>0 \\ -e^{-\omega_p\tau}e^{\omega_{p'}\tau'}\langle \hat{a}^\dagger_{\boldsymbol{p'}}(0)\hat{a}_{\boldsymbol{p}}(0)\rangle, & \tau-\tau'<0 \end{cases}$$

i.e.,

$$G^0_{\boldsymbol{pp'}}(\tau,\tau') = \begin{cases} -e^{-\omega_p\tau}e^{\omega_{p'}\tau'}\left[\langle \hat{a}^\dagger_{\boldsymbol{p'}}(0)\hat{a}_{\boldsymbol{p}}(0)\rangle + \delta_{\boldsymbol{pp'}}\right], \tau-\tau'>0 \\ -e^{-\omega_p\tau}e^{\omega_{p'}\tau'}\langle \hat{a}^\dagger_{\boldsymbol{p'}}(0)\hat{a}_{\boldsymbol{p}}(0)\rangle,\ \tau-\tau'<0 \end{cases}, \tag{S7.61}$$

where we have used Eq. (S7.54) for $\hat{a}_{\boldsymbol{p}}(\tau), \hat{a}^\dagger_{\boldsymbol{p'}}(\tau')$ and Commutation relation $\left[\hat{a}_{\boldsymbol{p}}(0),\hat{a}^\dagger_{\boldsymbol{p'}}(0)\right] = \delta_{\boldsymbol{pp'}}$. To calculate $\langle \hat{a}^\dagger_{\boldsymbol{p'}}(0)\hat{a}_{\boldsymbol{p}}(0)\rangle$, we first prove following equation:

$$e^{\hat{A}}\hat{B}e^{-\hat{A}} = \sum_{n=0}^{\infty}\frac{1}{n!}\left[\hat{A}^{(n)},\hat{B}\right], \tag{S7.62}$$

where $\left[\hat{A}^{(k)},\hat{B}\right] \equiv \left[\hat{A},\left[\hat{A}^{(k-1)},\hat{B}\right]\right]$. To prove this identity, we define the operator $\hat{f}(t) = e^{t\hat{A}}\hat{B}e^{-t\hat{A}}$ and taylor expand it around $t=0$:

$$\hat{f}(t) = \hat{f}(0) + t\hat{f}'(0) + \frac{t^2}{2}\hat{f}''(0) + \cdots = \sum_{n=0}^{\infty}\frac{t^n}{n!}\frac{d^n\hat{f}}{dt^n}\Big|_{t=0}, \tag{S7.63}$$

The corresponding derivatives are given by:

$$\begin{cases} \hat{f}'(t) = e^{t\hat{A}}\hat{A}\hat{B}e^{-t\hat{A}} - e^{t\hat{A}}\hat{B}\hat{A}e^{-t\hat{A}} = e^{t\hat{A}}\left[\hat{A},\hat{B}\right]e^{-t\hat{A}} \\ \hat{f}''(t) = e^{t\hat{A}}\left(\hat{A}\left[\hat{A},\hat{B}\right] - \left[\hat{A},\hat{B}\right]\hat{A}\right)e^{-t\hat{A}} = e^{t\hat{A}}\left[\hat{A}^{(2)},\hat{B}\right]e^{-t\hat{A}} \\ \vdots \\ \hat{f}^{(n)}(t) = e^{t\hat{A}}\left[\hat{A}^{(n)},\hat{B}\right]e^{-t\hat{A}} \end{cases}, \tag{S7.64}$$

Substituting Eq. (S7.64) into Eq. (S7.63), we have:

$$e^{t\hat{A}}\hat{B}e^{-t\hat{A}} = \sum_{n=0}^{\infty}\frac{t^n}{n!}\left[\hat{A}^{(n)},\hat{B}\right]. \tag{S7.65}$$

It's clear that Eq. (S7.61) is a spectial case of Eq. (S7.64) with $t = 1$. With this we can proceed as follows:

$$\langle\hat{a}^{\dagger}_{\boldsymbol{p}'}(0)\hat{a}_{\boldsymbol{p}}(0)\rangle = \frac{1}{Z_{H_0}}\mathrm{Tr}\left\{e^{-\beta H_0}\hat{a}^{\dagger}_{\boldsymbol{p}'}(0)\hat{a}_{\boldsymbol{p}}(0)\right\} = \frac{1}{Z_{H_0}}\mathrm{Tr}\left\{e^{-\beta H_0}\hat{a}^{\dagger}_{\boldsymbol{p}'}(0)e^{\beta H_0}e^{-\beta H_0}\hat{a}_{\boldsymbol{p}}(0)\right\}$$

$$= \frac{1}{Z_{H_0}}\mathrm{Tr}\left\{\sum_{n=0}^{\infty}\frac{(-\beta)^n}{n!}\left[\widehat{H}_0{}^{(n)},\hat{a}^{\dagger}_{\boldsymbol{p}'}(0)\right]e^{-\beta H_0}\hat{a}_{\boldsymbol{p}}(0)\right\}$$

Note that $\left[\widehat{H}_0,\hat{a}^{\dagger}_{\boldsymbol{p}'}(0)\right] = \hbar\omega_{\boldsymbol{p}'}\hat{a}^{\dagger}_{\boldsymbol{p}'}(0)$, we have

$$\left[\widehat{H}_0{}^{(n)},\hat{a}^{\dagger}_{\boldsymbol{p}'}(0)\right] = \left(\hbar\omega_{\boldsymbol{p}'}\right)^n\hat{a}^{\dagger}_{\boldsymbol{p}'}(0), \tag{S7.66}$$

such that:

$$\langle\hat{a}^{\dagger}_{\boldsymbol{p}'}(0)\hat{a}_{\boldsymbol{p}}(0)\rangle = \frac{1}{Z_{H_0}}\mathrm{Tr}\left\{\sum_{n=0}^{\infty}\frac{(-\beta)^n}{n!}\left[\widehat{H}_0{}^{(n)},\hat{a}^{\dagger}_{\boldsymbol{p}'}(0)\right]e^{-\beta H_0}\hat{a}_{\boldsymbol{p}}(0)\right\}$$

$$= \frac{1}{Z_{H_0}}\mathrm{Tr}\left\{\sum_{n=0}^{\infty}\frac{\left(-\beta\hbar\omega_{\boldsymbol{p}'}\right)^n}{n!}\hat{a}^{\dagger}_{\boldsymbol{p}'}(0)\,e^{-\beta H_0}\hat{a}_{\boldsymbol{p}}(0)\right\}$$

$$= e^{-\beta\hbar\omega_{\boldsymbol{p}'}}\frac{1}{Z_{H_0}}\mathrm{Tr}\left\{e^{-\beta H_0}\hat{a}_{\boldsymbol{p}}(0)\hat{a}^{\dagger}_{\boldsymbol{p}'}(0)\right\} = e^{-\beta\hbar\omega_{\boldsymbol{p}'}}\langle\hat{a}_{\boldsymbol{p}}(0)\hat{a}^{\dagger}_{\boldsymbol{p}'}(0)\rangle$$

$$= e^{-\beta\hbar\omega_{\boldsymbol{p}'}}\left(\langle\hat{a}^{\dagger}_{\boldsymbol{p}'}(0)\hat{a}_{\boldsymbol{p}}(0)\rangle + \delta_{\boldsymbol{p}\boldsymbol{p}'}\right)$$

therefore, we obtain $\langle\hat{a}^{\dagger}_{\boldsymbol{p}'}(0)\hat{a}_{\boldsymbol{p}}(0)\rangle\left(e^{\beta\hbar\omega_{\boldsymbol{p}'}}-1\right) = \delta_{\boldsymbol{p}\boldsymbol{p}'}$. For $\boldsymbol{p}' \neq \boldsymbol{p}$ and general $e^{\beta\hbar\omega_{\boldsymbol{p}'}}$ we have $\langle\hat{a}^{\dagger}_{\boldsymbol{p}'}(0)\hat{a}_{\boldsymbol{p}}(0)\rangle = 0$. For $\boldsymbol{p}' = \boldsymbol{p}$ we obtain $\langle\hat{a}^{\dagger}_{\boldsymbol{p}}(0)\hat{a}_{\boldsymbol{p}}(0)\rangle = \left[e^{\beta\hbar\omega_{\boldsymbol{p}}}-1\right]^{-1}$. Hence, we have:

$$\langle\hat{a}^{\dagger}_{\boldsymbol{p}'}(0)\hat{a}_{\boldsymbol{p}}(0)\rangle = \delta_{\boldsymbol{p}'\boldsymbol{p}}\frac{1}{e^{\beta\hbar\omega_{\boldsymbol{p}}}-1} \equiv \delta_{\boldsymbol{p}'\boldsymbol{p}}n_B\left(\omega_{\boldsymbol{p}}\right), \tag{S7.67}$$

where $n_B\left(\omega_{\boldsymbol{p}}\right)$ is the Bose-Einstein distribution for phonons. Substituting Eq. (S7.66) in Eq. (S7.61) we obtain:

$$G^0_{\boldsymbol{p}\boldsymbol{p}'}(\tau,\tau') = \begin{cases}-\delta_{\boldsymbol{p}\boldsymbol{p}'}\left[1+n_B\left(\omega_{\boldsymbol{p}}\right)\right]e^{-\omega_{\boldsymbol{p}}(\tau-\tau')}, & \tau-\tau'>0\\ -\delta_{\boldsymbol{p}\boldsymbol{p}'}n_B\left(\omega_{\boldsymbol{p}}\right)e^{-\omega_{\boldsymbol{p}}(\tau-\tau')}, & \tau-\tau'<0\end{cases}. \tag{S7.68}$$

Note that only those Green's functions of the form $G^0_{\boldsymbol{p}\boldsymbol{p}'}(\tau,\tau') = G^0_{\boldsymbol{p}}(\tau-\tau')\delta_{\boldsymbol{p}\boldsymbol{p}'}$ are non-zero due to the orthogonality of normal modes. Looking at the non-vanishing terms and setting $\tau' = 0$, without loss of generality, we can calculate the Fourier transform of $G^0_{\boldsymbol{p}}(\tau)$ from Eq. (S7.60):

$$G^0_{\boldsymbol{p}}(i\omega_n) = \int_0^{\beta\hbar}\mathrm{d}\tau e^{i\omega_n\tau}G^0_{\boldsymbol{p}}(\tau) = -\int_0^{\beta\hbar}\mathrm{d}\tau e^{i\omega_n\tau}\left[1+n_B\left(\omega_{\boldsymbol{p}}\right)\right]e^{-\omega_{\boldsymbol{p}}\tau} = -\frac{1+n_B(\omega_{\boldsymbol{p}})}{i\omega_n-\omega_{\boldsymbol{p}}}\left[e^{(i\omega_n-\omega_{\boldsymbol{p}})\beta\hbar}-1\right] = -\frac{1+\left(\frac{1}{e^{\beta\hbar\omega_{\boldsymbol{p}}}-1}\right)}{i\omega_n-\omega_{\boldsymbol{p}}}\left(e^{i\frac{2\pi n}{\beta\hbar}\beta\hbar}e^{-\beta\hbar\omega_{\boldsymbol{p}}}-1\right) = -\frac{e^{\beta\hbar\omega_{\boldsymbol{p}}}}{i\omega_n-\omega_{\boldsymbol{p}}}\frac{\left(e^{-\beta\hbar\omega_{\boldsymbol{p}}}-1\right)}{e^{\beta\hbar\omega_{\boldsymbol{p}}}-1} = -\frac{1}{i\omega_n-\omega_{\boldsymbol{p}}}\frac{1-e^{\beta\hbar\omega_{\boldsymbol{p}}}}{e^{\beta\hbar\omega_{\boldsymbol{p}}}-1} = \frac{1}{i\omega_n-\omega_{\boldsymbol{p}}},$$

i.e.,

$$G_{\boldsymbol{p}}^{0}(i\omega_n) == \frac{1}{i\omega_n - \omega_{\boldsymbol{p}}}. \tag{S7.69}$$

7.4.3 Interaction picture

Next, we can proceed with calculating the Green's function of the coupled system. To this end, we define the coupling Hamiltonian operator term in the interaction picture as:

$$\widehat{H}_C^I(\tau) = e^{\frac{\widehat{H}_0\tau}{\hbar}}\widehat{H}_C e^{-\frac{\widehat{H}_0\tau}{\hbar}}. \tag{S7.70}$$

The time evolution of $\widehat{H}_C(\tau)$ is then given by:

$$\hbar\frac{\partial\widehat{H}_C^I(\tau)}{\partial\tau} = \left[\widehat{H}_0, \widehat{H}_C^I(\tau)\right]. \tag{S7.71}$$

Note that the Green's function defined above was given in the Heisenberg picture. To proceed, we need to transform it to the interaction picture:

$$\begin{aligned} G_{\boldsymbol{p}\boldsymbol{p}'}(\tau,0) &= -\langle\hat{T}_\tau\hat{a}_{\boldsymbol{p}}(\tau)\hat{a}_{\boldsymbol{p}'}^{\dagger}(0)\rangle = -\mathrm{Tr}\left\{\hat{\rho}_H\hat{T}_\tau\left[e^{\frac{\widehat{H}\tau}{\hbar}}\hat{a}_{\boldsymbol{p}}(0)e^{-\frac{\widehat{H}\tau}{\hbar}}\hat{a}_{\boldsymbol{p}'}^{\dagger}(0)\right]\right\} \\ &= -\mathrm{Tr}\left\{\hat{\rho}_H\hat{T}_\tau\left[e^{\frac{\widehat{H}\tau}{\hbar}}e^{-\frac{\widehat{H}_0\tau}{\hbar}}\left(e^{\frac{\widehat{H}_0\tau}{\hbar}}\hat{a}_{\boldsymbol{p}}(0)e^{-\frac{\widehat{H}_0\tau}{\hbar}}\right)e^{\frac{\widehat{H}_0\tau}{\hbar}}e^{-\frac{\widehat{H}\tau}{\hbar}}\hat{a}_{\boldsymbol{p}'}^{\dagger}(0)\right]\right\} \\ &= -\mathrm{Tr}\left\{\hat{\rho}_H\hat{T}_\tau\left[\widehat{U}(0,\tau)\hat{a}_{\boldsymbol{p}}^I(\tau)\widehat{U}(\tau,0)\hat{a}_{\boldsymbol{p}'}^{\dagger}(0)\right]\right\} \end{aligned}$$

where,

$$\hat{a}_{\boldsymbol{p}}^I(\tau) \equiv e^{\frac{\widehat{H}_0\tau}{\hbar}}\hat{a}_{\boldsymbol{p}}(0)e^{-\frac{\widehat{H}_0\tau}{\hbar}}, \tag{S7.72}$$

is the operator in interaction picture and the operator $\widehat{U}$ is defined by:

$$\widehat{U}(\tau_1,\tau_2) \equiv e^{\frac{\widehat{H}_0\tau_1}{\hbar}}e^{-\frac{\widehat{H}(\tau_1-\tau_2)}{\hbar}}e^{-\frac{\widehat{H}_0\tau_2}{\hbar}}, \tag{S7.73}$$

Note that while $\widehat{U}$ is not unitary, it satisfies the following group property:

$$\widehat{U}(\tau_1,\tau_2)\widehat{U}(\tau_2,\tau_3) = \widehat{U}(\tau_1,\tau_3), \tag{S7.74}$$

and the boundary condition $\widehat{U}(\tau_1,\tau_1) = \hat{1}$. In addition, the τ derivative of $\widehat{U}$ is simply:

$$\begin{aligned} \hbar\frac{\partial\widehat{U}(\tau,\tau')}{\partial\tau} &= \left\{\widehat{H}_0 e^{\frac{\widehat{H}_0\tau}{\hbar}}e^{-\frac{\widehat{H}(\tau-\tau')}{\hbar}} - e^{\frac{\widehat{H}_0\tau}{\hbar}}\widehat{H}e^{-\frac{\widehat{H}(\tau-\tau')}{\hbar}}\right\}e^{-\frac{\widehat{H}_0\tau'}{\hbar}} \\ &= e^{\frac{\widehat{H}_0\tau}{\hbar}}\left(\widehat{H}_0-\widehat{H}\right)e^{-\frac{\widehat{H}_0\tau}{\hbar}}e^{\frac{\widehat{H}_0\tau}{\hbar}}e^{-\frac{\widehat{H}(\tau-\tau')}{\hbar}}e^{-\frac{\widehat{H}_0\tau'}{\hbar}} = e^{\frac{\widehat{H}_0\tau}{\hbar}}\left(-\widehat{H}_C\right)e^{-\frac{\widehat{H}_0\tau}{\hbar}}\widehat{U}(\tau,\tau') \\ &= -\widehat{H}_C^I(\tau)\widehat{U}(\tau,\tau') \end{aligned}$$

i.e.,

$$\hbar\frac{\partial\widehat{U}(\tau,\tau')}{\partial\tau} = -\widehat{H}_C^I(\tau)\widehat{U}(\tau,\tau'), \tag{S7.75}$$

The solution of Eq. (S7.75) is (see page 235 of Ref. [21]):

$$\hat{U}(\tau,\tau') = \sum_{n=0}^{\infty} \frac{\left(-\frac{1}{\hbar}\right)^n}{n!} \int_{\tau'}^{\tau} d\tau_1 \cdots \int_{\tau'}^{\tau} d\tau_n \, \hat{T}_\tau\left[\hat{H}_C^I(\tau_1)\cdots\hat{H}_C^I(\tau_n)\right], \tag{S7.76}$$

The exact thermal Green's function now may be rewritten in the interaction picture as:

$$\begin{aligned}
\hat{G}_{\boldsymbol{pp'}}(\tau,0) &= -\frac{1}{Z_H}\mathrm{Tr}\left\{e^{-\beta\hat{H}}\hat{T}_\tau\left[\hat{U}(0,\tau)\hat{a}_{\boldsymbol{p}}^I(\tau)\hat{U}(\tau,0)\right]\hat{a}_{\boldsymbol{p'}}^\dagger(0)\right\} \\
&= -\frac{\mathrm{Tr}\left\{e^{-\beta\hat{H}}\hat{T}_\tau\left[\hat{U}(0,\tau)\hat{a}_{\boldsymbol{p}}^I(\tau)\hat{U}(\tau,0)\hat{a}_{\boldsymbol{p'}}^\dagger(0)\right]\right\}}{\mathrm{Tr}\left\{e^{-\beta\hat{H}}\right\}} \\
&= -\frac{\mathrm{Tr}\left\{e^{-\beta\hat{H}_0}\hat{U}(\beta\hbar,0)\hat{T}_\tau\left[\hat{a}_{\boldsymbol{p}}^I(\tau)\hat{U}(0,\tau)\hat{U}(\tau,0)\hat{a}_{\boldsymbol{p'}}^\dagger(0)\right]\right\}}{\mathrm{Tr}\left\{e^{-\beta\hat{H}_0}\hat{U}(\beta\hbar,0)\right\}} \\
&= -\frac{\mathrm{Tr}\left\{e^{-\beta\hat{H}_0}\hat{U}(\beta\hbar,0)\hat{T}_\tau\left[\hat{a}_{\boldsymbol{p}}^I(\tau)\hat{U}(0,0)\hat{a}_{\boldsymbol{p'}}^\dagger(0)\right]\right\}}{\mathrm{Tr}\left\{e^{-\beta\hat{H}_0}\hat{U}(\beta\hbar,0)\right\}} = \\
&= -\frac{\mathrm{Tr}\left\{e^{-\beta\hat{H}_0}\hat{T}_\tau\left[\hat{U}(\beta\hbar,0)\hat{a}_{\boldsymbol{p}}^I(\tau)\hat{a}_{\boldsymbol{p'}}^\dagger(0)\right]\right\}}{\mathrm{Tr}\left\{e^{-\beta\hat{H}_0}\hat{U}(\beta\hbar,0)\right\}}
\end{aligned}$$

Where we used the fact that we are free to change the order of the operators within the time ordering operation (see pages 241-242 of Ref. [21]).

7.4.4 Wick's theorem

Thus the Green's function can be expanded as[21]

$$G_{\boldsymbol{pp'}}(\tau,0) = -\frac{\sum_{m=0}^{\infty}\frac{1}{m!}\left(-\frac{1}{\hbar}\right)^m \int_0^{\beta\hbar} d\tau_1 \cdots \int_0^{\beta\hbar} d\tau_m \langle T_\tau \hat{H}_C^I(\tau_1)\cdots\hat{H}_C^I(\tau_m)\hat{a}_{\boldsymbol{p}}^I(\tau)\hat{a}_{\boldsymbol{p'}}^\dagger(0)\rangle_0}{\sum_{m=0}^{\infty}\frac{1}{m!}\left(-\frac{1}{\hbar}\right)^m \int_0^{\beta\hbar} d\tau_1 \cdots \int_0^{\beta\hbar} d\tau_m \langle T_\tau \hat{H}_C^I(\tau_1)\cdots\hat{H}_C^I(\tau_m)\rangle_0}, \tag{S7.77}$$

where $\langle\cdots\rangle_0$ represents the ensemble average with respect to the non-interacting basis $\mathrm{Tr}\left\{e^{-\beta\hat{H}_0}(\cdots)\right\}$. Or explicitly,

$$G_{\boldsymbol{pp'}}(\tau,0) = -\frac{G^0_{\boldsymbol{pp'}}(\tau) - \frac{1}{\hbar}\int_0^{\beta\hbar} d\tau_1 \langle T_\tau \hat{H}_C^I(\tau_1)\hat{a}_{\boldsymbol{p}}(\tau)\hat{a}_{\boldsymbol{p'}}^\dagger(0)\rangle_0 + \frac{1}{2\hbar^2}\int_0^{\beta\hbar} d\tau_1 \int_0^{\beta\hbar} d\tau_2 \langle T_\tau \hat{H}_C^I(\tau_1)\hat{H}_C^I(\tau_2)\hat{a}_{\boldsymbol{p}}(\tau)\hat{a}_{\boldsymbol{p'}}^\dagger(0)\rangle_0 + \cdots}{1 - \frac{1}{\hbar}\int_0^{\beta\hbar} d\tau_1 \langle T_\tau \hat{H}_C^I(\tau_1)\rangle_0 + \frac{1}{2\hbar^2}\int_0^{\beta\hbar} d\tau_1 \int_0^{\beta\hbar} d\tau_2 \langle T_\tau \hat{H}_C^I(\tau_1)H_C^I(\tau_2)\rangle_0 + \cdots}, \tag{S7.78}$$

For consiceness we introduce the following notation:

$$D_m \equiv \frac{1}{m!}\left(-\frac{1}{\hbar}\right)^m \int_0^{\beta\hbar} d\tau_1 \cdots \int_0^{\beta\hbar} d\tau_m \, \langle T_\tau \hat{H}_C^I(\tau_1)\cdots\hat{H}_C^I(\tau_m)\rangle_0, \tag{S7.79}$$

To simplify the calculation in Eq. (S7.77), we adopt Wick's theorem (see pages 237-241 of Ref. [21]),which can be expressed as follows:

$$\langle T_\tau\left[\hat{A}\hat{B}\hat{C}\hat{D}\cdots\hat{Y}\hat{Z}\right]\rangle_0 = \langle T_\tau\left[\hat{A}\hat{B}\right]\rangle_0\langle T_\tau\left[\hat{C}\hat{D}\right]\rangle_0\cdots\langle T_\tau\left[\hat{Y}\hat{Z}\right]\rangle_0 + \langle T_\tau\left[\hat{A}\hat{C}\right]\rangle_0\langle T_\tau\left[\hat{B}\hat{D}\right]\rangle_0\cdots\langle T_\tau\left[\hat{X}\hat{Z}\right]\rangle_0 + \cdots, \tag{7.80}$$

Here $\hat{A},\hat{B},\ldots,\hat{Y},\hat{Z}$ represent $\hat{a}_{\boldsymbol{p}}(\tau)$ or $\hat{a}_{\boldsymbol{p}}^\dagger(\tau)$. In Eq. (7.80), each term corresponds to a particular pairing of the operators $\hat{A}\hat{B}\hat{C}\hat{D}\cdots\hat{Y}\hat{Z}$ and all possible pairings are taken into account. Here, the only

non-vanishing propagators will have the form [see Eq. (S7.68)]:

$$\langle T_\tau \left[\hat{a}^\dagger_{\boldsymbol{p}'}(\tau')\hat{a}_{\boldsymbol{p}}(\tau)\right]\rangle_0 = -\langle T_\tau \left[\hat{a}_{\boldsymbol{p}}(\tau)\hat{a}^\dagger_{\boldsymbol{p}'}(\tau')\right]\rangle_0 = G^0_{\boldsymbol{p}\boldsymbol{p}'}(\tau,\tau') = G^0_{\boldsymbol{p}}(\tau-\tau')\delta_{\boldsymbol{p}\boldsymbol{p}'}. \quad \text{(S7.81)}$$

Therefore, the second term in the numerator of Eq. (S7.78) can be calculated as:

$$\begin{aligned} I_2 &= -\frac{1}{\hbar}\int_0^{\beta\hbar} d\tau_1 \langle T_\tau \widehat{H}^I_C(\tau_1)\hat{a}_{\boldsymbol{p}}(\tau)\hat{a}^\dagger_{\boldsymbol{p}'}(0)\rangle_0 \\ &= -\frac{1}{\hbar}\int_0^{\beta\hbar} d\tau_1 \langle T_\tau \widehat{H}^I_C(\tau_1)\rangle_0 \langle T_\tau \hat{a}^\dagger_{\boldsymbol{p}'}(0)\hat{a}_{\boldsymbol{p}}(\tau)\rangle_0 - \frac{1}{\hbar}\int_0^{\beta\hbar} d\tau_1 \langle T_\tau \widehat{H}^I_C(\tau_1)\hat{a}_{\boldsymbol{p}}(\tau)\hat{a}^\dagger_{\boldsymbol{p}'}(0)\rangle_{0,c} \\ &= G^0_{\boldsymbol{p}\boldsymbol{p}'}(\tau,0)\left[-\frac{1}{\hbar}\int_0^{\beta\hbar} d\tau_1 \langle T_\tau \widehat{H}^I_C(\tau_1)\rangle_0\right] - \frac{1}{\hbar}\int_0^{\beta\hbar} d\tau_1 \langle T_\tau \widehat{H}^I_C(\tau_1)\hat{a}_{\boldsymbol{p}}(\tau)\hat{a}^\dagger_{\boldsymbol{p}'}(0)\rangle_{0,c} \end{aligned}$$

The first term in above equation is called disconnected part since the pairing is performed separately on $\widehat{H}_C(\tau_1)$ and $\hat{a}_{\boldsymbol{p}}(\tau)\hat{a}^\dagger_{\boldsymbol{p}'}(0)$. All other terms have pairs that mix creation and annihilation operators of the Hamiltonian with $\hat{a}_{\boldsymbol{p}}(\tau)$ or $\hat{a}^\dagger_{\boldsymbol{p}'}(0)$ and are said to have connected party. For simplicity we include all these terms in the notation $\langle T_\tau \widehat{H}_C(\tau_1)\hat{a}_{\boldsymbol{p}}(\tau)\hat{a}^\dagger_{\boldsymbol{p}'}(0)\rangle_{0,c}$. Furthermore, we define $G^{(1)}_{\boldsymbol{p}\boldsymbol{p}'}(\tau) \equiv -\frac{1}{\hbar}\int_0^{\beta\hbar} d\tau_1 \langle T_\tau \widehat{H}_C(\tau_1)\hat{a}_{\boldsymbol{p}}(\tau)\hat{a}^\dagger_{\boldsymbol{p}'}(0)\rangle_{0,c}$. Then we have,

$$I_3 = -\frac{1}{\hbar}\int_0^{\beta\hbar} d\tau_1 \langle T_\tau \widehat{H}^I_C(\tau_1)\hat{a}_{\boldsymbol{p}}(\tau)\hat{a}^\dagger_{\boldsymbol{p}'}(0)\rangle_0 = G^0_{\boldsymbol{p}\boldsymbol{p}'}(\tau,0)D_1 + G^{(1)}_{\boldsymbol{p}\boldsymbol{p}'}(\tau), \quad \text{(S7.82)}$$

Using this method, the third term in the numerator of Eq. (S7.78) can be calculated as:

$$\begin{aligned} I_3 &= \tfrac{1}{2\hbar^2}\int_0^{\beta\hbar} d\tau_1 \int_0^{\beta\hbar} d\tau_2 \langle T_\tau \widehat{H}^I_C(\tau_1)\widehat{H}^I_C(\tau_2)\hat{a}_{\boldsymbol{p}}(\tau)\hat{a}^\dagger_{\boldsymbol{p}'}(0)\rangle_0 = \tfrac{1}{2\hbar^2}\int_0^{\beta\hbar} d\tau_1 \int_0^{\beta\hbar} d\tau_2 \langle T_\tau \widehat{H}^I_C(\tau_1)\widehat{H}^I_C(\tau_2)\rangle_0 \langle T_\tau \hat{a}^\dagger_{\boldsymbol{p}'}(0)\hat{a}_{\boldsymbol{p}}(\tau)\rangle_0 + \\ &\tfrac{1}{2\hbar^2}\int_0^{\beta\hbar} d\tau_1 \int_0^{\beta\hbar} d\tau_2 \langle T_\tau \widehat{H}^I_C(\tau_2)\rangle_0 \langle T_\tau \widehat{H}^I_C(\tau_1)\hat{a}_{\boldsymbol{p}}(\tau)\hat{a}^\dagger_{\boldsymbol{p}'}(0)\rangle_{0,c} + \tfrac{1}{2\hbar^2}\int_0^{\beta\hbar} d\tau_1 \int_0^{\beta\hbar} d\tau_2 \langle T_\tau \widehat{H}^I_C(\tau_1)\rangle_0 \langle T_\tau \widehat{H}^I_C(\tau_2)\hat{a}_{\boldsymbol{p}}(\tau)\hat{a}^\dagger_{\boldsymbol{p}'}(0)\rangle_{0,c} + \\ &\tfrac{1}{2\hbar^2}\int_0^{\beta\hbar} d\tau_1 \int_0^{\beta\hbar} d\tau_2 \langle T_\tau \widehat{H}^I_C(\tau_1)\widehat{H}^I_C(\tau_2)\hat{a}_{\boldsymbol{p}}(\tau)\hat{a}^\dagger_{\boldsymbol{p}'}(0)\rangle_{0,c} = G^0_{\boldsymbol{p}\boldsymbol{p}'}(\tau,0)\left[\tfrac{1}{2\hbar^2}\int_0^{\beta\hbar} d\tau_1 \int_0^{\beta\hbar} d\tau_2 \langle T_\tau \widehat{H}^I_C(\tau_1)\widehat{H}^I_C(\tau_2)\rangle_0\right] + \\ &\tfrac{1}{2\hbar^2}\int_0^{\beta\hbar} d\tau_2 \langle T_\tau \widehat{H}^I_C(\tau_2)\rangle_0 \int_0^{\beta\hbar} d\tau_1 \langle T_\tau \widehat{H}^I_C(\tau_1)\hat{a}_{\boldsymbol{p}}(\tau)\hat{a}^\dagger_{\boldsymbol{p}'}(0)\rangle_{0,c} + \tfrac{1}{2\hbar^2}\int_0^{\beta\hbar} d\tau_1 \langle T_\tau \widehat{H}^I_C(\tau_1)\rangle_0 \int_0^{\beta\hbar} d\tau_2 \langle T_\tau \widehat{H}^I_C(\tau_2)\hat{a}_{\boldsymbol{p}}(\tau)\hat{a}^\dagger_{\boldsymbol{p}'}(0)\rangle_{0,c} + \\ &\tfrac{1}{2\hbar^2}\int_0^{\beta\hbar} d\tau_1 \int_0^{\beta\hbar} d\tau_2 \langle T_\tau \widehat{H}^I_C(\tau_1)\widehat{H}^I_C(\tau_2)\hat{a}_{\boldsymbol{p}}(\tau)\hat{a}^\dagger_{\boldsymbol{p}'}(0)\rangle_{0,c}. \end{aligned}$$

Here, the last term is denoted as $G^{(2)}_{\boldsymbol{p}\boldsymbol{p}'}(\tau)$.

Using Eq. (S7.82), the second and third terms on the right hand above equation can be simplified as follows:

$$\frac{1}{2\hbar^2}\int_0^{\beta\hbar} d\tau_2 \langle T_\tau \hat{H}_C^I(\tau_2)\rangle_0 \int_0^{\beta\hbar} d\tau_1 \langle T_\tau \hat{H}_C^I(\tau_1)\hat{a}_{\boldsymbol{p}}(\tau)\hat{a}_{\boldsymbol{p}'}^\dagger(0)\rangle_{0,c} + \frac{1}{2\hbar^2}\int_0^{\beta\hbar} d\tau_1 \langle T_\tau \hat{H}_C^I(\tau_1)\rangle_0 \int_0^{\beta\hbar} d\tau_2 \langle T_\tau \hat{H}_C^I(\tau_2)\hat{a}_{\boldsymbol{p}}(\tau)\hat{a}_{\boldsymbol{p}'}^\dagger(0)\rangle_{0,c}$$

$$= \frac{1}{2}\left[\frac{-1}{\hbar}\int_0^{\beta\hbar} d\tau_2 \langle T_\tau \hat{H}_C^I(\tau_2)\rangle_0\right]\left[\frac{-1}{\hbar}\int_0^{\beta\hbar} d\tau_1 \langle T_\tau \hat{H}_C^I(\tau_1)\hat{a}_{\boldsymbol{p}}(\tau)\hat{a}_{\boldsymbol{p}'}^\dagger(0)\rangle_{0,c}\right]$$

$$+ \frac{1}{2}\left[\frac{-1}{\hbar}\int_0^{\beta\hbar} d\tau_1 \langle T_\tau \hat{H}_C^I(\tau_1)\rangle_0\right]\left[\frac{-1}{\hbar}\int_0^{\beta\hbar} d\tau_2 \langle T_\tau \hat{H}_C^I(\tau_2)\hat{a}_{\boldsymbol{p}}(\tau)\hat{a}_{\boldsymbol{p}'}^\dagger(0)\rangle_{0,c}\right]$$

$$= \frac{1}{2}\left[\frac{-1}{\hbar}\int_0^{\beta\hbar} d\tau_2 \langle T_\tau \hat{H}_C^I(\tau_2)\rangle_0\right]\left[\frac{-1}{\hbar}\int_0^{\beta\hbar} d\tau_1 \langle T_\tau \hat{H}_C^I(\tau_1)\hat{a}_{\boldsymbol{p}}(\tau)\hat{a}_{\boldsymbol{p}'}^\dagger(0)\rangle_{0,c}\right]$$

$$+ \frac{1}{2}\left[\frac{-1}{\hbar}\int_0^{\beta\hbar} d\tau_2 \langle T_\tau \hat{H}_C^I(\tau_2)\rangle_0\right]\left[\frac{-1}{\hbar}\int_0^{\beta\hbar} d\tau_1 \langle T_\tau \hat{H}_C^I(\tau_1)\hat{a}_{\boldsymbol{p}}(\tau)\hat{a}_{\boldsymbol{p}'}^\dagger(0)\rangle_{0,c}\right]$$

$$= \left[\frac{-1}{\hbar}\int_0^{\beta\hbar} d\tau_2 \langle T_\tau \hat{H}_C^I(\tau_2)\rangle_0\right]\left[\frac{-1}{\hbar}\int_0^{\beta\hbar} d\tau_1 \langle T_\tau \hat{H}_C^I(\tau_1)\hat{a}_{\boldsymbol{p}}(\tau)\hat{a}_{\boldsymbol{p}'}^\dagger(0)\rangle_{0,c}\right] = D_1 G_{\boldsymbol{pp}'}^{(1)}(\tau)$$

Where, we performed the following integration variables interchange $\tau_1 \leftrightarrow \tau_2$. Thus we have

$$I_3 = G_{\boldsymbol{pp}'}^{(2)}(\tau) + G_{\boldsymbol{pp}'}^{(1)}(\tau)D_1 + G_{\boldsymbol{pp}'}^{0}(\tau,0)D_2, \tag{S7.83}$$

Similarity, we can calculate the fourth term of Eq. (S7.78) as:

$I_4 = \frac{-1}{6\hbar^3}\int_0^{\beta\hbar} d\tau_1 \int_0^{\beta\hbar} d\tau_2 \int_0^{\beta\hbar} d\tau_3 \langle T_\tau \hat{H}_C^I(\tau_1)\hat{H}_C^I(\tau_2)\hat{H}_C^I(\tau_3)\hat{a}_{\boldsymbol{p}}(\tau)\hat{a}_{\boldsymbol{p}'}^\dagger(0)\rangle_0 =$

$\frac{-1}{6\hbar^3}\int_0^{\beta\hbar} d\tau_1 \int_0^{\beta\hbar} d\tau_2 \int_0^{\beta\hbar} d\tau_3 \langle T_\tau \hat{H}_C^I(\tau_1)\hat{H}_C^I(\tau_2)\hat{H}_C^I(\tau_3)\rangle_0 \langle T_\tau \hat{a}_{\boldsymbol{p}}(\tau)\hat{a}_{\boldsymbol{p}'}^\dagger(0)\rangle_0 + 3 \times$

$\frac{-1}{6\hbar^3}\int_0^{\beta\hbar} d\tau_1 \int_0^{\beta\hbar} d\tau_2 \int_0^{\beta\hbar} d\tau_3 \langle T_\tau \hat{H}_C^I(\tau_2)\hat{H}_C^I(\tau_3)\rangle_0 \langle T_\tau \hat{H}_C^I(\tau_1)\hat{a}_{\boldsymbol{p}}(\tau)\hat{a}_{\boldsymbol{p}'}^\dagger(0)\rangle_{0,c} + 3 \times$

$\frac{-1}{6\hbar^3}\int_0^{\beta\hbar} d\tau_1 \int_0^{\beta\hbar} d\tau_2 \int_0^{\beta\hbar} d\tau_3 \langle T_\tau \hat{H}_C^I(\tau_1)\rangle_0 \langle T_\tau \hat{H}_C^I(\tau_2)\hat{H}_C^I(\tau_3)\hat{a}_{\boldsymbol{p}}(\tau)\hat{a}_{\boldsymbol{p}'}^\dagger(0)\rangle_{0,c} +$

$\frac{-1}{6\hbar^3}\int_0^{\beta\hbar} d\tau_1 \int_0^{\beta\hbar} d\tau_2 \int_0^{\beta\hbar} d\tau_3 \langle T_\tau \hat{H}_C^I(\tau_1)\hat{H}_C^I(\tau_2)\hat{H}_C^I(\tau_3)\hat{a}_{\boldsymbol{p}}(\tau)\hat{a}_{\boldsymbol{p}'}^\dagger(0)\rangle_{0,c} =$

$G_{\boldsymbol{pp}'}^{0}(\tau,0)\left[\frac{-1}{6\hbar^3}\int_0^{\beta\hbar} d\tau_1 \int_0^{\beta\hbar} d\tau_2 \int_0^{\beta\hbar} d\tau_3 \langle T_\tau \hat{H}_C^I(\tau_1)\hat{H}_C^I(\tau_2)\hat{H}_C^I(\tau_3)\rangle_0\right] +$

$\frac{1}{2\hbar^2}\int_0^{\beta\hbar} d\tau_2 \int_0^{\beta\hbar} d\tau_3 \langle T_\tau \hat{H}_C^I(\tau_2)\hat{H}_C^I(\tau_3)\rangle_0 \left[\frac{-1}{\hbar}\int_0^{\beta\hbar} d\tau_1 \langle T_\tau \hat{H}_C^I(\tau_1)\hat{a}_{\boldsymbol{p}}(\tau)\hat{a}_{\boldsymbol{p}'}^\dagger(0)\rangle_{0,c}\right] +$

$\frac{1}{2\hbar^2}\int_0^{\beta\hbar} d\tau_2 \int_0^{\beta\hbar} d\tau_3 \langle T_\tau \hat{H}_C^I(\tau_2)\hat{H}_C^I(\tau_3)\hat{a}_{\boldsymbol{p}}(\tau)\hat{a}_{\boldsymbol{p}'}^\dagger(0)\rangle_{0,c} \left[\frac{-1}{\hbar}\int_0^{\beta\hbar} d\tau_1 \langle T_\tau \hat{H}_C^I(\tau_1)\rangle_0\right] + G_{\boldsymbol{pp}'}^{(3)}(\tau) = G_{\boldsymbol{pp}'}^{(3)}(\tau) +$

$G_{\boldsymbol{pp}'}^{(2)}(\tau)D_1 + G_{\boldsymbol{pp}'}^{(1)}(\tau)D_2 + G_{\boldsymbol{pp}'}^{0}(\tau,0)D_3.$

Higher order terms can be treated in the same manner (see pages 95-96 of Ref. [21]). Then when substituting I_2, I_3, I_4 and all higher order terms into Eq. (S7.78), we can simplify the numerator as follows:

$$G_{\boldsymbol{pp}'}^{0}(\tau) - \frac{1}{\hbar}\int_0^{\beta\hbar} d\tau_1 \langle T_\tau \hat{H}_C^I(\tau_1)\hat{a}_{\boldsymbol{p}}(\tau)\hat{a}_{\boldsymbol{p}'}^\dagger(0)\rangle_0$$

$$+ \frac{1}{2\hbar^2}\int_0^{\beta\hbar} d\tau_1 \int_0^{\beta\hbar} d\tau_2 \langle T_\tau \hat{H}_C^I(\tau_1)\hat{H}_C^I(\tau_2)\hat{a}_{\boldsymbol{p}}(\tau)\hat{a}_{\boldsymbol{p}'}^\dagger(0)\rangle_0 + \cdots$$

$$= \left[G_{\boldsymbol{pp}'}^{0}(\tau) + G_{\boldsymbol{pp}'}^{(1)}(\tau) + G_{\boldsymbol{pp}'}^{(2)}(\tau) + \cdots\right](1 + D_1 + D_2 + \cdots)$$

Noting that the expression $(1 + D_1 + D_2 + \cdots)$ is exactly canceled with the denominator, the Green's function can be simplified as:

$$G_{\boldsymbol{pp'}}(\tau) = G^{0}_{\boldsymbol{pp'}}(\tau) + G^{(1)}_{\boldsymbol{pp'}}(\tau) + G^{(2)}_{\boldsymbol{pp'}}(\tau) + \cdots, \tag{S7.84}$$

where,

$$\begin{cases} G^{(1)}_{\boldsymbol{pp'}}(\tau) = -\frac{1}{\hbar}\int_0^{\beta\hbar} d\tau_1 \langle T_\tau \widehat{H}^I_C(\tau_1)\hat{a}_{\boldsymbol{q}\lambda}(\tau)\hat{a}^\dagger_{\boldsymbol{q'}\lambda'}(0)\rangle_{0,c} \\ G^{(2)}_{\boldsymbol{pp'}}(\tau) = \frac{1}{2\hbar^2}\int_0^{\beta\hbar} d\tau_1 \int_0^{\beta\hbar} d\tau_2 \langle T_\tau \widehat{H}^I_C(\tau_1)\widehat{H}^I_C(\tau_2)\hat{a}_{\boldsymbol{q}\lambda}(\tau)\hat{a}^\dagger_{\boldsymbol{q'}\lambda'}(0)\rangle_{0,c} \end{cases}. \tag{S7.85}$$

7.5 Calculation of Green's function

7.5.1 First order appriximation

In Eq. (S7.85), we go back to the full notation $\hat{a}_{\boldsymbol{q}\lambda}$ to distinguish phonons of different branches, then $G^{(1)}_{\boldsymbol{pp'}}(\tau)$ is calculated as:

$$\begin{aligned} G^{(1)}_{\boldsymbol{pp'}}(\tau) = -\frac{1}{\hbar}\frac{1}{2}\int_0^{\beta\hbar} d\tau_1 \langle T_\tau \Bigg[& \sum_{\boldsymbol{k}}\sum_{j=1}^{3r/2}\sum_{j'=\frac{3r}{2}+1}^{3r} V_{jj'}(\boldsymbol{k})\hat{Q}_{\boldsymbol{k}j}(\tau_1)\hat{\tilde{Q}}^\dagger_{\boldsymbol{k}j'}(\tau_1) \\ & + \sum_{\boldsymbol{k}}\sum_{j=1}^{3r/2}\sum_{j'=\frac{3r}{2}+1}^{3r} V^*_{jj'}(\boldsymbol{k})\hat{\tilde{Q}}_{\boldsymbol{k}j'}(\tau_1)\hat{Q}^\dagger_{\boldsymbol{k}j}(\tau_1)\Bigg]\hat{a}_{\boldsymbol{q}\lambda}(\tau)\hat{a}^\dagger_{\boldsymbol{q'}\lambda'}(0)\rangle_{0,c} \\ = -\frac{1}{2\hbar}\int_0^{\beta\hbar} d\tau_1 \langle T_\tau \Bigg\{ & \sum_{\boldsymbol{k}}\sum_{j=1}^{3r/2}\sum_{j'=\frac{3r}{2}+1}^{3r} \frac{\hbar V_{jj'}(\boldsymbol{k})}{2\sqrt{\omega_{\boldsymbol{k}j}\widetilde{\omega}_{\boldsymbol{k}j'}}}\left[\hat{a}_{\boldsymbol{k}j}(\tau_1) + \hat{a}^\dagger_{-\boldsymbol{k}j}(\tau_1)\right]\left[\hat{\tilde{a}}_{-\boldsymbol{k}j'}(\tau_1) + \hat{\tilde{a}}^\dagger_{\boldsymbol{k}j'}(\tau_1)\right] \\ & + \sum_{\boldsymbol{k}}\sum_{j=1}^{3r/2}\sum_{j'=\frac{3r}{2}+1}^{3r} \frac{\hbar V^*_{jj'}(\boldsymbol{k})}{2\sqrt{\omega_{\boldsymbol{k}j}\widetilde{\omega}_{\boldsymbol{k}j'}}}\left[\hat{\tilde{a}}_{\boldsymbol{k}j'}(\tau_1) + \hat{\tilde{a}}^\dagger_{-\boldsymbol{k}j'}(\tau_1)\right]\left[\hat{a}_{-\boldsymbol{k}j}(\tau_1) + \hat{a}^\dagger_{\boldsymbol{k}j}(\tau_1)\right]\Bigg\}\hat{a}_{\boldsymbol{q}\lambda}(\tau)\hat{a}^\dagger_{\boldsymbol{q'}\lambda'}(0)\rangle_{0,c} \end{aligned}$$

According to Wick's theorem[21], the terms that contain $a_{\boldsymbol{k}j}a_{-\boldsymbol{k}j'}$ and $a^\dagger_{-\boldsymbol{k}j}a^\dagger_{\boldsymbol{k}j'}$ are equal to zero, thus the first term of above equation are calculated as:

$$\begin{aligned} g_{11} = -\frac{1}{4}\sum_{\boldsymbol{k}}\sum_{j=1}^{\frac{3r}{2}}\sum_{j'=\frac{3r}{2}+1}^{3r} & \frac{V_{jj'}(\boldsymbol{k})}{\sqrt{\omega_{\boldsymbol{k}j}\widetilde{\omega}_{\boldsymbol{k}j'}}}\int_0^{\beta\hbar} d\tau_1 \Big\{\langle T_\tau \hat{a}^\dagger_{-\boldsymbol{k}j}(\tau_1)\hat{\tilde{a}}_{-\boldsymbol{k}j'}(\tau_1)\hat{a}_{\boldsymbol{q}\lambda}(\tau)\hat{a}^\dagger_{\boldsymbol{q'}\lambda'}(0)\rangle_{0,c} \\ & + \langle T_\tau \hat{a}_{\boldsymbol{k}j}(\tau_1)\hat{\tilde{a}}^\dagger_{\boldsymbol{k}j'}(\tau_1)\hat{a}_{\boldsymbol{q}\lambda}(\tau)\hat{a}^\dagger_{\boldsymbol{q'}\lambda'}(0)\rangle_{0,c}\Big\} \\ = -\frac{1}{4}\sum_{\boldsymbol{k}}\sum_{j=1}^{3r/2}\sum_{j'=\frac{3r}{2}+1}^{3r} & \frac{V_{jj'}(\boldsymbol{k})}{\sqrt{\omega_{\boldsymbol{k}j}\widetilde{\omega}_{\boldsymbol{k}j'}}}\int_0^{\beta\hbar} d\tau_1 \Big\{\langle T_\tau \hat{a}^\dagger_{-\boldsymbol{k}j}(\tau_1)\hat{a}_{\boldsymbol{q}\lambda}(\tau)\rangle_0 \langle T_\tau \hat{a}^\dagger_{\boldsymbol{q'}\lambda'}(0)\hat{\tilde{a}}_{-\boldsymbol{k}j'}(\tau_1)\rangle_0 \\ & + \langle T_\tau \hat{\tilde{a}}^\dagger_{\boldsymbol{k}j'}(\tau_1)\hat{a}_{\boldsymbol{q}\lambda}(\tau)\rangle_0 \langle T_\tau \hat{a}^\dagger_{\boldsymbol{q'}\lambda'}(0)\hat{a}_{\boldsymbol{k}j}(\tau_1)\rangle_0\Big\} \\ = -\frac{1}{4}\sum_{\boldsymbol{k}}\sum_{j=1}^{3r/2}\sum_{j'=\frac{3r}{2}+1}^{3r} & \frac{V_{jj'}(\boldsymbol{k})}{\sqrt{\omega_{\boldsymbol{k}j}\widetilde{\omega}_{\boldsymbol{k}j'}}}\int_0^{\beta\hbar} d\tau_1 \Big\{G^0_{\boldsymbol{q}\lambda}(\tau,\tau_1)\delta_{\boldsymbol{q},-\boldsymbol{k}}\delta_{\lambda j}G^0_{\boldsymbol{q'}\lambda'}(\tau_1,0)\delta_{\boldsymbol{q'},-\boldsymbol{k}}\delta_{\lambda' j'} \\ & + G^0_{\boldsymbol{q}\lambda}(\tau,\tau_1)\delta_{\boldsymbol{q},\boldsymbol{k}}\delta_{\lambda j'}G^0_{\boldsymbol{q'}\lambda'}(\tau_1,0)\delta_{\boldsymbol{q'},\boldsymbol{k}}\delta_{\lambda' j}\Big\} \end{aligned}$$

Simplification of above equation gives:

$$g_{11}=\begin{cases}\frac{-V_{\lambda\lambda'}(-\boldsymbol{q})}{4\sqrt{\omega_{\boldsymbol{q}\lambda}\widetilde{\omega}_{\boldsymbol{q}\lambda'}}}\int_0^{\beta\hbar}d\tau_1\,G^0_{\boldsymbol{q}\lambda}(\tau,\tau_1)G^0_{\boldsymbol{q}'\lambda'}(\tau_1,0)\delta_{\boldsymbol{q}\boldsymbol{q}'}, & 1\le\lambda\le\frac{3r}{2}<\lambda'\le 3r\\ \frac{-V_{\lambda'\lambda}(\boldsymbol{q})}{4\sqrt{\widetilde{\omega}_{\boldsymbol{q}\lambda}\omega_{\boldsymbol{q}\lambda'}}}\int_0^{\beta\hbar}d\tau_1\,G^0_{\boldsymbol{q}\lambda}(\tau,\tau_1)G^0_{\boldsymbol{q}'\lambda'}(\tau_1,0)\delta_{\boldsymbol{q}\boldsymbol{q}'}, & 1\le\lambda'\le\frac{3r}{2}<\lambda\le 3r\\ 0 & \text{else}\end{cases}. \tag{S7.86}$$

Similarity, the second term of $G^{(1)}_{\boldsymbol{p}\boldsymbol{p}'}(\tau)$ is calculated as:

$$\begin{aligned}g_{12}=-\frac{1}{4}\sum_{\boldsymbol{k}}\sum_{j=1}^{\frac{3r}{2}}\sum_{j'=\frac{3r}{2}+1}^{3r}\frac{-V^*_{jj'}(\boldsymbol{k})}{4\sqrt{\omega_{\boldsymbol{k}j}\widetilde{\omega}_{\boldsymbol{k}j'}}}\int_0^{\beta\hbar}d\tau_1\Big\{&\langle T_\tau\hat{\tilde{a}}_{\boldsymbol{k}j'}(\tau_1)\hat{a}^\dagger_{\boldsymbol{k}j}(\tau_1)\hat{a}_{\boldsymbol{q}\lambda}(\tau)\hat{a}^\dagger_{\boldsymbol{q}'\lambda'}(0)\rangle_{0,c}\\&+\langle T_\tau\hat{\tilde{a}}^\dagger_{-\boldsymbol{k}j'}(\tau_1)\hat{a}_{-\boldsymbol{k}j}(\tau_1)\hat{a}_{\boldsymbol{q}\lambda}(\tau)\hat{a}^\dagger_{\boldsymbol{q}'\lambda'}(0)\rangle_{0,c}\Big\}\\=-\frac{1}{4}\sum_{\boldsymbol{k}}\sum_{j=1}^{\frac{3r}{2}}\sum_{j'=\frac{3r}{2}+1}^{3r}\frac{-V^*_{jj'}(\boldsymbol{k})}{4\sqrt{\omega_{\boldsymbol{k}j}\widetilde{\omega}_{\boldsymbol{k}j'}}}\int_0^{\beta\hbar}d\tau_1\Big\{&\langle T_\tau\hat{a}^\dagger_{\boldsymbol{q}'\lambda'}(0)\hat{\tilde{a}}_{\boldsymbol{k}j'}(\tau_1)\rangle_0\,\langle T_\tau\hat{a}^\dagger_{\boldsymbol{k}j}(\tau_1)\hat{a}_{\boldsymbol{q}\lambda}(\tau)\rangle_0\\&+\langle T_\tau\hat{a}^\dagger_{\boldsymbol{q}'\lambda'}(0)\hat{a}_{-\boldsymbol{k}j}(\tau_1)\rangle_0\,\langle T_\tau\hat{\tilde{a}}^\dagger_{-\boldsymbol{k}j'}(\tau_1)\hat{a}_{\boldsymbol{q}\lambda}(\tau)\rangle_0\Big\}\end{aligned}$$

i.e.,

$$g_{12}=\begin{cases}\frac{-V^*_{\lambda\lambda'}(\boldsymbol{q})}{4\sqrt{\omega_{\boldsymbol{q}\lambda}\widetilde{\omega}_{\boldsymbol{q}\lambda'}}}\int_0^{\beta\hbar}d\tau_1\,G^0_{\boldsymbol{q}'\lambda'}(\tau_1,0)G^0_{\boldsymbol{q}\lambda}(\tau,\tau_1)\delta_{\boldsymbol{q}\boldsymbol{q}'}, & 1\le\lambda\le\frac{3r}{2}<\lambda'\le 3r\\ \frac{-V^*_{\lambda'\lambda}(-\boldsymbol{q})}{4\sqrt{\widetilde{\omega}_{\boldsymbol{q}\lambda}\omega_{\boldsymbol{q}\lambda'}}}\int_0^{\beta\hbar}d\tau_1\,G^0_{\boldsymbol{q}'\lambda'}(\tau_1,0)G^0_{\boldsymbol{q}\lambda}(\tau,\tau_1)\delta_{\boldsymbol{q}\boldsymbol{q}'}, & 1\le\lambda'\le\frac{3r}{2}<\lambda\le 3r\\ 0 & \text{else}\end{cases}. \tag{S7.87}$$

Note that since $V^*_{\lambda\lambda'}(\boldsymbol{q})=V_{\lambda\lambda'}(-\boldsymbol{q})$ [Eq. (S7.44)], the first order approximation of Green's function can be written as

$$G^{(1)}_{\boldsymbol{q}\lambda,\boldsymbol{q}'\lambda'}(\tau)=\begin{cases}\frac{-V_{\lambda\lambda'}(-\boldsymbol{q})}{2\sqrt{\omega_{\boldsymbol{q}\lambda}\widetilde{\omega}_{\boldsymbol{q}\lambda'}}}\int_0^{\beta\hbar}d\tau_1\,G^0_{\boldsymbol{q}\lambda}(\tau,\tau_1)G^0_{\boldsymbol{q}'\lambda'}(\tau_1,0)\delta_{\boldsymbol{q}\boldsymbol{q}'}, & 1\le\lambda\le\frac{3r}{2}<\lambda'\le 3r\\ \frac{-V_{\lambda'\lambda}(\boldsymbol{q})}{2\sqrt{\widetilde{\omega}_{\boldsymbol{q}\lambda}\omega_{\boldsymbol{q}\lambda'}}}\int_0^{\beta\hbar}d\tau_1\,G^0_{\boldsymbol{q}\lambda}(\tau,\tau_1)G^0_{\boldsymbol{q}'\lambda'}(\tau_1,0)\delta_{\boldsymbol{q}\boldsymbol{q}'}, & 1\le\lambda'\le\frac{3r}{2}<\lambda\le 3r\\ 0 & \text{else}\end{cases}. \tag{S7.88}$$

To derive the Green's function in frequency domain, we use the expression for Fourier series, then we have:

$$\begin{aligned}\int_0^{\beta\hbar}d\tau_1\,G^0_{\boldsymbol{q}\lambda}(\tau,\tau_1)G^0_{\boldsymbol{q}'\lambda'}(\tau_1,0)&=\int_0^{\beta\hbar}d\tau_1\left[\frac{1}{\beta\hbar}\sum_n e^{-i\omega_n(\tau-\tau_1)}G^0_{\boldsymbol{q}\lambda}(i\omega_n)\right]\left[\frac{1}{\beta\hbar}\sum_{n'}e^{-i\omega_{n'}\tau_1}G^0_{\boldsymbol{q}'\lambda'}(i\omega_{n'})\right]\\&=\frac{1}{(\beta\hbar)^2}\sum_{n,n'}e^{-i\omega_n\tau}\left[\int_0^{\beta\hbar}d\tau_1\,e^{i(\omega_n-\omega_{n'})\tau_1}\right]G^0_{\boldsymbol{q}\lambda}(i\omega_n)G^0_{\boldsymbol{q}'\lambda'}(i\omega_{n'})=\\&=\frac{1}{(\beta\hbar)^2}\sum_{n,n'}e^{-i\omega_n\tau}[\beta\hbar\delta_{nn'}]G^0_{\boldsymbol{q}\lambda}(i\omega_n)G^0_{\boldsymbol{q}'\lambda'}(i\omega_{n'})=\frac{1}{\beta\hbar}\sum_n e^{-i\omega_n\tau}G^0_{\boldsymbol{q}\lambda}(i\omega_n)G^0_{\boldsymbol{q}'\lambda'}(i\omega_n)\end{aligned}$$

According to the definition of Fourier series [see Eq. (S7.60)], we get the Fourier coefficient of

$G^{(1)}_{\boldsymbol{q}\lambda,\boldsymbol{q}'\lambda'}(\tau)$:

$$G^{(1)}_{\boldsymbol{q}\lambda,\boldsymbol{q}'\lambda'}(i\omega_n)=\begin{cases}\frac{-V_{\lambda\lambda'}(-\boldsymbol{q})}{2\sqrt{\omega_{\boldsymbol{q}\lambda}\widetilde{\omega}_{\boldsymbol{q}\lambda'}}}G^0_{\boldsymbol{q}\lambda}(i\omega_n)G^0_{\boldsymbol{q}'\lambda'}(i\omega_n)\delta_{\boldsymbol{q}\boldsymbol{q}'}, & 1\le\lambda\le\frac{3r}{2}<\lambda'\le 3r\\ \frac{-V_{\lambda'\lambda}(\boldsymbol{q})}{2\sqrt{\widetilde{\omega}_{\boldsymbol{q}\lambda}\omega_{\boldsymbol{q}\lambda'}}}G^0_{\boldsymbol{q}\lambda}(i\omega_n)G^0_{\boldsymbol{q}'\lambda'}(i\omega_n)\delta_{\boldsymbol{q}\boldsymbol{q}'}, & 1\le\lambda'\le\frac{3r}{2}<\lambda\le 3r\\ 0, & \text{else}\end{cases} \tag{S7.89}$$

where $G^{(1)}_{\boldsymbol{q}\lambda,\boldsymbol{q}'\lambda'}(i\omega_n)=G^0_{\boldsymbol{q}\lambda}(i\omega_n)\times\Sigma^{(1)}_{\boldsymbol{q}\lambda,\boldsymbol{q}'\lambda'}(i\omega_n)\times G^0_{\boldsymbol{q}'\lambda'}(i\omega_n)$ and $\Sigma^{(1)}_{\boldsymbol{q}\lambda,\boldsymbol{q}'\lambda'}(i\omega_n)$ is defined as

$$\Sigma^{(1)}_{\boldsymbol{q}\lambda,\boldsymbol{q}'\lambda'}(i\omega_n)=\begin{cases}\frac{-V_{\lambda\lambda'}(-\boldsymbol{q})}{2\sqrt{\omega_{\boldsymbol{q}\lambda}\widetilde{\omega}_{\boldsymbol{q}\lambda'}}}\delta_{\boldsymbol{q}\boldsymbol{q}'}, & 1\le\lambda\le\frac{3r}{2}<\lambda'\le 3r\\ \frac{-V_{\lambda'\lambda}(\boldsymbol{q})}{2\sqrt{\widetilde{\omega}_{\boldsymbol{q}\lambda}\omega_{\boldsymbol{q}\lambda'}}}\delta_{\boldsymbol{q}\boldsymbol{q}'}, & 1\le\lambda'\le\frac{3r}{2}<\lambda\le 3r\\ 0, & \text{else}\end{cases} \tag{S7.90}$$

7.5.2 Second order approximation

The second order approximation of the Green's function in Eq. (S7.85), $G^{(2)}_{\boldsymbol{q}\lambda,\boldsymbol{q}'\lambda'}(\tau)$, is calculated as:

$$\begin{aligned}G^{(2)}_{\boldsymbol{q}\lambda,\boldsymbol{q}'\lambda'}(\tau)=\frac{1}{8\hbar^2}\int_0^{\beta\hbar}d\tau_1\int_0^{\beta\hbar}d\tau_2\,\langle T_\tau\Bigg[&\sum_{\boldsymbol{k}_1}\sum_{j_1=1}^{\frac{3r}{2}}\sum_{j_1'=\frac{3r}{2}+1}^{3r}V_{j_1j_1'}(\boldsymbol{k}_1)\hat{Q}_{\boldsymbol{k}_1j_1}(\tau_1)\hat{\tilde{Q}}^\dagger_{\boldsymbol{k}_1j_1'}(\tau_1)\\&+\sum_{\boldsymbol{k}_1}\sum_{i_1=1}^{\frac{3r}{2}}\sum_{i_1'=\frac{3r}{2}+1}^{3r}V^*_{i_1i_1'}(\boldsymbol{k}_1)\hat{\tilde{Q}}_{\boldsymbol{k}_1i_1'}(\tau_1)\hat{Q}^\dagger_{\boldsymbol{k}_1i_1}(\tau_1)\Bigg]\Bigg[\sum_{\boldsymbol{k}_2}\sum_{j_2=1}^{\frac{3r}{2}}\sum_{j_2'=\frac{3r}{2}+1}^{3r}V_{j_2j_2'}(\boldsymbol{k}_2)\hat{Q}_{\boldsymbol{k}_2j_2}(\tau_2)\hat{\tilde{Q}}^\dagger_{\boldsymbol{k}_2j_2'}(\tau_2)\\&+\sum_{\boldsymbol{k}_2}\sum_{i_2=1}^{\frac{3r}{2}}\sum_{i_2'=\frac{3r}{2}+1}^{3r}V^*_{i_2i_2'}(\boldsymbol{k}_2)\hat{\tilde{Q}}_{\boldsymbol{k}_2i_2'}(\tau_2)\hat{Q}^\dagger_{\boldsymbol{k}_2i_2}(\tau_2)\Bigg]\hat{a}_{\boldsymbol{q}\lambda}(\tau)\hat{a}^\dagger_{\boldsymbol{q}'\lambda'}(0)\rangle_{0,c}=g_1+g_2+g_3+g_4\end{aligned}$$

where,

$$g_1=\tfrac{1}{8\hbar^2}\textstyle\int_0^{\beta\hbar}d\tau_1\int_0^{\beta\hbar}d\tau_2\begin{Bmatrix}\sum_{\boldsymbol{k}_1j_1j_1'}^{1\le j_1\le\frac{3r}{2}<j_1'\le 3r}\sum_{\boldsymbol{k}_2j_2j_2'}^{1\le j_2\le\frac{3r}{2}<j_2'\le 3r}V_{j_1j_1'}(\boldsymbol{k}_1)V_{j_2j_2'}(\boldsymbol{k}_2)\\ \times\langle T_\tau\hat{Q}_{\boldsymbol{k}_1j_1}(\tau_1)\hat{\tilde{Q}}^\dagger_{\boldsymbol{k}_1j_1'}(\tau_1)\hat{Q}_{\boldsymbol{k}_2j_2}(\tau_2)\hat{\tilde{Q}}^\dagger_{\boldsymbol{k}_2j_2'}(\tau_2)\hat{a}_{\boldsymbol{q}\lambda}(\tau)\hat{a}^\dagger_{\boldsymbol{q}'\lambda'}(0)\rangle_{0,c}\end{Bmatrix} \tag{S7.91}$$

$$g_2=\tfrac{1}{8\hbar^2}\textstyle\int_0^{\beta\hbar}d\tau_1\int_0^{\beta\hbar}d\tau_2\begin{Bmatrix}\sum_{\boldsymbol{k}_1j_1j_1'}^{1\le j_1\le\frac{3r}{2}<j_1'\le 3r}\sum_{\boldsymbol{k}_2i_2i_2'}^{1\le i_2\le\frac{3r}{2}<i_2'\le 3r}V_{j_1j_1'}(\boldsymbol{k}_1)V^*_{i_2i_2'}(\boldsymbol{k}_2)\\ \times\langle T_\tau\hat{Q}_{\boldsymbol{k}_1j_1}(\tau_1)\hat{\tilde{Q}}^\dagger_{\boldsymbol{k}_1j_1'}(\tau_1)\hat{\tilde{Q}}_{\boldsymbol{k}_2i_2'}(\tau_2)\hat{Q}^\dagger_{\boldsymbol{k}_2i_2}(\tau_2)\hat{a}_{\boldsymbol{q}\lambda}(\tau)\hat{a}^\dagger_{\boldsymbol{q}'\lambda'}(0)\rangle_{0,c}\end{Bmatrix} \tag{S7.92}$$

$$g_3=\tfrac{1}{8\hbar^2}\textstyle\int_0^{\beta\hbar}d\tau_1\int_0^{\beta\hbar}d\tau_2\begin{Bmatrix}\sum_{\boldsymbol{k}_1i_1i_1'}^{1\le i_1\le\frac{3r}{2}<i_1'\le 3r}\sum_{\boldsymbol{k}_2j_2j_2'}^{1\le j_2\le\frac{3r}{2}<j_2'\le 3r}V^*_{i_1i_1'}(\boldsymbol{k}_1)V_{j_2j_2'}(\boldsymbol{k}_2)\\ \times\langle T_\tau\hat{\tilde{Q}}_{\boldsymbol{k}_1i_1'}(\tau_1)\hat{Q}^\dagger_{\boldsymbol{k}_1i_1}(\tau_1)\hat{Q}_{\boldsymbol{k}_2j_2}(\tau_2)\hat{\tilde{Q}}^\dagger_{\boldsymbol{k}_2j_2'}(\tau_2)\hat{a}_{\boldsymbol{q}\lambda}(\tau)\hat{a}^\dagger_{\boldsymbol{q}'\lambda'}(0)\rangle_{0,c}\end{Bmatrix} \tag{S7.93}$$

$$g_4 = \frac{1}{8\hbar^2}\int_0^{\beta\hbar} d\tau_1 \int_0^{\beta\hbar} d\tau_2 \begin{Bmatrix} \sum_{\boldsymbol{k_1} i_1 i_1'}^{1\le i_1 \le \frac{3r}{2} < i_1' \le 3r} \sum_{\boldsymbol{k_2} i_2 i_2'}^{1\le i_2 \le \frac{3r}{2} < i_2' \le 3r} V^*_{i_1 i_1'}(\boldsymbol{k_1}) V^*_{i_2 i_2'}(\boldsymbol{k_2}) \\ \times \langle T_\tau \hat{\tilde{Q}}_{\boldsymbol{k_1} i_1'}(\tau_1) \hat{Q}^\dagger_{\boldsymbol{k_1} i_1}(\tau_1) \hat{\tilde{Q}}_{\boldsymbol{k_2} i_2'}(\tau_2) \hat{Q}^\dagger_{\boldsymbol{k_2} i_2}(\tau_2) \hat{a}_{\boldsymbol{q}\lambda}(\tau) \hat{a}^\dagger_{\boldsymbol{q}'\lambda'}(0) \rangle_{0,c} \end{Bmatrix} \quad \text{(S7.94)}$$

In what follows we will expand the term g_2. The expansion of all other terms follows the same lines and eventually results in the same expression. Expanding the product $\hat{Q}_{\boldsymbol{k_1} j_1} \hat{\tilde{Q}}^\dagger_{\boldsymbol{k_1} j_1'} \hat{\tilde{Q}}_{\boldsymbol{k_2} i_2'} \hat{Q}^\dagger_{\boldsymbol{k_2} i_2}$, we can rewrite Eq. (S7.92) as follows

$$g_2 = \frac{1}{32}\int_0^{\beta\hbar} d\tau_1 \int_0^{\beta\hbar} d\tau_2 \left\{ \sum_{\boldsymbol{k_1} j_1 j_1'}^{1\le j_1 \le \frac{3r}{2} < j_1' \le 3r} \sum_{\boldsymbol{k_2} i_2 i_2'}^{1\le i_2 \le \frac{3r}{2} < i_2' \le 3r} \frac{V_{j_1 j_1'}(\boldsymbol{k_1}) V^*_{i_2 i_2'}(\boldsymbol{k_2})}{\sqrt{\omega_{\boldsymbol{k_1} j_1} \tilde{\omega}_{\boldsymbol{k_1} j_1'} \omega_{\boldsymbol{k_2} i_2} \tilde{\omega}_{\boldsymbol{k_2} i_2'}}} \times I \right\} \quad \text{(S7.95)}$$

Where

$$\begin{aligned} I &= \langle T_\tau \left[\hat{a}_{\boldsymbol{k_1} j_1}(\tau_1) + \hat{a}^\dagger_{-\boldsymbol{k_1} j_1}(\tau_1)\right] \left[\hat{\tilde{a}}_{-\boldsymbol{k_1} j_1'}(\tau_1) + \hat{\tilde{a}}^\dagger_{\boldsymbol{k_1} j_1'}(\tau_1)\right] \left[\hat{\tilde{a}}_{\boldsymbol{k_2} i_2'}(\tau_2) + \hat{\tilde{a}}^\dagger_{-\boldsymbol{k_2} i_2'}(\tau_2)\right] \left[\hat{a}_{-\boldsymbol{k_2} i_2}(\tau_2) + \hat{a}^\dagger_{\boldsymbol{k_2} i_2}(\tau_2)\right] \hat{a}_{\boldsymbol{q}\lambda}(\tau) \hat{a}^\dagger_{\boldsymbol{q}'\lambda'}(0) \rangle_{0,c} \\ &= \langle T_\tau \left[\hat{a}_{\boldsymbol{k_1} j_1} \hat{\tilde{a}}_{-\boldsymbol{k_1} j_1'} + \hat{a}_{\boldsymbol{k_1} j_1} \hat{\tilde{a}}^\dagger_{\boldsymbol{k_1} j_1'} + \hat{a}^\dagger_{-\boldsymbol{k_1} j_1} \hat{\tilde{a}}_{-\boldsymbol{k_1} j_1'} + \hat{a}^\dagger_{-\boldsymbol{k_1} j_1} \hat{\tilde{a}}^\dagger_{\boldsymbol{k_1} j_1'}\right]_{\tau_1} \left[\hat{\tilde{a}}_{\boldsymbol{k_2} i_2'} \hat{a}_{-\boldsymbol{k_2} i_2} + \hat{\tilde{a}}_{\boldsymbol{k_2} i_2'} \hat{a}^\dagger_{\boldsymbol{k_2} i_2} + \hat{\tilde{a}}^\dagger_{-\boldsymbol{k_2} i_2'} \hat{a}_{-\boldsymbol{k_2} i_2} \right. \\ &\quad \left. + \hat{\tilde{a}}^\dagger_{-\boldsymbol{k_2} i_2'} \hat{a}^\dagger_{\boldsymbol{k_2} i_2}\right]_{\tau_2} \hat{a}_{\boldsymbol{q}\lambda}(\tau) \hat{a}^\dagger_{\boldsymbol{q}'\lambda'}(0) \rangle_{0,c} \\ &= \langle T_\tau \left[\hat{a}_{\boldsymbol{k_1} j_1} \hat{\tilde{a}}^\dagger_{\boldsymbol{k_1} j_1'} + \hat{a}^\dagger_{-\boldsymbol{k_1} j_1} \hat{\tilde{a}}_{-\boldsymbol{k_1} j_1'}\right]_{\tau_1} \left[\hat{\tilde{a}}_{\boldsymbol{k_2} i_2'} \hat{a}^\dagger_{\boldsymbol{k_2} i_2} + \hat{\tilde{a}}^\dagger_{-\boldsymbol{k_2} i_2'} \hat{a}_{-\boldsymbol{k_2} i_2}\right]_{\tau_2} \hat{a}_{\boldsymbol{q}\lambda}(\tau) \hat{a}^\dagger_{\boldsymbol{q}'\lambda'}(0) \rangle_{0,c} \end{aligned}$$

Where the symbol $[...]_{\tau_1}$ signifies that the operators in the brackets are given in the interaction picture. The last equality in above equation comes from the fact that the contractions of the product of the operators are equal to zero when the number of creation and annihilation operators are not the same (see Wick's theorem in Ref. [21]). Using Wick's theorem[21], we are able to calculate the above equation term by term as follows:

$$\begin{cases} I_1 = \langle T_\tau \hat{a}_{\boldsymbol{k_1} j_1}(\tau_1) \hat{\tilde{a}}^\dagger_{\boldsymbol{k_1} j_1'}(\tau_1) \hat{\tilde{a}}_{\boldsymbol{k_2} i_2'}(\tau_2) \hat{a}^\dagger_{\boldsymbol{k_2} i_2}(\tau_2) \hat{a}_{\boldsymbol{q}\lambda}(\tau) \hat{a}^\dagger_{\boldsymbol{q}'\lambda'}(0) \rangle_{0,c} \\ I_2 = \langle T_\tau \hat{a}_{\boldsymbol{k_1} j_1}(\tau_1) \hat{\tilde{a}}^\dagger_{\boldsymbol{k_1} j_1'}(\tau_1) \hat{\tilde{a}}^\dagger_{-\boldsymbol{k_2} i_2'}(\tau_2) \hat{a}_{-\boldsymbol{k_2} i_2}(\tau_2) \hat{a}_{\boldsymbol{q}\lambda}(\tau) \hat{a}^\dagger_{\boldsymbol{q}'\lambda'}(0) \rangle_{0,c} \\ I_3 = \langle T_\tau \hat{a}^\dagger_{-\boldsymbol{k_1} j_1}(\tau_1) \hat{\tilde{a}}_{-\boldsymbol{k_1} j_1'}(\tau_1) \hat{\tilde{a}}_{\boldsymbol{k_2} i_2'}(\tau_2) \hat{a}^\dagger_{\boldsymbol{k_2} i_2}(\tau_2) \hat{a}_{\boldsymbol{q}\lambda}(\tau) \hat{a}^\dagger_{\boldsymbol{q}'\lambda'}(0) \rangle_{0,c} \\ I_4 = \langle T_\tau \hat{a}^\dagger_{-\boldsymbol{k_1} j_1}(\tau_1) \hat{\tilde{a}}_{-\boldsymbol{k_1} j_1'}(\tau_1) \hat{\tilde{a}}^\dagger_{-\boldsymbol{k_2} i_2'}(\tau_2) \hat{a}_{-\boldsymbol{k_2} i_2}(\tau_2) \hat{a}_{\boldsymbol{q}\lambda}(\tau) \hat{a}^\dagger_{\boldsymbol{q}'\lambda'}(0) \rangle_{0,c} \end{cases} . \quad \text{(S7.96)}$$

We shall now calculate them term by term:

$$
\begin{aligned}
I_1 = \langle T_\tau \hat{a}_{\boldsymbol{k_1} j_1}(\tau_1) \hat{\tilde{a}}^\dagger_{\boldsymbol{k_1} j_1'}(\tau_1) \hat{\tilde{a}}_{\boldsymbol{k_2} i_2'}(\tau_2) \hat{a}^\dagger_{\boldsymbol{k_2} i_2}(\tau_2) \hat{a}_{\boldsymbol{q}\lambda}(\tau) a^\dagger_{\boldsymbol{q}'\lambda'}(0) \rangle_{0,c} \\
&= \langle T_\tau \hat{a}^\dagger_{\boldsymbol{q}'\lambda'}(0) \hat{a}_{\boldsymbol{k_1} j_1}(\tau_1) \rangle_0 \langle T_\tau \hat{a}^\dagger_{\boldsymbol{k_2} i_2}(\tau_2) \hat{\tilde{a}}_{\boldsymbol{k_2} i_2'}(\tau_2) \rangle_0 \langle T_\tau \hat{\tilde{a}}^\dagger_{\boldsymbol{k_1} j_1'}(\tau_1) \hat{a}_{\boldsymbol{q}\lambda}(\tau) \rangle_0 \\
&+ \langle T_\tau \hat{a}^\dagger_{\boldsymbol{k_2} i_2}(\tau_2) \hat{a}_{\boldsymbol{k_1} j_1}(\tau_1) \rangle_0 \langle T_\tau \hat{a}^\dagger_{\boldsymbol{q}'\lambda'}(0) \hat{\tilde{a}}_{\boldsymbol{k_2} i_2'}(\tau_2) \rangle_0 \langle T_\tau \hat{\tilde{a}}^\dagger_{\boldsymbol{k_1} j_1'}(\tau_1) \hat{a}_{\boldsymbol{q}\lambda}(\tau) \rangle_0 \\
&+ \langle T_\tau \hat{a}^\dagger_{\boldsymbol{q}'\lambda'}(0) \hat{\tilde{a}}_{\boldsymbol{k_2} i_2'}(\tau_2) \rangle_0 \langle T_\tau \hat{\tilde{a}}^\dagger_{\boldsymbol{k_1} j_1'}(\tau_1) \hat{a}_{\boldsymbol{k_1} j_1}(\tau_1) \rangle_0 \langle T_\tau \hat{a}^\dagger_{\boldsymbol{k_2} i_2}(\tau_2) \hat{a}_{\boldsymbol{q}\lambda}(\tau) \rangle_0 \\
&+ \langle T_\tau \hat{\tilde{a}}^\dagger_{\boldsymbol{k_1} j_1'}(\tau_1) \hat{\tilde{a}}_{\boldsymbol{k_2} i_2'}(\tau_2) \rangle_0 \langle T_\tau \hat{a}^\dagger_{\boldsymbol{q}'\lambda'}(0) \hat{a}_{\boldsymbol{k_1} j_1}(\tau_1) \rangle_0 \langle T_\tau \hat{a}^\dagger_{\boldsymbol{k_2} i_2}(\tau_2) \hat{a}_{\boldsymbol{q}\lambda}(\tau) \rangle_{0,c} \\
&= \left[G^0_{\boldsymbol{q}'\lambda'}(\tau_1, 0) \delta_{\boldsymbol{k_1 q}'} \delta_{j_1 \lambda'} \cdot G^0_{\boldsymbol{k_2} j_2}(\tau_2, \tau_2) \delta_{i_2 i_2'} \cdot G^0_{\boldsymbol{q}\lambda}(\tau, \tau_1) \delta_{\boldsymbol{k_1 q}} \delta_{j_1' \lambda} \right] \\
&+ \left[G^0_{\boldsymbol{k_1} j_1}(\tau_1, \tau_2) \delta_{\boldsymbol{k_1 k_2}} \delta_{j_1 i_2} \cdot G^0_{\boldsymbol{q}'\lambda'}(\tau_2, 0) \delta_{\boldsymbol{k_2 q}'} \delta_{i_2' \lambda'} \cdot G^0_{\boldsymbol{q}\lambda}(\tau, \tau_1) \delta_{\boldsymbol{k_1 q}} \delta_{j_1' \lambda} \right] \\
&+ \left[G^0_{\boldsymbol{q}'\lambda'}(\tau_2, 0) \delta_{\boldsymbol{k_2 q}'} \delta_{i_2' \lambda'} \cdot G^0_{\boldsymbol{k_1} j_1}(\tau_1, \tau_1) \delta_{j_1 j_1'} \cdot G^0_{\boldsymbol{q}\lambda}(\tau, \tau_2) \delta_{\boldsymbol{k_2 q}} \delta_{i_2 \lambda} \right] \\
&+ \left[G^0_{\boldsymbol{k_1} j_1'}(\tau_2, \tau_1) \delta_{\boldsymbol{k_1 k_2}} \delta_{i_2' j_1'} \cdot G^0_{\boldsymbol{q}'\lambda'}(\tau_1, 0) \delta_{\boldsymbol{k_1 q}'} \delta_{j_1 \lambda'} \cdot G^0_{\boldsymbol{q}\lambda}(\tau, \tau_2) \delta_{\boldsymbol{k_2 q}} \delta_{i_2 \lambda} \right] \\
&= \left[G^0_{\boldsymbol{k_1} j_1}(\tau_1, \tau_2) \delta_{\boldsymbol{k_1 k_2}} \delta_{j_1 i_2} \cdot G^0_{\boldsymbol{q}'\lambda'}(\tau_2, 0) \delta_{\boldsymbol{k_2 q}'} \delta_{i_2' \lambda'} \cdot G^0_{\boldsymbol{q}\lambda}(\tau, \tau_1) \delta_{\boldsymbol{k_1 q}} \delta_{j_1' \lambda} \right] \\
&+ \left[G^0_{\boldsymbol{k_1} j_1'}(\tau_2, \tau_1) \delta_{\boldsymbol{k_1 k_2}} \delta_{i_2' j_1'} \cdot G^0_{\boldsymbol{q}'\lambda'}(\tau_1, 0) \delta_{\boldsymbol{k_1 q}'} \delta_{j_1 \lambda'} \cdot G^0_{\boldsymbol{q}\lambda}(\tau, \tau_2) \delta_{\boldsymbol{k_2 q}} \delta_{i_2 \lambda} \right]
\end{aligned}
$$

The last equality results from the fact that j_1 and j_1' are indices of different ranges (belonging to different subsystems) and the same holds for i_2 and i_2'. Similarity,

$$
\begin{aligned}
I_4 = \langle T_\tau \hat{a}^\dagger_{-\boldsymbol{k_1} j_1}(\tau_1) \hat{\tilde{a}}_{-\boldsymbol{k_1} j_1'}(\tau_1) \hat{\tilde{a}}^\dagger_{-\boldsymbol{k_2} i_2'}(\tau_2) \hat{a}_{-\boldsymbol{k_2} i_2}(\tau_2) \hat{a}_{\boldsymbol{q}\lambda}(\tau) \hat{\tilde{a}}^\dagger_{\boldsymbol{q}'\lambda'}(0) \rangle_{0,c} \\
&= \langle T_\tau \hat{\tilde{a}}^\dagger_{\boldsymbol{q}'\lambda'}(0) \hat{\tilde{a}}_{-\boldsymbol{k_1} j_1'}(\tau_1) \rangle_0 \langle T_\tau \hat{a}^\dagger_{-\boldsymbol{k_1} j_1}(\tau_1) \hat{a}_{\boldsymbol{q}\lambda}(\tau) \rangle_0 \langle T_\tau \hat{\tilde{a}}^\dagger_{-\boldsymbol{k_2} i_2'}(\tau_2) \hat{a}_{-\boldsymbol{k_2} i_2}(\tau_2) \rangle_0 \\
&+ \langle T_\tau \hat{a}^\dagger_{\boldsymbol{q}'\lambda'}(0) \hat{a}_{-\boldsymbol{k_2} i_2}(\tau_2) \rangle_0 \langle T_\tau \hat{a}^\dagger_{-\boldsymbol{k_1} j_1}(\tau_1) \hat{a}_{\boldsymbol{q}\lambda}(\tau) \rangle_0 \langle T_\tau \hat{\tilde{a}}^\dagger_{-\boldsymbol{k_2} i_2'}(\tau_2) \hat{\tilde{a}}_{-\boldsymbol{k_1} j_1'}(\tau_1) \rangle_0 \\
&+ \langle T_\tau \hat{a}^\dagger_{\boldsymbol{q}'\lambda'}(0) \hat{a}_{-\boldsymbol{k_2} i_2}(\tau_2) \rangle_0 \langle T_\tau \hat{\tilde{a}}^\dagger_{-\boldsymbol{k_2} i_2'}(\tau_2) \hat{a}_{\boldsymbol{q}\lambda}(\tau) \rangle_0 \langle T_\tau \hat{a}^\dagger_{-\boldsymbol{k_1} j_1}(\tau_1) \hat{\tilde{a}}_{-\boldsymbol{k_1} j_1'}(\tau_1) \rangle_0 \\
&+ \langle T_\tau \hat{a}^\dagger_{\boldsymbol{q}'\lambda'}(0) \hat{\tilde{a}}_{-\boldsymbol{k_1} j_1'}(\tau_1) \rangle_0 \langle T_\tau \hat{\tilde{a}}^\dagger_{-\boldsymbol{k_2} i_2'}(\tau_2) \hat{a}_{\boldsymbol{q}\lambda}(\tau) \rangle_0 \langle T_\tau \hat{a}^\dagger_{-\boldsymbol{k_1} j_1}(\tau_1) \hat{a}_{-\boldsymbol{k_2} i_2}(\tau_2) \rangle_0 \\
&= \left[G^0_{\boldsymbol{q}'\lambda'}(\tau_1, 0) \delta_{-\boldsymbol{k_1 q}'} \delta_{j_1' \lambda'} \cdot G^0_{\boldsymbol{q}\lambda}(\tau, \tau_1) \delta_{-\boldsymbol{k_1 q}} \delta_{j_1 \lambda} \cdot G^0_{-\boldsymbol{k_2} i_2}(\tau_2, \tau_2) \delta_{i_2 i_2'} \right] \\
&+ \left[G^0_{\boldsymbol{q}'\lambda'}(\tau_2, 0) \delta_{-\boldsymbol{k_2 q}'} \delta_{i_2 \lambda'} \cdot G^0_{\boldsymbol{q}\lambda}(\tau, \tau_1) \delta_{-\boldsymbol{k_1 q}} \delta_{j_1 \lambda} \cdot G^0_{-\boldsymbol{k_1} j_1'}(\tau_1, \tau_2) \delta_{\boldsymbol{k_1 k_2}} \delta_{j_1' i_2'} \right] \\
&+ \left[G^0_{\boldsymbol{q}'\lambda'}(\tau_2, 0) \delta_{-\boldsymbol{k_2 q}'} \delta_{i_2 \lambda'} \cdot G^0_{\boldsymbol{q}\lambda}(\tau, \tau_2) \delta_{-\boldsymbol{k_2 q}} \delta_{i_2' \lambda} \cdot G^0_{-\boldsymbol{k_1} j_1}(\tau_1, \tau_1) \delta_{j_1 j_1'} \right] \\
&+ \left[G^0_{\boldsymbol{q}'\lambda'}(\tau_1, 0) \delta_{-\boldsymbol{k_1 q}'} \delta_{j_1' \lambda'} \cdot G^0_{\boldsymbol{q}\lambda}(\tau, \tau_2) \delta_{-\boldsymbol{k_2 q}} \delta_{i_2' \lambda} \cdot G^0_{-\boldsymbol{k_1} j_1}(\tau_2, \tau_1) \delta_{\boldsymbol{k_1 k_2}} \delta_{j_1 i_2} \right] \\
&= \left[G^0_{\boldsymbol{q}'\lambda'}(\tau_2, 0) \delta_{-\boldsymbol{k_2 q}'} \delta_{i_2 \lambda'} \cdot G^0_{\boldsymbol{q}\lambda}(\tau, \tau_1) \delta_{-\boldsymbol{k_1 q}} \delta_{j_1 \lambda} \cdot G^0_{-\boldsymbol{k_1} j_1'}(\tau_1, \tau_2) \delta_{\boldsymbol{k_1 k_2}} \delta_{j_1' i_2'} \right] \\
&+ \left[G^0_{\boldsymbol{q}'\lambda'}(\tau_1, 0) \delta_{-\boldsymbol{k_1 q}'} \delta_{j_1' \lambda'} \cdot G^0_{\boldsymbol{q}\lambda}(\tau, \tau_2) \delta_{-\boldsymbol{k_2 q}} \delta_{i_2' \lambda} \cdot G^0_{-\boldsymbol{k_1} j_1}(\tau_2, \tau_1) \delta_{\boldsymbol{k_1 k_2}} \delta_{j_1 i_2} \right].
\end{aligned}
$$

Where, again, the last equality results from the fact that j_1 and j_1' are indices of different ranges (belonging to different subsystems) and the same holds for i_2 and i_2'. Similarly, we obtain $I_2 = I_3 = 0$ for the same reason, as shown below:

$$
\begin{aligned}
I_2 = \langle T_\tau \hat{a}_{\boldsymbol{k_1} j_1}(\tau_1) \hat{\tilde{a}}^\dagger_{\boldsymbol{k_1} j_1'}(\tau_1) \hat{\tilde{a}}^\dagger_{-\boldsymbol{k_2} i_2'}(\tau_2) \hat{a}_{-\boldsymbol{k_2} i_2}(\tau_2) \hat{a}_{\boldsymbol{q}\lambda}(\tau) \hat{a}^\dagger_{\boldsymbol{q}'\lambda'}(0) \rangle_{0,c} \\
= \langle T_\tau \hat{a}^\dagger_{\boldsymbol{q}'\lambda'}(0) \hat{a}_{\boldsymbol{k_1} j_1}(\tau_1) \rangle_0 \langle T_\tau \hat{\tilde{a}}^\dagger_{\boldsymbol{k_1} j_1'}(\tau_1) \hat{a}_{\boldsymbol{q}\lambda}(\tau) \rangle_0 \langle T_\tau \hat{\tilde{a}}^\dagger_{-\boldsymbol{k_2} i_2'}(\tau_2) \hat{a}_{-\boldsymbol{k_2} i_2}(\tau_2) \rangle_0 \\
+ \langle T_\tau \hat{\tilde{a}}^\dagger_{-\boldsymbol{k_2} i_2'}(\tau_2) \hat{a}_{\boldsymbol{k_1} j_1}(\tau_1) \rangle_0 \langle T_\tau \hat{a}^\dagger_{\boldsymbol{q}'\lambda'}(0) \hat{a}_{-\boldsymbol{k_2} i_2}(\tau_2) \rangle_0 \langle T_\tau \hat{\tilde{a}}^\dagger_{\boldsymbol{k_1} j_1'}(\tau_1) \hat{a}_{\boldsymbol{q}\lambda}(\tau) \rangle_0 \\
+ \langle T_\tau \hat{a}^\dagger_{\boldsymbol{q}'\lambda'}(0) \hat{a}_{-\boldsymbol{k_2} i_2}(\tau_2) \rangle_0 \langle T_\tau \hat{\tilde{a}}^\dagger_{-\boldsymbol{k_2} i_2'}(\tau_2) \hat{a}_{\boldsymbol{q}\lambda}(\tau) \rangle_0 \langle T_\tau \hat{\tilde{a}}^\dagger_{\boldsymbol{k_1} j_1'}(\tau_1) \hat{a}_{\boldsymbol{k_1} j_1}(\tau_1) \rangle_0 \\
+ \langle T_\tau \hat{\tilde{a}}^\dagger_{\boldsymbol{k_1} j_1'}(\tau_1) \hat{a}_{-\boldsymbol{k_2} i_2}(\tau_2) \rangle_0 \langle T_\tau \hat{a}^\dagger_{\boldsymbol{q}'\lambda'}(0) \hat{a}_{\boldsymbol{k_1} j_1}(\tau_1) \rangle_0 \langle T_\tau \hat{\tilde{a}}^\dagger_{-\boldsymbol{k_2} i_2'}(\tau_2) \hat{a}_{\boldsymbol{q}\lambda}(\tau) \rangle_0 \\
= \left[G^0_{\boldsymbol{q}'\lambda'}(\tau_1, 0) \delta_{\boldsymbol{k_1 q}'} \delta_{j_1 \lambda'} \cdot G^0_{\boldsymbol{q}\lambda}(\tau, \tau_1) \delta_{\boldsymbol{k_1 q}} \delta_{j_1' \lambda} \cdot G^0_{-\boldsymbol{k_2} i_2}(\tau_2, \tau_2) \delta_{i_2 i_2'} \right] \\
+ \left[G^0_{\boldsymbol{k_1} j_1}(\tau_1, \tau_2) \delta_{-\boldsymbol{k_2 k_1}} \delta_{j_1 i_2'} \cdot G^0_{\boldsymbol{q}'\lambda'}(\tau_2, 0) \delta_{-\boldsymbol{k_2 q}'} \delta_{i_2 \lambda'} \cdot G^0_{\boldsymbol{q}\lambda}(\tau, \tau_1) \delta_{\boldsymbol{k_1 q}} \delta_{j_1' \lambda} \right] \\
+ \left[G^0_{\boldsymbol{q}'\lambda'}(\tau_2, 0) \delta_{-\boldsymbol{k_2 q}'} \delta_{i_2 \lambda'} \cdot G^0_{\boldsymbol{q}\lambda}(\tau, \tau_2) \delta_{-\boldsymbol{k_2 q}} \delta_{i_2' \lambda} \cdot G^0_{\boldsymbol{k_1} j_1}(\tau_1, \tau_1) \delta_{j_1 j_1'} \right] \\
+ \left[G^0_{\boldsymbol{k_1} j_1'}(\tau_2, \tau_1) \delta_{-\boldsymbol{k_2 k_1}} \delta_{i_2 j_1'} \cdot G^0_{\boldsymbol{q}'\lambda'}(\tau_1, 0) \delta_{\boldsymbol{k_1 q}'} \delta_{j_1 \lambda'} \cdot G^0_{\boldsymbol{q}\lambda}(\tau, \tau_2) \delta_{-\boldsymbol{k_2 q}} \delta_{i_2' \lambda} \right] = 0.
\end{aligned}
$$

$$
\begin{aligned}
I_3 = \langle T_\tau \hat{a}^\dagger_{-\boldsymbol{k_1} j_1}(\tau_1) \hat{\tilde{a}}_{-\boldsymbol{k_1} j_1'}(\tau_1) \hat{\tilde{a}}_{\boldsymbol{k_2} i_2'}(\tau_2) \hat{a}^\dagger_{\boldsymbol{k_2} i_2}(\tau_2) \hat{a}_{\boldsymbol{q}\lambda}(\tau) \hat{a}^\dagger_{\boldsymbol{q}'\lambda'}(0) \rangle_{0,c} \\
= \langle T_\tau \hat{a}^\dagger_{\boldsymbol{q}'\lambda'}(0) \hat{\tilde{a}}_{-\boldsymbol{k_1} j_1'}(\tau_1) \rangle_0 \langle T_\tau \hat{a}^\dagger_{-\boldsymbol{k_1} j_1}(\tau_1) \hat{a}_{\boldsymbol{q}\lambda}(\tau) \rangle_0 \langle T_\tau \hat{a}^\dagger_{\boldsymbol{k_2} i_2}(\tau_2) \hat{\tilde{a}}_{\boldsymbol{k_2} i_2'}(\tau_2) \rangle_0 \\
+ \langle T_\tau \hat{a}^\dagger_{\boldsymbol{k_2} i_2}(\tau_2) \hat{\tilde{a}}_{-\boldsymbol{k_1} j_1'}(\tau_1) \rangle_0 \langle T_\tau \hat{a}^\dagger_{\boldsymbol{q}'\lambda'}(0) \hat{\tilde{a}}_{\boldsymbol{k_2} i_2'}(\tau_2) \rangle_0 \langle T_\tau \hat{a}^\dagger_{-\boldsymbol{k_1} j_1}(\tau_1) \hat{a}_{\boldsymbol{q}\lambda}(\tau) \rangle_0 \\
+ \langle T_\tau \hat{a}^\dagger_{\boldsymbol{q}'\lambda'}(0) \hat{\tilde{a}}_{\boldsymbol{k_2} i_2'}(\tau_2) \rangle_0 \langle T_\tau \hat{a}^\dagger_{\boldsymbol{k_2} i_2}(\tau_2) \hat{a}_{\boldsymbol{q}\lambda}(\tau) \rangle_0 \langle T_\tau \hat{a}^\dagger_{-\boldsymbol{k_1} j_1}(\tau_1) \hat{\tilde{a}}_{-\boldsymbol{k_1} j_1'}(\tau_1) \rangle_0 \\
+ \langle T_\tau \hat{a}^\dagger_{-\boldsymbol{k_1} j_1}(\tau_1) \hat{\tilde{a}}_{\boldsymbol{k_2} i_2'}(\tau_2) \rangle_0 \langle T_\tau \hat{a}^\dagger_{\boldsymbol{q}'\lambda'}(0) \hat{\tilde{a}}_{-\boldsymbol{k_1} j_1'}(\tau_1) \rangle_0 \langle T_\tau \hat{a}^\dagger_{\boldsymbol{k_2} i_2}(\tau_2) \hat{a}_{\boldsymbol{q}\lambda}(\tau) \rangle_0 \\
= \left[G^0_{\boldsymbol{q}'\lambda'}(\tau_1, 0) \delta_{-\boldsymbol{k_1 q}'} \delta_{j_1' \lambda'} \cdot G^0_{\boldsymbol{q}\lambda}(\tau, \tau_1) \delta_{-\boldsymbol{k_1 q}} \delta_{j_1 \lambda} \cdot G^0_{\boldsymbol{k_2} i_2}(\tau_2, \tau_2) \delta_{i_2 i_2'} \right] \\
+ \left[G^0_{\boldsymbol{k_2} i_2}(\tau_1, \tau_2) \delta_{-\boldsymbol{k_1 k_2}} \delta_{j_1' i_2} \cdot G^0_{\boldsymbol{q}'\lambda'}(\tau_2, 0) \delta_{\boldsymbol{k_2 q}'} \delta_{i_2' \lambda'} \cdot G^0_{\boldsymbol{q}\lambda}(\tau, \tau_1) \delta_{-\boldsymbol{k_1 q}} \delta_{j_1 \lambda} \right] \\
+ \left[G^0_{\boldsymbol{q}'\lambda'}(\tau_2, 0) \delta_{\boldsymbol{k_2 q}'} \delta_{i_2' \lambda'} \cdot G^0_{\boldsymbol{q}\lambda}(\tau, \tau_2) \delta_{\boldsymbol{k_2 q}} \delta_{i_2 \lambda} \cdot G^0_{-\boldsymbol{k_1} j_1}(\tau_1, \tau_1) \delta_{j_1 j_1'} \right] \\
+ \left[G^0_{\boldsymbol{k_2} i_2'}(\tau_2, \tau_1) \delta_{-\boldsymbol{k_1 k_2}} \delta_{i_2' j_1} \cdot G^0_{\boldsymbol{q}'\lambda'}(\tau_1, 0) \delta_{-\boldsymbol{k_1 q}'} \delta_{j_1' \lambda'} \cdot G^0_{\boldsymbol{q}\lambda}(\tau, \tau_2) \delta_{\boldsymbol{k_2 q}} \delta_{i_2 \lambda} \right] = 0.
\end{aligned}
$$

The two non-vanishing terms (I_1 and I_4) produce the following contributions to g_2 of Eq. (S7.95):

$$
g_{21} = \frac{1}{32} \int_0^{\beta\hbar} d\tau_1 \int_0^{\beta\hbar} d\tau_2 \left\{ \sum_{\boldsymbol{k_1} j_1 j_1'}^{1 \le j_1 \le \frac{3r}{2} < j_1' \le 3r} \sum_{\boldsymbol{k_2} i_2 i_2'}^{1 \le i_2 \le \frac{3r}{2} < i_2' \le 3r} \frac{V_{j_1 j_1'}(\boldsymbol{k_1}) V^*_{i_2 i_2'}(\boldsymbol{k_2})}{\sqrt{\omega_{\boldsymbol{k_1} j_1} \tilde{\omega}_{\boldsymbol{k_1} j_1'} \omega_{\boldsymbol{k_2} i_2} \tilde{\omega}_{\boldsymbol{k_2} i_2'}}} I_1 \right\} =
$$

$$
\frac{1}{32} \int_0^{\beta\hbar} d\tau_1 \int_0^{\beta\hbar} d\tau_2 \sum_{\boldsymbol{k_1} j_1 j_1'}^{1 \le j_1 \le \frac{3r}{2} < j_1' \le 3r} \sum_{\boldsymbol{k_2} i_2 i_2'}^{1 \le i_2 \le \frac{3r}{2} < i_2' \le 3r} \frac{V_{j_1 j_1'}(\boldsymbol{k_1}) V^*_{i_2 i_2'}(\boldsymbol{k_2})}{\sqrt{\omega_{\boldsymbol{k_1} j_1} \tilde{\omega}_{\boldsymbol{k_1} j_1'} \omega_{\boldsymbol{k_2} i_2} \tilde{\omega}_{\boldsymbol{k_2} i_2'}}} \left[G^0_{\boldsymbol{k_1} j_1}(\tau_1, \tau_2) \delta_{\boldsymbol{k_1 k_2}} \delta_{j_1 i_2} \cdot G^0_{\boldsymbol{q}'\lambda'}(\tau_2, 0) \delta_{\boldsymbol{k_2 q}'} \delta_{i_2' \lambda'} \cdot \right.
$$

$$
\left. G^0_{\boldsymbol{q}\lambda}(\tau, \tau_1) \delta_{\boldsymbol{k_1 q}} \delta_{j_1' \lambda} \right] + \frac{1}{32} \int_0^{\beta\hbar} d\tau_1 \int_0^{\beta\hbar} d\tau_2 \sum_{\boldsymbol{k_1} j_1 j_1'}^{1 \le j_1 \le \frac{3r}{2} < j_1' \le 3r} \sum_{\boldsymbol{k_2} i_2 i_2'}^{1 \le i_2 \le \frac{3r}{2} < i_2' \le 3r} \frac{V_{j_1 j_1'}(\boldsymbol{k_1}) V^*_{i_2 i_2'}(\boldsymbol{k_2})}{\sqrt{\omega_{\boldsymbol{k_1} j_1} \tilde{\omega}_{\boldsymbol{k_1} j_1'} \omega_{\boldsymbol{k_2} i_2} \tilde{\omega}_{\boldsymbol{k_2} i_2'}}} \left[G^0_{\boldsymbol{k_1} j_1'}(\tau_2, \tau_1) \delta_{\boldsymbol{k_1 k_2}} \delta_{i_2' j_1'} \cdot \right.
$$

$$
\left. G^0_{\boldsymbol{q}'\lambda'}(\tau_1, 0) \delta_{\boldsymbol{k_1 q}'} \delta_{j_1 \lambda'} \cdot G^0_{\boldsymbol{q}\lambda}(\tau, \tau_2) \delta_{\boldsymbol{k_2 q}} \delta_{i_2 \lambda} \right] =
$$

$$
\begin{cases}
\frac{\delta_{\boldsymbol{q}\boldsymbol{q}'}}{32} \int_0^{\beta\hbar} d\tau_1 \int_0^{\beta\hbar} d\tau_2 \sum_{j_1=1}^{\frac{3r}{2}} \frac{V_{j_1\lambda}(\boldsymbol{q}) V^*_{j_1\lambda'}(\boldsymbol{q}')}{\omega_{\boldsymbol{q}j_1} \sqrt{\omega_{\boldsymbol{q}\lambda} \omega_{\boldsymbol{q}'\lambda'}}} \left[G^0_{\boldsymbol{q}j_1}(\tau_1, \tau_2) \cdot G^0_{\boldsymbol{q}'\lambda'}(\tau_2, 0) G^0_{\boldsymbol{q}\lambda}(\tau, \tau_1) \right], & \lambda, \lambda' \in \left[\frac{3r}{2} + 1, 3r \right] \\
\frac{\delta_{\boldsymbol{q}\boldsymbol{q}'}}{32} \int_0^{\beta\hbar} d\tau_1 \int_0^{\beta\hbar} d\tau_2 \sum_{j_1'=\frac{3r}{2}+1}^{3r} \frac{V_{\lambda' j_1'}(\boldsymbol{q}') V^*_{\lambda j_1'}(\boldsymbol{q})}{\omega_{\boldsymbol{q}j_1'} \sqrt{\omega_{\boldsymbol{q}\lambda} \omega_{\boldsymbol{q}'\lambda'}}} \left[G^0_{\boldsymbol{q}j_1'}(\tau_2, \tau_1) \cdot G^0_{\boldsymbol{q}'\lambda'}(\tau_1, 0) G^0_{\boldsymbol{q}\lambda}(\tau, \tau_2) \right], & \lambda, \lambda' \in \left[1, \frac{3r}{2} \right] \\
0 & \text{else}
\end{cases}
$$

and

$$g_{24}=\frac{1}{32}\int_0^{\beta\hbar}d\tau_1\int_0^{\beta\hbar}d\tau_2\left\{\sum_{\boldsymbol{k_1}j_1j_1'}^{1\le j_1\le\frac{3r}{2}<j_1'\le 3r}\sum_{\boldsymbol{k_2}i_2i_2'}^{1\le i_2\le\frac{3r}{2}<i_2'\le 3r}\frac{V_{j_1j_1'}(\boldsymbol{k_1})V^*_{i_2i_2'}(\boldsymbol{k_2})}{\sqrt{\omega_{\boldsymbol{k_1}j_1}\widetilde{\omega}_{\boldsymbol{k_1}j_1'}\omega_{\boldsymbol{k_2}i_2}\widetilde{\omega}_{\boldsymbol{k_2}i_2'}}}I_4\right\}=$$

$$\frac{1}{32}\int_0^{\beta\hbar}d\tau_1\int_0^{\beta\hbar}d\tau_2\sum_{\boldsymbol{k_1}j_1j_1'}^{1\le j_1\le\frac{3r}{2}<j_1'\le 3r}\sum_{\boldsymbol{k_2}i_2i_2'}^{1\le i_2\le\frac{3r}{2}<i_2'\le 3r}\frac{V_{j_1j_1'}(\boldsymbol{k_1})V^*_{i_2i_2'}(\boldsymbol{k_2})}{\sqrt{\omega_{\boldsymbol{k_1}j_1}\widetilde{\omega}_{\boldsymbol{k_1}j_1'}\omega_{\boldsymbol{k_2}i_2}\widetilde{\omega}_{\boldsymbol{k_2}i_2'}}}\Big[G^0_{\boldsymbol{q}'\lambda'}(\tau_2,0)\delta_{-\boldsymbol{k_2}\boldsymbol{q}'}\delta_{i_2\lambda'}\cdot G^0_{\boldsymbol{q}\lambda}(\tau,\tau_1)\delta_{-\boldsymbol{k_1}\boldsymbol{q}}\delta_{j_1\lambda}\cdot$$

$$G^0_{-\boldsymbol{k_1}j_1'}(\tau_1,\tau_2)\delta_{\boldsymbol{k_1}\boldsymbol{k_2}}\delta_{j_1'i_2'}\Big]+\frac{1}{32}\int_0^{\beta\hbar}d\tau_1\int_0^{\beta\hbar}d\tau_2\sum_{\boldsymbol{k_1}j_1j_1'}^{1\le j_1\le\frac{3r}{2}<j_1'\le 3r}\sum_{\boldsymbol{k_2}i_2i_2'}^{1\le i_2\le\frac{3r}{2}<i_2'\le 3r}\frac{V_{j_1j_1'}(\boldsymbol{k_1})V^*_{i_2i_2'}(\boldsymbol{k_2})}{\sqrt{\omega_{\boldsymbol{k_1}j_1}\widetilde{\omega}_{\boldsymbol{k_1}j_1'}\omega_{\boldsymbol{k_2}i_2}\widetilde{\omega}_{\boldsymbol{k_2}i_2'}}}\Big[G^0_{\boldsymbol{q}'\lambda'}(\tau_1,0)\delta_{-\boldsymbol{k_1}\boldsymbol{q}'}\delta_{j_1'\lambda'}\cdot$$

$$G^0_{\boldsymbol{q}\lambda}(\tau,\tau_2)\delta_{-\boldsymbol{k_2}\boldsymbol{q}}\delta_{i_2'\lambda}\cdot G^0_{-\boldsymbol{k_1}j_1}(\tau_2,\tau_1)\delta_{\boldsymbol{k_1}\boldsymbol{k_2}}\delta_{j_1i_2}\Big]=$$

$$\begin{cases}\frac{\delta_{\boldsymbol{q}\boldsymbol{q}'}}{32}\int_0^{\beta\hbar}d\tau_1\int_0^{\beta\hbar}d\tau_2\sum_{j_1'=\frac{3r}{2}+1}^{3r}\frac{V_{\lambda'j_1'}(\boldsymbol{q}')V^*_{\lambda j_1'}(\boldsymbol{q})}{\omega_{\boldsymbol{q}j_1'}\sqrt{\omega_{\boldsymbol{q}\lambda}\omega_{\boldsymbol{q}'\lambda'}}}\Big[G^0_{\boldsymbol{q}j_1'}(\tau_1,\tau_2)G^0_{\boldsymbol{q}'\lambda'}(\tau_2,0)G^0_{\boldsymbol{q}\lambda}(\tau,\tau_1)\Big], & \lambda,\lambda'\in\left[1,\frac{3r}{2}\right]\\ \frac{\delta_{\boldsymbol{q}\boldsymbol{q}'}}{32}\int_0^{\beta\hbar}d\tau_1\int_0^{\beta\hbar}d\tau_2\sum_{j_1=1}^{\frac{3r}{2}}\frac{V_{j_1\lambda}(\boldsymbol{q})V^*_{j_1\lambda'}(\boldsymbol{q}')}{\omega_{\boldsymbol{q}j_1}\sqrt{\omega_{\boldsymbol{q}\lambda}\omega_{\boldsymbol{q}'\lambda'}}}\Big[G^0_{\boldsymbol{q}j_1}(\tau_2,\tau_1)G^0_{\boldsymbol{q}'\lambda'}(\tau_1,0)G^0_{\boldsymbol{q}\lambda}(\tau,\tau_2)\Big], & \lambda,\lambda'\in\left[\frac{3r}{2}+1,3r\right]\\ 0 & \text{else}\end{cases}.$$

Here we used the following properties: $\omega_{-\boldsymbol{q}\lambda}=\omega_{\boldsymbol{q}\lambda}$ and $V_{\lambda j_1'}(-\boldsymbol{q})=V^*_{\lambda j_1'}\ (\boldsymbol{q})$ [see Eqs. (S7.12) and (S7.44)].

The equivalence of g_{21} and g_{24} can be seen by changing the integration variables $\tau_2\leftrightarrow\tau_1$. Substituting g_{21} and g_{24} into Eq. (S7.95), g_2 is given by:

$$g_2=\begin{cases}\frac{\delta_{\boldsymbol{q}\boldsymbol{q}'}}{16}\int_0^{\beta\hbar}d\tau_1\int_0^{\beta\hbar}d\tau_2\sum_{j_1=1}^{\frac{3r}{2}}\frac{V_{j_1\lambda}(\boldsymbol{q})V^*_{j_1\lambda'}(\boldsymbol{q}')}{\omega_{\boldsymbol{q}j_1}\sqrt{\omega_{\boldsymbol{q}\lambda}\omega_{\boldsymbol{q}'\lambda'}}}\Big[G^0_{\boldsymbol{q}j_1}(\tau_1,\tau_2)G^0_{\boldsymbol{q}'\lambda'}(\tau_2,0)G^0_{\boldsymbol{q}\lambda}(\tau,\tau_1)\Big], & \lambda,\lambda'\in\left[\frac{3r}{2}+1,3r\right]\\ \frac{\delta_{\boldsymbol{q}\boldsymbol{q}'}}{16}\int_0^{\beta\hbar}d\tau_1\int_0^{\beta\hbar}d\tau_2\sum_{j_1'=\frac{3r}{2}+1}^{3r}\frac{V_{\lambda'j_1'}(\boldsymbol{q}')V^*_{\lambda j_1'}(\boldsymbol{q})}{\omega_{\boldsymbol{q}j_1'}\sqrt{\omega_{\boldsymbol{q}\lambda}\omega_{\boldsymbol{q}'\lambda'}}}\Big[G^0_{\boldsymbol{q}j_1'}(\tau_2,\tau_1)G^0_{\boldsymbol{q}'\lambda'}(\tau_1,0)G^0_{\boldsymbol{q}\lambda}(\tau,\tau_2)\Big], & \lambda,\lambda'\in\left[1,\frac{3r}{2}\right]\\ 0 & \text{else}\end{cases}\tag{S7.97}$$

By changing the indices and integration variables, it's straightforward to show that the other three terms (g_1,g_3,g_4) are identical to g_2, thus the final expression of $G^{(2)}_{\boldsymbol{q}\lambda,\boldsymbol{q}'\lambda'}(\tau)$ [Eq. (S7.85)) can be calculated as:

$$G^{(2)}_{\boldsymbol{q}\lambda,\boldsymbol{q}'\lambda'}(\tau)=4g_2=\begin{cases}\frac{\delta_{\boldsymbol{q}\boldsymbol{q}'}}{4}\int_0^{\beta\hbar}d\tau_1\int_0^{\beta\hbar}d\tau_2\sum_{j_1'=\frac{3r}{2}+1}^{3r}\frac{V_{\lambda'j_1'}(\boldsymbol{q}')V^*_{\lambda j_1'}(\boldsymbol{q})}{\omega_{\boldsymbol{q}j_1'}\sqrt{\omega_{\boldsymbol{q}\lambda}\omega_{\boldsymbol{q}'\lambda'}}}\Big[G^0_{\boldsymbol{q}j_1'}(\tau_2,\tau_1)G^0_{\boldsymbol{q}'\lambda'}(\tau_1,0)G^0_{\boldsymbol{q}\lambda}(\tau,\tau_2)\Big], & \lambda,\lambda'\in\left[1,\frac{3r}{2}\right]\\ \frac{\delta_{\boldsymbol{q}\boldsymbol{q}'}}{4}\int_0^{\beta\hbar}d\tau_1\int_0^{\beta\hbar}d\tau_2\sum_{j_1=1}^{\frac{3r}{2}}\frac{V_{j_1\lambda}(\boldsymbol{q})V^*_{j_1\lambda'}(\boldsymbol{q}')}{\omega_{\boldsymbol{q}j_1}\sqrt{\omega_{\boldsymbol{q}\lambda}\omega_{\boldsymbol{q}'\lambda'}}}\Big[G^0_{\boldsymbol{q}j_1}(\tau_1,\tau_2)G^0_{\boldsymbol{q}'\lambda'}(\tau_2,0)G^0_{\boldsymbol{q}\lambda}(\tau,\tau_1)\Big], & \lambda,\lambda'\in\left[\frac{3r}{2}+1,3r\right]\\ 0 & \text{else}\end{cases}\tag{S7.98}$$

To calculate $G^{(2)}_{\boldsymbol{q}\lambda,\boldsymbol{q}'\lambda'}$ in frequency space, we expand $G^{(2)}_{\boldsymbol{q}\lambda,\boldsymbol{q}'\lambda'}(\tau)$ in a Fourier series:

$$\begin{cases}G^{(2)}_{\boldsymbol{q}\lambda,\boldsymbol{q}'\lambda'}(\tau)=\frac{1}{\beta\hbar}\sum_n e^{-i\omega_n\tau}G^{(2)}_{\boldsymbol{q}\lambda,\boldsymbol{q}'\lambda'}(i\omega_n)\\ G^{(2)}_{\boldsymbol{q}\lambda,\boldsymbol{q}'\lambda'}(i\omega_n)=\int_0^{\beta\hbar}\mathrm{d}\tau e^{i\omega_n\tau}G^{(2)}_{\boldsymbol{q}\lambda,\boldsymbol{q}'\lambda'}(\tau)\end{cases}\tag{S7.99}$$

Using Eq. (S7.69) we get for $\lambda,\lambda'\in\left[1,\frac{3r}{2}\right]$,

$$G^{(2)}_{\boldsymbol{q}\lambda,\boldsymbol{q}'\lambda'}(\tau)=\frac{\delta_{\boldsymbol{q}\boldsymbol{q}'}}{4}\int_0^{\beta\hbar}d\tau_1\int_0^{\beta\hbar}d\tau_2\sum_{j_1'=\frac{3r}{2}+1}^{3r}\frac{V_{\lambda' j_1'}(\boldsymbol{q}')V^*_{\lambda j_1'}(\boldsymbol{q})}{\omega_{\boldsymbol{q}j_1'}\sqrt{\omega_{\boldsymbol{q}\lambda}\omega_{\boldsymbol{q}'\lambda'}}}\left[G^0_{\boldsymbol{q}j_1'}(\tau_2,\tau_1)G^0_{\boldsymbol{q}\lambda'}(\tau_1,0)G^0_{\boldsymbol{q}\lambda}(\tau,\tau_2)\right]$$

$$=\frac{\delta_{\boldsymbol{q}\boldsymbol{q}'}}{4}\sum_{j_1'=\frac{3r}{2}+1}^{3r}\frac{V_{\lambda' j_1'}(\boldsymbol{q}')V^*_{\lambda j_1'}(\boldsymbol{q})}{\omega_{\boldsymbol{q}j_1'}\sqrt{\omega_{\boldsymbol{q}\lambda}\omega_{\boldsymbol{q}'\lambda'}}}\int_0^{\beta\hbar}d\tau_1\int_0^{\beta\hbar}d\tau_2\left[\frac{1}{\beta\hbar}\sum_{n_2}e^{-i\omega_{n_2}(\tau_2-\tau_1)}G^0_{\boldsymbol{q}j_1'}(i\omega_{n_2})\cdot\frac{1}{\beta\hbar}\sum_{n_1}e^{-i\omega_{n_1}\tau_1}G^0_{\boldsymbol{q}\lambda'}(i\omega_{n_1})\right.$$

$$\left.\cdot\frac{1}{\beta\hbar}\sum_{n}e^{-i\omega_n(\tau-\tau_2)}G^0_{\boldsymbol{q}\lambda}(i\omega_n)\right]$$

$$=\frac{\delta_{\boldsymbol{q}\boldsymbol{q}'}}{4}\sum_{j_1'=\frac{3r}{2}+1}^{3r}\frac{V_{\lambda' j_1'}(\boldsymbol{q}')V^*_{\lambda j_1'}(\boldsymbol{q})}{\omega_{\boldsymbol{q}j_1'}\sqrt{\omega_{\boldsymbol{q}\lambda}\omega_{\boldsymbol{q}'\lambda'}}}\frac{1}{\beta\hbar}\sum_{n,n_1,n_2}e^{-i\omega_n\tau}G^0_{\boldsymbol{q}\lambda}(i\omega_n)G^0_{\boldsymbol{q}\lambda'}(i\omega_{n_1})G^0_{\boldsymbol{q}j_1'}(i\omega_{n_2})\left\{\begin{array}{l}\frac{1}{\beta\hbar}\int_0^{\beta\hbar}d\tau_1\,e^{-i(\omega_{n_1}-\omega_{n_2})\tau_1}\\ \times\frac{1}{\beta\hbar}\int_0^{\beta\hbar}d\tau_2\,e^{-i(\omega_{n_2}-\omega_n)\tau_2}\end{array}\right\}$$

$$=\frac{\delta_{\boldsymbol{q}\boldsymbol{q}'}}{4}\sum_{j_1'=\frac{3r}{2}+1}^{3r}\frac{V_{\lambda' j_1'}(\boldsymbol{q}')V^*_{\lambda j_1'}(\boldsymbol{q})}{\omega_{\boldsymbol{q}j_1'}\sqrt{\omega_{\boldsymbol{q}\lambda}\omega_{\boldsymbol{q}'\lambda'}}}\frac{1}{\beta\hbar}\sum_{n,n_1,n_2}e^{-i\omega_n\tau}G^0_{\boldsymbol{q}\lambda}(i\omega_n)\,G^0_{\boldsymbol{q}\lambda'}(i\omega_{n_1})G^0_{\boldsymbol{q}j_1'}(i\omega_{n_2})\delta_{n_1n_2}\delta_{nn_2}$$

$$=\frac{\delta_{\boldsymbol{q}\boldsymbol{q}'}}{\beta\hbar}\sum_{n}e^{-i\omega_n\tau}\left\{G^0_{\boldsymbol{q}\lambda}(i\omega_n)\left[\frac{1}{4}\sum_{j_1'=\frac{3r}{2}+1}^{3r}\frac{V_{\lambda' j_1'}(\boldsymbol{q}')V^*_{\lambda j_1'}(\boldsymbol{q})}{\omega_{\boldsymbol{q}j_1'}\sqrt{\omega_{\boldsymbol{q}\lambda}\omega_{\boldsymbol{q}'\lambda'}}}G^0_{\boldsymbol{q}j_1'}(i\omega_n)\right]G^0_{\boldsymbol{q}\lambda'}(i\omega_n)\right\}$$

Comparing above expression with Eq. (S7.99), the Fourier transform of $G^{(2)}_{\boldsymbol{q}\lambda,\boldsymbol{q}\lambda'}(\tau)$ reads as

$$G^{(2)}_{\boldsymbol{q}\lambda,\boldsymbol{q}'\lambda'}(i\omega_n)=G^0_{\boldsymbol{q}\lambda}(i\omega_n)\left[\frac{\delta_{\boldsymbol{q}\boldsymbol{q}'}}{4}\sum_{j_1'=\frac{3r}{2}+1}^{3r}\frac{V_{\lambda' j_1'}(\boldsymbol{q}')V^*_{\lambda j_1'}(\boldsymbol{q})}{\omega_{\boldsymbol{q}j_1'}\sqrt{\omega_{\boldsymbol{q}\lambda}\omega_{\boldsymbol{q}'\lambda'}}}G^0_{\boldsymbol{q}j_1'}(i\omega_n)\right]G^0_{\boldsymbol{q}\lambda'}(i\omega_n)\qquad\text{(S7.100)}$$

where we have introduced the notation:

$$\Sigma^{(2)}_{\boldsymbol{q}\lambda,\boldsymbol{q}'\lambda'}(i\omega_n)\equiv\frac{\delta_{\boldsymbol{q}\boldsymbol{q}'}}{4}\sum_{j_1'=\frac{3r}{2}+1}^{3r}\frac{V_{\lambda' j_1'}(\boldsymbol{q}')V^*_{\lambda j_1'}(\boldsymbol{q})}{\omega_{\boldsymbol{q}j_1'}\sqrt{\omega_{\boldsymbol{q}\lambda}\omega_{\boldsymbol{q}'\lambda'}}}G^0_{\boldsymbol{q}j_1'}(i\omega_n)\qquad\text{(S7.101)}$$

and $G^{(2)}_{\boldsymbol{q}\lambda,\boldsymbol{q}'\lambda'}(i\omega_n)=G^0_{\boldsymbol{q}\lambda}(i\omega_n)\cdot\Sigma^{(2)}_{\boldsymbol{q}\lambda,\boldsymbol{q}\lambda'}(i\omega_n)\cdot G^0_{\boldsymbol{q}\lambda'}(i\omega_n)$. Similarly, for $\lambda,\lambda'\in\left[\frac{3r}{2}+1,3r\right]$ we have:

$$\Sigma^{(2)}_{\boldsymbol{q}\lambda,\boldsymbol{q}'\lambda'}(i\omega_n)=\frac{\delta_{\boldsymbol{q}\boldsymbol{q}'}}{4}\sum_{j_1=1}^{\frac{3r}{2}}\frac{V_{j_1\lambda}(\boldsymbol{q})V^*_{j_1\lambda'}(\boldsymbol{q}')}{\omega_{\boldsymbol{q}j_1}\sqrt{\omega_{\boldsymbol{q}\lambda}\omega_{\boldsymbol{q}'\lambda'}}}G^0_{\boldsymbol{q}j_1}(i\omega_n)\qquad\text{(S7.102)}$$

and all together we have for $\Sigma^{(2)}_{\boldsymbol{q}\lambda,\boldsymbol{q}'\lambda'}(i\omega_n)$:

$$\Sigma^{(2)}_{\boldsymbol{q}\lambda,\boldsymbol{q}'\lambda'}(i\omega_n)=\begin{cases}\frac{\delta_{\boldsymbol{q}\boldsymbol{q}'}}{4}\sum_{j_1'=\frac{3r}{2}+1}^{3r}\frac{V_{\lambda' j_1'}(\boldsymbol{q}')V^*_{\lambda j_1'}(\boldsymbol{q})}{\omega_{\boldsymbol{q}j_1'}\sqrt{\omega_{\boldsymbol{q}\lambda}\omega_{\boldsymbol{q}'\lambda'}}}G^0_{\boldsymbol{q}j_1'}(i\omega_n), & \lambda,\lambda'\in\left[1,\frac{3r}{2}\right]\\ \frac{\delta_{\boldsymbol{q}\boldsymbol{q}'}}{4}\sum_{j_1=1}^{\frac{3r}{2}}\frac{V_{j_1\lambda}(\boldsymbol{q})V^*_{j_1\lambda'}(\boldsymbol{q}')}{\omega_{\boldsymbol{q}j_1}\sqrt{\omega_{\boldsymbol{q}\lambda}\omega_{\boldsymbol{q}'\lambda'}}}G^0_{\boldsymbol{q}j_1}(i\omega_n), & \lambda,\lambda'\in\left[\frac{3r}{2}+1,3r\right]\\ 0 & \text{else}\end{cases}\qquad\text{(S7.103)}$$

7.5.3 Dyson's equation

Substituting Eqs. (S7.90) and (S7.103) into Eq. (S7.85) and performing a Fourier transform, we have:

$$\begin{aligned} G_{\boldsymbol{q}\lambda,\boldsymbol{q}'\lambda'}(i\omega_n) &= G^0_{\boldsymbol{q}\lambda,\boldsymbol{q}'\lambda'}(i\omega_n) + G^{(1)}_{\boldsymbol{q}\lambda,\boldsymbol{q}'\lambda'}(i\omega_n) + G^{(2)}_{\boldsymbol{q}\lambda,\boldsymbol{q}'\lambda'}(i\omega_n) + \cdots \\ &= G^0_{\boldsymbol{q}\lambda}(i\omega_n)\delta_{\boldsymbol{q}\boldsymbol{q}'}\delta_{\lambda\lambda'} + G^0_{\boldsymbol{q}\lambda}(i\omega_n)\cdot\Sigma^{(1)}_{\boldsymbol{q}\lambda,\boldsymbol{q}'\lambda'}(i\omega_n)\cdot G^0_{\boldsymbol{q}'\lambda'}(i\omega_n) + G^0_{\boldsymbol{q}\lambda}(i\omega_n)\cdot\Sigma^{(2)}_{\boldsymbol{q}\lambda,\boldsymbol{q}'\lambda'}(i\omega_n) \\ &\cdot G^0_{\boldsymbol{q}'\lambda'}(i\omega_n) + \cdots = G^0_{\boldsymbol{q}\lambda}(i\omega_n)\delta_{\boldsymbol{q}\boldsymbol{q}'}\delta_{\lambda\lambda'} + G^0_{\boldsymbol{q}\lambda}(i\omega_n)\cdot\Sigma_{\boldsymbol{q}\lambda,\boldsymbol{q}'\lambda'}(i\omega_n)\cdot G^0_{\boldsymbol{q}'\lambda'}(i\omega_n) \end{aligned}$$

or

$$G_{\boldsymbol{q}\lambda,\boldsymbol{q}'\lambda'}(i\omega_n) = G^0_{\boldsymbol{q}\lambda}(i\omega_n)\delta_{\boldsymbol{q}\boldsymbol{q}'}\delta_{\lambda\lambda'} + G^0_{\boldsymbol{q}\lambda}(i\omega_n)\cdot\Sigma_{\boldsymbol{q}\lambda,\boldsymbol{q}'\lambda'}(i\omega_n)\cdot G^0_{\boldsymbol{q}'\lambda'}(i\omega_n) \tag{S7.104}$$

Eq. (S7.104) is the so-called Dyson's equation (see Ref. [21]), where

$$\Sigma_{\boldsymbol{q}\lambda,\boldsymbol{q}\lambda'}(i\omega_n) = \Sigma^{(1)}_{\boldsymbol{q}\lambda,\boldsymbol{q}'\lambda'}(i\omega_n) + \Sigma^{(2)}_{\boldsymbol{q}\lambda,\boldsymbol{q}'\lambda'}(i\omega_n) + \cdots$$

is called self-energy and $\Sigma^{(n)}_{\boldsymbol{q}\lambda,\boldsymbol{q}\lambda'}(i\omega_n), n = 1,2,\cdots$ is the self-energy of n^{th} order approximation. Up to the second order approximation, the self-energy is written as

$$\Sigma_{\boldsymbol{q}\lambda,\boldsymbol{q}'\lambda'}(i\omega_n) = \begin{cases} -\frac{\delta_{\boldsymbol{q}\boldsymbol{q}'}}{2}\frac{V^*_{\lambda\lambda'}(\boldsymbol{q})}{\sqrt{\omega_{\boldsymbol{q}\lambda}\widetilde{\omega}_{\boldsymbol{q}\lambda'}}}, & 1 \le \lambda \le \frac{3r}{2} < \lambda' \le 3r \\ -\frac{\delta_{\boldsymbol{q}\boldsymbol{q}'}}{2}\frac{V_{\lambda'\lambda}(\boldsymbol{q})}{\sqrt{\widetilde{\omega}_{\boldsymbol{q}\lambda}\omega_{\boldsymbol{q}\lambda'}}}, & 1 \le \lambda' \le \frac{3r}{2} < \lambda \le 3r \\ \frac{\delta_{\boldsymbol{q}\boldsymbol{q}'}}{4}\sum_{j_1'=\frac{3r}{2}+1}^{3r}\frac{V_{\lambda' j_1'}(\boldsymbol{q}')V^*_{\lambda j_1'}(\boldsymbol{q})}{\widetilde{\omega}_{\boldsymbol{q}j_1'}\sqrt{\omega_{\boldsymbol{q}\lambda}\omega_{\boldsymbol{q}'\lambda'}}}G^0_{\boldsymbol{q}j_1'}(i\omega_n), & \lambda,\lambda' \in \left[1,\frac{3r}{2}\right] \\ \frac{\delta_{\boldsymbol{q}\boldsymbol{q}'}}{4}\sum_{j_1=1}^{\frac{3r}{2}}\frac{V_{j_1\lambda}(\boldsymbol{q})V^*_{j_1\lambda'}(\boldsymbol{q}')}{\omega_{\boldsymbol{q}j_1}\sqrt{\widetilde{\omega}_{\boldsymbol{q}\lambda}\widetilde{\omega}_{\boldsymbol{q}'\lambda'}}}G^0_{\boldsymbol{q}j_1}(i\omega_n), & \lambda,\lambda' \in \left[\frac{3r}{2}+1,3r\right] \end{cases} \tag{S7.105}$$

7.6 Fermi's golden Rule

To get the Fermi's golden Rule, we need to calculate the retarded Green's function, which can be calculated from $G_{\boldsymbol{q}\lambda,\boldsymbol{q}\lambda'}(i\omega_n)$ by analytic continuation to the real axis via $i\omega_n \to \omega + i\eta$ with an infinitesimal positive η[20, 21]:

$$G^r_{\boldsymbol{q}\lambda,\boldsymbol{q}\lambda'}(\omega) \equiv G_{\boldsymbol{q}\lambda,\boldsymbol{q}\lambda'}(i\omega_n \to \omega + i\eta), \eta \to 0 \tag{S7.106}$$

Similarity, the retarded self-energy is defined as

$$\Sigma^r_{\boldsymbol{q}\lambda,\boldsymbol{q}\lambda'}(\omega) \equiv \Sigma_{\boldsymbol{q}\lambda,\boldsymbol{q}\lambda'}(i\omega_n \to \omega + i\eta), \eta \to 0 \tag{S7.107}$$

The transition rate of phonons of branch λ at $\boldsymbol{q}$, $\Gamma_{\boldsymbol{q}\lambda}(\omega)$, is related to the retarded self energy $\Sigma^r_{\boldsymbol{q}\lambda}(\omega)$ via[20, 22]:

$$\Gamma_{\boldsymbol{q}\lambda}(\omega) = -2\mathrm{Im}\Sigma^r_{\boldsymbol{q}\lambda,\boldsymbol{q}\lambda}(\omega). \tag{S7.108}$$

Using the expression for $G^0_{\boldsymbol{q}\lambda}(i\omega_n)$ [Eq. (S7.69)] and focused on the second order approximation[20, 22] we have:

$$\Sigma^r_{\boldsymbol{q}\lambda,\boldsymbol{q}\lambda}(i\omega_n)=\begin{cases}\frac{1}{4}\sum_{j_1'=\frac{3r}{2}+1}^{3r}\frac{\left|V_{\lambda j_1'}(\boldsymbol{q})\right|^2}{\widetilde{\omega}_{\boldsymbol{q}j_1'}\omega_{\boldsymbol{q}\lambda}}\frac{1}{\left(\omega-\omega_{\boldsymbol{q}j_1'}\right)+i\eta}, & \lambda\in\left[1,\frac{3r}{2}\right]\\ \frac{1}{4}\sum_{j_1=1}^{\frac{3r}{2}}\frac{\left|V_{j_1\lambda}(\boldsymbol{q})\right|^2}{\omega_{\boldsymbol{q}j_1}\widetilde{\omega}_{\boldsymbol{q}\lambda}}\frac{1}{(\omega-\omega_{\boldsymbol{q}j_1})+i\eta}, & \lambda\in\left[\frac{3r}{2}+1,3r\right]\end{cases}. \tag{S7.109}$$

Using the relation:

$$\mathrm{Im}\left[\frac{1}{\left(\omega-\omega_{\boldsymbol{q}j_1'}\right)+i\eta}\right]=-\pi\delta\left(\omega-\omega_{\boldsymbol{q}j_1'}\right). \tag{S7.110}$$

The transition rate reads as

$$\Gamma_{\boldsymbol{q}\lambda}(\omega)=\begin{cases}\frac{\pi}{2}\sum_{j_1'=\frac{3r}{2}+1}^{3r}\frac{\left|V_{\lambda j_1'}(\boldsymbol{q})\right|^2}{\widetilde{\omega}_{\boldsymbol{q}j_1'}\omega_{\boldsymbol{q}\lambda}}\delta\left(\omega-\omega_{\boldsymbol{q}j_1'}\right), & \lambda\in\left[1,\frac{3r}{2}\right]\\ \frac{\pi}{2}\sum_{j_1=1}^{\frac{3r}{2}}\frac{\left|V_{j_1\lambda}(\boldsymbol{q})\right|^2}{\omega_{\boldsymbol{q}j_1}\widetilde{\omega}_{\boldsymbol{q}\lambda}}\delta\left(\omega-\omega_{\boldsymbol{q}j_1}\right), & \lambda\in\left[\frac{3r}{2}+1,3r\right]\end{cases}. \tag{S7.111}$$

Or equivalently,

$$\Gamma_{\boldsymbol{q}\lambda}(E=\hbar\omega)=\begin{cases}\frac{\pi\hbar^3}{2}\sum_{j_1'=\frac{3r}{2}+1}^{3r}\frac{\left|V_{\lambda j_1'}(\boldsymbol{q})\right|^2}{E_{\boldsymbol{q}j_1'}E_{\boldsymbol{q}\lambda}}\delta\left(E-E_{\boldsymbol{q}j_1'}\right), & \lambda\in\left[1,\frac{3r}{2}\right]\\ \frac{\pi\hbar^3}{2}\sum_{j_1=1}^{\frac{3r}{2}}\frac{\left|V_{j_1\lambda}(\boldsymbol{q})\right|^2}{E_{\boldsymbol{q}j_1}E_{\boldsymbol{q}\lambda}}\delta\left(E-E_{\boldsymbol{q}j_1}\right), & \lambda\in\left[\frac{3r}{2}+1,3r\right]\end{cases}. \tag{S7.112}$$

$\Gamma_{\boldsymbol{q}\lambda}(E)$ represents the probability per unit time of a transition with energy E from phonon branch λ at wave number $\boldsymbol{q}$ in subsystem I (II) to a set of phonon branches in subsystem II (I) with the same wave number. Here, state $\boldsymbol{q}\lambda$ in one subsystem is coupled to state $\boldsymbol{q}j_1'$ in the other subsystem via: $V_{\lambda j_1'}(\boldsymbol{q})$. Since the two expressions in Eq. (S7.112) are completely equivalent just representing transitions of opposite directions we consider only the first one in what follows. Assuming that subsystem II sufficiently large such that its density of states is nearly continuous, the sum over its states in the above expression can be replaced by an integral over the energy $\sum_j(\cdots)\rightarrow\int(\cdots)\rho\left(E_{\boldsymbol{q}}\right)\mathrm{d}E_{\boldsymbol{q}}$ giving:

$$\Gamma_{\boldsymbol{q}\lambda}(E)=\frac{\pi\hbar^3}{2}\int\mathrm{d}E'_{\boldsymbol{q}}\rho\left(E'_{\boldsymbol{q}}\right)\frac{\left\{\left|V_{\lambda j'}(\boldsymbol{q})\right|^2\right\}_{E_{\boldsymbol{q}j'}=E'_{\boldsymbol{q}}}}{E'_{\boldsymbol{q}}E_{\boldsymbol{q}\lambda}}\delta\left(E-E'_{\boldsymbol{q}}\right)=\frac{\pi\hbar^3}{2}\rho(E)\frac{\left\{\left|V_{\lambda j'}(\boldsymbol{q})\right|^2\right\}_{E_{\boldsymbol{q}j'}=E}}{EE_{\boldsymbol{q}\lambda}}. \tag{S7.113}$$

Eq. (S7.113) represents the transition rate of the phonons with energy E from branch λ and wave number $\boldsymbol{q}$ in subsystem I to the continuous manifold of states in subsystem II. The total transition rate between the two subsystems is then given by the sum of transition rates from all states in subsystem I, weighted by their phonon populations, to the manifold of states in subsystem II.

Assuming that the two subsystems are weakly coupled such that the width of state $\boldsymbol{q}\lambda$ in subsystem I is small and the probability to leave it at an energy other than $E_{\boldsymbol{q}\lambda}$ is negligible we can now write total transition rate as:

$$\Gamma_{\text{tot}} = \sum_{\boldsymbol{q}\lambda} \frac{1}{Z} e^{-\beta E_{\boldsymbol{q}\lambda}} \Gamma_{\boldsymbol{q}\lambda}\left(E_{\boldsymbol{q}\lambda}\right) = \frac{\pi\hbar^3}{2} \sum_{\boldsymbol{q}\lambda} \frac{e^{-\beta E_{\boldsymbol{q}\lambda}}}{Z} \frac{\rho\left(E_{\boldsymbol{q}\lambda}\right)\left\{\left|V_{\lambda j'}(\boldsymbol{q})\right|^2\right\}_{E_{\boldsymbol{q}j'}=E_{\boldsymbol{q}\lambda}}}{E_{\boldsymbol{q}\lambda}^2}$$

$$= \frac{\pi\hbar^3}{2} \sum_{\boldsymbol{q}\lambda} \frac{e^{-\beta E_{\boldsymbol{q}\lambda}}}{Z} \frac{\rho\left(E_{\boldsymbol{q}\lambda}\right)\left|V_{\lambda,\lambda+\frac{3r}{2}}(\boldsymbol{q})\right|^2}{E_{\boldsymbol{q}\lambda}^2}.$$

Finally we get

$$\Gamma_{\text{tot}} = \Gamma_{\boldsymbol{q}\lambda}(E) = \frac{\pi\hbar^3}{2} \sum_{\boldsymbol{q}\lambda} \frac{e^{-\beta E_{\boldsymbol{q}\lambda}}}{Z} \frac{\rho\left(E_{\boldsymbol{q}\lambda}\right)\left|V_{\lambda,\lambda+\frac{3r}{2}}(\boldsymbol{q})\right|^2}{E_{\boldsymbol{q}\lambda}^2}. \tag{S7.114}$$

where $Z = \sum_{\boldsymbol{q}\lambda} e^{-\beta E_{\boldsymbol{q}\lambda}}$ is the partition function. Here, we choose the index of phonon branches λ such that the phonon branch with lower energy has a smaller index, i.e., $E_{\boldsymbol{q}\lambda_1} < E_{\boldsymbol{q}\lambda_2}$ for index $\lambda_1 < \lambda_2$. Note that phonon branches λ and j_1' belong to the subsystem I (with index from 1 to $3r/2$) and subsystem II (with index from 1 to $1 + 3r/2$ to $3r$), respectively, we choose $j' = \lambda + \frac{3r}{2}$ to make sure that $E_{\boldsymbol{q}j'} = E_{\boldsymbol{q}\lambda}$ since phonon energy of two uncoupled system is identical. Eq. (S7.114) is the Fermi's golden rule for inter-phonon coupling.

References

(1) Wei, Z.; Yang, J.; Chen, W.; Bi, K.; Li, D.; Chen, Y. Phonon mean free path of graphite along the c-axis. *Appl. Phys. Lett.* **2014,** *104* (8), 081903.
(2) Brenner, D. W.; Shenderova, O. A.; Harrison, J. A.; Stuart, S. J.; Ni, B.; Sinnott, S. B. A second-generation reactive empirical bond order (REBO) potential energy expression for hydrocarbons. *J. Phys.: Condens. Matter* **2002,** *14* (4), 783-802.
(3) Kınacı, A.; Haskins, J. B.; Sevik, C.; Çağın, T. Thermal conductivity of BN-C nanostructures. *Phys. Rev. B* **2012,** *86* (11).
(4) Ouyang, W.; Azuri, I.; Mandelli, D.; Tkatchenko, A.; Kronik, L.; Urbakh, M.; Hod, O. Mechanical and Tribological Properties of Layered Materials under High Pressure: Assessing the Importance of Many-Body Dispersion Effects. *J. Chem. Theory Comput.* **2020,** *16* (1), 666-676.
(5) Plimpton, S. Fast Parallel Algorithms for Short-Range Molecular Dynamics. *J. Comput. Phys.* **1995,** *117* (1), 1-19.
(6) Ouyang, W.; Mandelli, D.; Urbakh, M.; Hod, O. Nanoserpents: Graphene Nanoribbon Motion on Two-Dimensional Hexagonal Materials. *Nano Lett.* **2018,** *18* (9), 6009-6016.
(7) Pollack, G. L. Kapitza Resistance. *Rev. Mod. Phys.* **1969,** *41* (1), 48-81.
(8) Yang, H.-S.; Bai, G. R.; Thompson, L. J.; Eastman, J. A. Interfacial thermal resistance in nanocrystalline yttria-stabilized zirconia. *Acta Mater.* **2002,** *50* (9), 2309-2317.
(9) Shinoda, W.; Shiga, M.; Mikami, M. Rapid estimation of elastic constants by molecular dynamics simulation under constant stress. *Phys. Rev. B* **2004,** *69* (13), 134103.
(10) Chen, J.; Walther, J. H.; Koumoutsakos, P. Strain Engineering of Kapitza Resistance in Few-Layer Graphene. *Nano Lett.* **2014,** *14* (2), 819-825.
(11) Wirtz, L.; Rubio, A. The phonon dispersion of graphite revisited. *Solid State Commun.* **2004,** *131* (3), 141-152.
(12) Zhang, J.; Hong, Y.; Yue, Y. Thermal transport across graphene and single layer hexagonal boron nitride. *J. Appl. Phys.* **2015,** *117* (13), 134307.
(13) Liu, B.; Meng, F.; Reddy, C. D.; Baimova, J. A.; Srikanth, N.; Dmitriev, S. V.; Zhou, K. Thermal transport in a graphene–MoS2 bilayer heterostructure: a molecular dynamics study. *RSC Adv.* **2015,** *5* (37), 29193-29200.
(14) Ding, Z.; Pei, Q.-X.; Jiang, J.-W.; Huang, W.; Zhang, Y.-W. Interfacial thermal conductance in graphene/MoS2 heterostructures. *Carbon* **2016,** *96*, 888-896.
(15) Nam, N. N. T.; Koshino, M. Lattice relaxation and energy band modulation in twisted bilayer graphene. *Phys. Rev. B* **2017,** *96* (7), 075311.
(16) Ramíarez, R.; Böhm, M. C. Simple geometric generation of special points in brillouin-zone integrations. Two-dimensional bravais lattices. *Int. J. Quantum Chem.* **1986,** *30* (3), 391-411.
(17) Cunningham, S. L. Special points in the two-dimensional Brillouin zone. *Phys. Rev. B* **1974,** *10* (12), 4988-4994.
(18) Monkhorst, H. J.; Pack, J. D. Special points for Brillouin-zone integrations. *Phys. Rev. B* **1976,** *13* (12), 5188-5192.
(19) Chadi, D. J. Special points for Brillouin-zone integrations. *Phys. Rev. B* **1977,** *16* (4), 1746-1747.
(20) Xu, Y.; Wang, J.-S.; Duan, W.; Gu, B.-L.; Li, B. Nonequilibrium Green's function method for phonon-phonon interactions and ballistic-diffusive thermal transport. *Phys. Rev. B* **2008,** *78* (22), 224303.
(21) Fetter, A. L.; Walecka, J. D., *Quantum theory of many-particle systems*. Courier Corporation: New York, USA, 2012.
(22) Stedman, G. E. Fermi's Golden Rule—An Exercise in Quantum Field Theory. *Am. J. Phys.* **1971,** *39* (2), 205-214.